

# 5

## FORMULATION AND CALCULATION OF ISOPARAMETRIC FINITE ELEMENT MATRICES

### 5.1 INTRODUCTION

A very important phase of a finite element analysis is the calculation of the finite element matrices. In Chapter 4 we discussed the formulation and calculation of generalized coordinate finite element models. The aim in the presentation of the generalized coordinate finite elements was primarily to enhance the understanding of the finite element method. We already pointed out that in most practical analyses the use of isoparametric finite elements is more effective.<sup>1-14</sup>

Our objective in this chapter is to present the formulation of isoparametric finite elements and describe effective implementations. In the derivation of generalized coordinate finite element models, we used local element coordinate systems  $x, y, z$  and assumed the element displacements  $u(x, y, z), v(x, y, z)$ , and  $w(x, y, z)$  in the form of polynomials in  $x, y$ , and  $z$  with undetermined constant coefficients  $\alpha_i, \beta_i$ , and  $\gamma_i$ ,  $i = 1, 2, \dots$ , identified as generalized coordinates. It was not possible to associate a priori a physical meaning to the generalized coordinates; however, on evaluation we found that the generalized coordinates are linear combinations of the element nodal point displacements.

The principal idea of the isoparametric finite element formulation is to achieve the relationship between the element displacements at any point and the element nodal point displacements directly through the use of *interpolation functions* (also called *shape functions*). This means that the transformation matrix  $\mathbf{A}^{-1}$  (see (4.55)) is not evaluated; instead, the element matrices corresponding to the required degrees of freedom are obtained directly.

### 5.2 ISOPARAMETRIC DERIVATION OF BAR ELEMENT STIFFNESS MATRIX

Consider the example of a bar element to illustrate the procedure of an isoparametric stiffness formulation. In order to simplify the explanation, assume that the bar lies in the global  $X$ -coordinate axis, as shown in Fig. 5.1. The first step is to relate the actual global coordinates  $X$  to a *natural coordinate system* with variable  $r$ , where  $-1 \leq r \leq 1$  (Fig. 5.1). This transformation is given by

$$X := \frac{1}{2}(1 - r)X_1 + \frac{1}{2}(1 + r)X_2 \quad (5.1)$$

$$\text{or} \quad X := \sum_{i=1}^2 h_i X_i \quad (5.2)$$

where  $h_1 = \frac{1}{2}(1 - r)$  and  $h_2 = \frac{1}{2}(1 + r)$  are the interpolation or shape functions. Note that (5.2) establishes a unique relationship between the coordinates  $X$  and  $r$  on the bar.

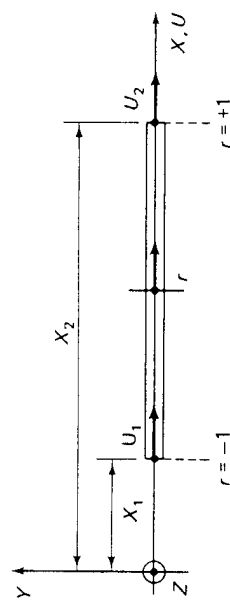


FIGURE 5.1 Element in global and natural coordinate system.

The bar global displacements are expressed in the same way as the global coordinates:

$$U = \sum_{i=1}^2 h_i U_i \quad (5.3)$$

where in this case a linear displacement variation is specified. *The interpolation of the element coordinates and element displacements using the same interpolation functions, which are defined in a natural coordinate system, is the basis of the isoparametric finite element formulation.*

For the calculation of the element stiffness matrix we need to find the element strains  $\epsilon = dU/dX$ . Here we use

$$\epsilon = \frac{dU}{dX} \frac{dr}{dX} \quad (5.4)$$

where, from (5.3),

$$\frac{dU}{dr} = U_2 - U_1 \quad (5.5)$$

and using (5.2) we obtain

$$\frac{dX}{dr} = \frac{X_2 - X_1}{2} = \frac{L}{2} \quad (5.6)$$

where  $L$  is the length of the bar. Hence, as expected, we have

$$\epsilon = \frac{U_2 - U_1}{L} \quad (5.7)$$

The strain-displacement transformation matrix corresponding to (4.28) is therefore

$$\mathbf{B} = \frac{1}{L} [-1 \quad 1] \quad (5.8)$$

In general, the strain-displacement transformation matrix is a function of the natural coordinates and we therefore evaluate the stiffness matrix volume integral in (4.29) by integrating over the natural coordinates. Following this general procedure, although in this example it is not necessary, we have

$$\mathbf{K} = \frac{AE}{L^2} \int_{-1}^1 \begin{bmatrix} -1 & 1 \\ 1 & -1 \end{bmatrix} [I \quad I] J dr \quad (5.9)$$

where the bar area  $A$  and modulus of elasticity  $E$  have been assumed constant, and  $J$  is the Jacobian relating an element length in the global coordinate system to an element length in the natural coordinate system; i.e.,

$$dX = J dr \quad (5.10)$$

$$J = \frac{L}{2} \quad (5.11)$$

From (5.6) we have

$$r = \frac{X - [X_1 + X_2]/2}{L/2} \quad (5.12)$$

Then evaluating (5.9) we obtain the well-known matrix

$$\mathbf{K} = \frac{AE}{L} \begin{bmatrix} 1 & -1 \\ -1 & 1 \end{bmatrix} \quad (5.13)$$

As was stated in the introduction, the isoparametric formulation avoids the construction of the transformation matrix  $\mathbf{A}^{-1}$ . In order to compare the above formulation with the generalized coordinate formulation, we need to solve from (5.1) for  $r$  and then substitute for  $r$  into (5.3). We obtain

$$r = \frac{X - [(X_1 + X_2)/2]}{L/2} \quad (5.14)$$

and then

$$\left. \begin{aligned} \boldsymbol{\alpha}_0 &= \frac{1}{2}(U_1 + U_2) - \frac{X_1 + X_2}{2L}(U_2 - U_1) \\ \boldsymbol{\alpha}_1 &= \frac{1}{L}(U_2 - U_1) \end{aligned} \right\} \quad (5.15)$$

$$\text{or } \boldsymbol{\alpha} = \begin{bmatrix} \frac{1}{2} + \frac{X_1 + X_2}{2L} & \frac{1}{2} - \frac{X_1 + X_2}{2L} \\ -\frac{1}{L} & \frac{1}{L} \end{bmatrix} \mathbf{U} \quad (5.16)$$

where

$$\boldsymbol{\alpha}^T = [\boldsymbol{\alpha}_0 \quad \boldsymbol{\alpha}_1]; \quad \mathbf{U}^T = [U_1 \quad U_2] \quad (5.17)$$

and the matrix relating in (5.16)  $\boldsymbol{\alpha}$  to  $\mathbf{U}$  is  $\mathbf{A}^{-1}$ . It should be noted that in this example the generalized coordinates  $\boldsymbol{\alpha}_0$  and  $\boldsymbol{\alpha}_1$  relate the global element displacements to the global element coordinates.

### 5.3 FORMULATION OF CONTINUUM ELEMENTS

Considering the calculation of a continuum element, it is in most cases effective to directly calculate the element matrices corresponding to the global degrees of freedom. However, we shall first present the formulation of the matrices that only the relevant coordinate axes and the appropriate interpolation functions.

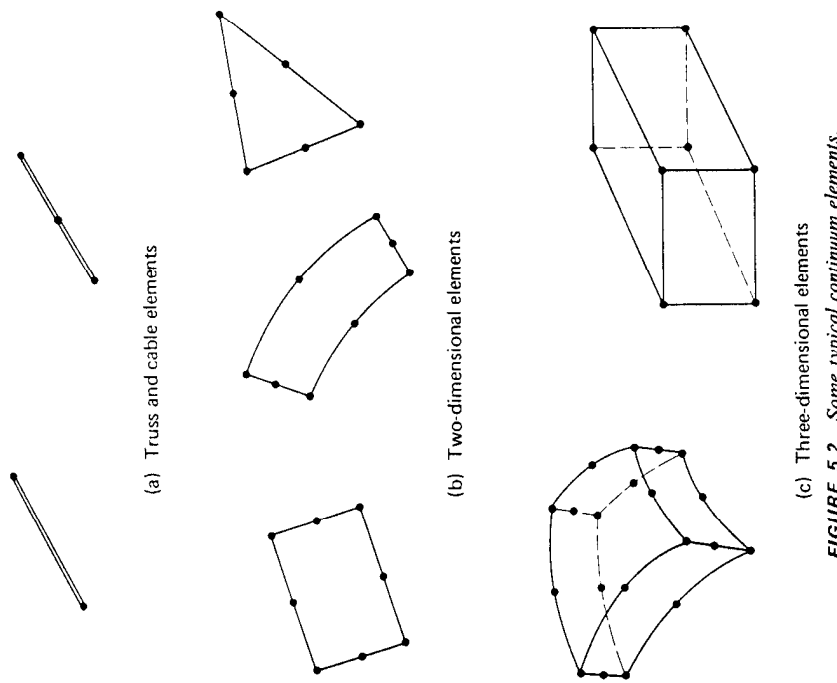


FIGURE 5.2 Some typical continuum elements.

#### 5.3.1 Rectangular Elements

The basic procedure in the isoparametric finite element formulation is to express the element coordinates and element displacements in the form of interpolations using the natural coordinate system of the element. This coordinate system is one-, two-, or three-dimensional, depending on the dimensionality of the element. The formulation of the element matrices is the same whether we deal with a one-, two-, or three-dimensional element. For this reason we use in the following general presentation the equations of a three-dimensional element. However, the one- and two-dimensional elements are included by simply using only the relevant coordinate axes and the appropriate interpolation functions.

Considering a general three-dimensional element, the coordinate interpolations are

$$\left. \begin{aligned} x &= \sum_{i=1}^q h_i x_i \\ y &= \sum_{i=1}^q h_i y_i \\ z &= \sum_{i=1}^q h_i z_i \end{aligned} \right\} \quad (5.18)$$

where  $x$ ,  $y$ , and  $z$  are the coordinates at any point of the element (here local coordinates), and  $x_i, y_i, z_i, i = 1, \dots, q$ , are the coordinates of the  $q$  element nodes. The interpolation functions  $h_i$  are defined in the natural coordinate system of the element, which has variables  $r$ ,  $s$ , and  $t$  that each vary from  $-1$  to  $+1$ . For one- or two-dimensional elements, only the relevant equations in (5.18) would be employed, and the interpolation functions would depend only on the natural coordinate variables  $r$  and  $r, s$ , respectively.

The unknown quantities in (5.18) are so far the interpolation functions  $h_i$ . The fundamental property of the interpolation function  $h_i$  is that its value in the natural coordinate system is unity at node  $i$  and is zero at all other nodes. Using these conditions the functions  $h_i$  corresponding to a specific nodal point layout could be solved for in a systematic manner. However, it is convenient to construct them by inspection, which is demonstrated in the following simple example.

**EXAMPLE 5.1:** Construct the interpolation functions corresponding to the three-node truss element in Fig. 5.3.

A first observation is that for the three-node truss element we want interpolation polynomials that involve  $r^2$  as the highest power of  $r$ ; in other words, the interpolation functions shall be parabolas. The function  $h_2$  can thus be constructed without much effort. Namely, the parabola that satisfies the conditions to be equal to zero at  $r = \pm 1$  and equal to 1 at  $r = 0$  is given by  $(1 - r^2)$ . The other two interpolation functions  $h_1$  and  $h_3$  are constructed by superimposing a linear function and a parabola. Consider the interpolation function  $h_3$ . Using  $\frac{1}{2}(1 + r)$ , the condition that the function shall be zero at  $r = -1$  and 1 at  $r = +1$  are satisfied. To assure that  $h_3$  is also zero at  $r = 0$ , we need to use  $h_3 = \frac{1}{2}(1 + r) - \frac{1}{2}(1 - r^2)$ . The interpolation function  $h_1$  is obtained in a similar manner.

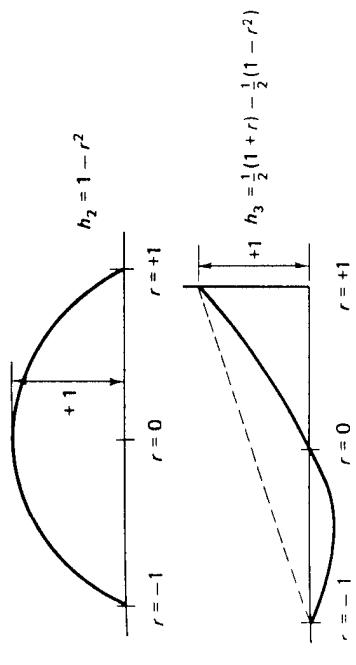
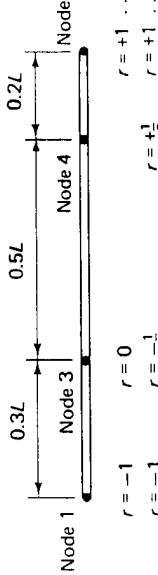


FIGURE 5.3 (cont.)

The procedure used in Example 5.1 of constructing the final required interpolation functions suggests an attractive formulation of an element with a variable number of nodes. This formulation is achieved by constructing first the interpolations corresponding to a basic two-node element. The addition of another node then results into an additional interpolation function and a correction to be applied to the already existing interpolation functions. Figure 5.4 gives the interpolation functions of the one-dimensional element considered in Example 5.1, with an additional fourth node possible. As shown the element can have from two to four nodes. We should note that nodes 3 and 4 are now intermediate nodes, because nodes 1 and 2 are used to define the two-node element.



(a) Two to 4 variable-nodes truss element

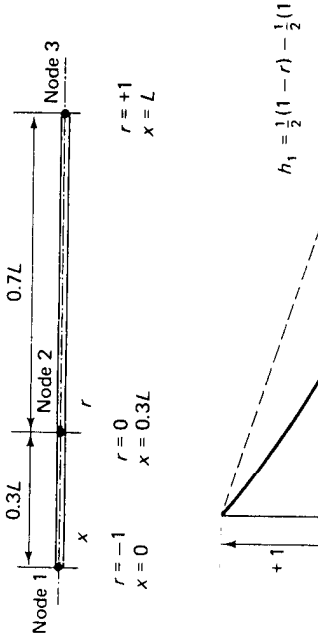


FIGURE 5.4 Interpolation functions of two to four variable-number-nodes one-dimensional element.  
 FIGURE 5.3 One-dimensional interpolation functions of a truss element.

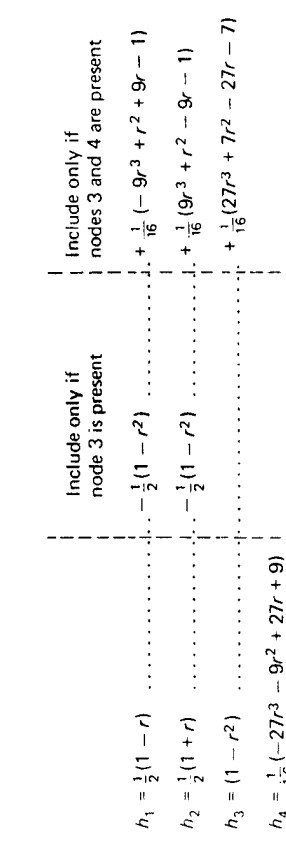
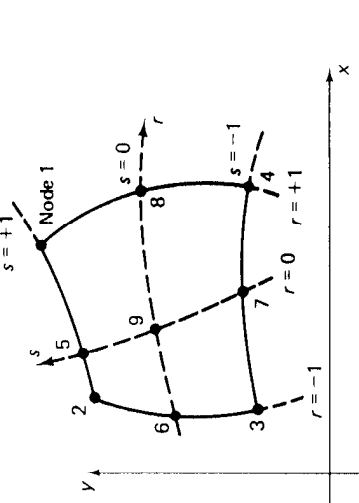


FIGURE 5.4 Interpolation functions of two to four variable-number-nodes one-dimensional element.  
 FIGURE 5.3 One-dimensional interpolation functions of a truss element.

This procedure of constructing the element interpolation functions for one-dimensional analysis can be directly generalized for use in two and three dimensions. Figure 5.5 shows the interpolation functions of a four to nine variable-number-nodes two-dimensional element and Fig. 5.6 gives the interpolation functions for three-dimensional eight- to twenty-node elements. The two- and three-dimensional interpolations have been established in a manner analogous to the one-dimensional interpolations, where the basic functions used are, in fact, those already employed in Fig. 5.4. We consider in Figs. 5.5 and 5.6 at most parabolic interpolation, but variable-number-nodes elements with interpolations of higher order could be derived in an analogous way.

The attractiveness of the elements in Figs. 5.4 to 5.6 lies in that the elements can have any number of nodes between the minimum and the maximum, and triangular elements can also be formed (see Section 5.3.2). However, to obtain

(b) Interpolation functions



(a) Four to 9 variable-number-nodes two-dimensional element

Include only if node  $i$  is defined

$$\begin{aligned} h_1 &= \frac{1}{4}(1+r)(1+s) \\ h_2 &= \frac{1}{4}(1-r)(1+s) \\ h_3 &= \frac{1}{4}(1-r)(1-s) \\ h_4 &= \frac{1}{4}(1+r)(1-s) \\ h_5 &= \frac{1}{2}(1-r^2)(1+s) \\ h_6 &= \frac{1}{2}(1-s^2)(1-r) \\ h_7 &= \frac{1}{2}(1-r^2)(1-s) \\ h_8 &= \frac{1}{2}(1-s^2)(1+r) \\ h_9 &= (1-r^2)(1-s^2) \end{aligned}$$

(b) Interpolation functions

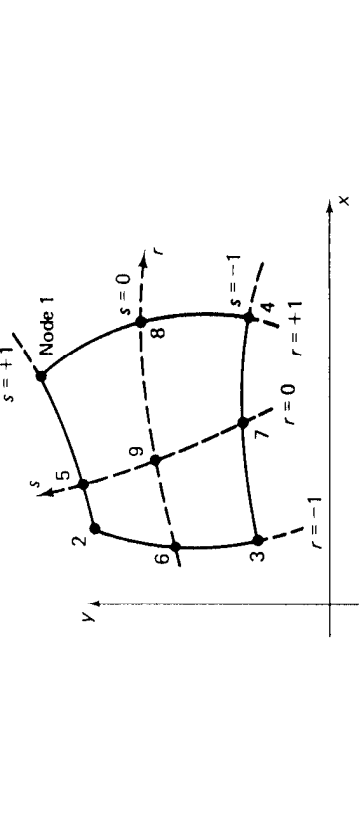
**FIGURE 5.5** Interpolation functions of four to nine variable-number-nodes two-dimensional element.

maximum accuracy, the variable-number-nodes elements should be as nearly rectangular (in three-dimensional analysis, rectangular in each local plane) as possible and the noncorner nodes should in general be located at their natural coordinate positions, e.g., for the 9-node two-dimensional element the intermediate side nodes should in general be located at the midpoints between the corner nodes and the ninth node should be at the center of the element (for some exceptions see Section 5.3.2).

Considering the geometry of the two- and three-dimensional elements in Figs. 5.5 and 5.6 we note that by means of the coordinate interpolations in (5.18), the elements can have, without any difficulties, curved boundaries. This is an important advantage over the generalized coordinate finite element formulation. Another important advantage is the ease with which the element displacement functions can be constructed.

The attractiveness of the elements in Figs. 5.4 to 5.6 lies in that the elements can have any number of nodes between the minimum and the maximum, and triangular elements can also be formed (see Section 5.3.2). However, to obtain

(b) Interpolation functions



(a) Eight to 20 variable-number-nodes three-dimensional element

Include only if node  $i$  is not included; otherwise,

$$g_i = G(r, r_i) G(s, s_i) G(t, t_i)$$

$$G(\beta, \beta_i) = \frac{1}{2}(1 + \beta_i \beta) \quad \text{for } \beta_i = \pm 1$$

$$G(\beta, \beta_i) = (1 - \beta^2) \quad \text{for } \beta_i = 0$$

(b) Interpolation functions

**FIGURE 5.6** Interpolation functions of eight to twenty variable-number-nodes three-dimensional element.

$$\begin{aligned} h_1 &= g_1 - |g_9 + g_{12} + g_{17}|/2 \\ h_2 &= g_2 - |g_9 + g_{10} + g_{18}|/2 \\ h_3 &= g_3 - |g_{10} + g_{11} + g_{19}|/2 \\ h_4 &= g_4 - |g_{11} + g_{12} + g_{20}|/2 \\ h_5 &= g_5 - |g_{13} + g_{16} + g_{17}|/2 \\ h_6 &= g_6 = g_1 - (g_{13} + g_{14} + g_{18})/2 \\ h_7 &= g_7 = g_1 - (g_{14} + g_{15} + g_{19})/2 \\ h_8 &= g_8 = g_1 - (g_{15} + g_{16} + g_{20})/2 \\ h_9 &= g_9 = 0 \quad \text{if node } i \text{ is not included; otherwise,} \\ h_{10} &= G(r, r_i) G(s, s_i) G(t, t_i) \\ G(\beta, \beta_i) &= \frac{1}{2}(1 + \beta_i \beta) \quad \text{for } \beta_i = \pm 1 \\ G(\beta, \beta_i) &= (1 - \beta^2) \quad \text{for } \beta_i = 0 \end{aligned}$$

In the isoparametric formulation the element displacements are interpolated in the same way as the geometry; i.e., we use

$$u = \sum_{i=1}^q h_i u_i; \quad v = \sum_{i=1}^q h_i v_i; \quad w = \sum_{i=1}^q h_i w_i \quad (5.19)$$

where  $u$ ,  $v$ , and  $w$  are the local element displacements at any point of the element and  $u_i$ ,  $v_i$ , and  $w_i$ ,  $i = 1, \dots, q$ , are the corresponding element displacements at its nodes. Therefore, it is assumed that to each nodal point coordinate necessary to describe the geometry of the element, there corresponds one nodal point displacement.

To be able to evaluate the stiffness matrix of an element, we need to calculate the strain-displacement transformation matrix. The element strains are obtained in terms of derivatives of element displacements with respect to the local coordinates. Because the element displacements are defined in the natural coordinate system using (5.19), we need to relate the  $x$ ,  $y$ , and  $z$  derivatives to the  $r$ ,  $s$ , and  $t$  derivatives, where we realize that (5.18) is of the form

$$x = f_1(r, s, t); \quad y = f_2(r, s, t); \quad z = f_3(r, s, t); \quad (5.20)$$

where  $f_i$  denotes "function of." The inverse relationship is

$$r = f_4(x, y, z); \quad s = f_5(x, y, z); \quad t = f_6(x, y, z) \quad (5.21)$$

We require the derivatives  $\partial/\partial x$ ,  $\partial/\partial y$ , and  $\partial/\partial z$  and it seems natural to use the chain rule in the following form:

$$\frac{\partial}{\partial x} = \frac{\partial r}{\partial x} + \frac{\partial s}{\partial x} + \frac{\partial t}{\partial x} \quad (5.22)$$

with similar relationships for  $\partial/\partial y$  and  $\partial/\partial z$ . However, to evaluate  $\partial/\partial x$  in (5.22), we need to calculate  $\partial r/\partial x$ ,  $\partial s/\partial x$ , and  $\partial t/\partial x$ , which means that the explicit inverse relationships in (5.21) would need to be evaluated. These inverse relationships are in general difficult to establish explicitly, and it is necessary to evaluate the required derivatives in the following way. Using the chain rule, we have

$$\begin{bmatrix} \frac{\partial}{\partial r} \\ \frac{\partial}{\partial s} \\ \frac{\partial}{\partial t} \end{bmatrix} = \begin{bmatrix} \frac{\partial x}{\partial r} & \frac{\partial y}{\partial r} & \frac{\partial z}{\partial r} \\ \frac{\partial x}{\partial s} & \frac{\partial y}{\partial s} & \frac{\partial z}{\partial s} \\ \frac{\partial x}{\partial t} & \frac{\partial y}{\partial t} & \frac{\partial z}{\partial t} \end{bmatrix} \begin{bmatrix} \frac{\partial}{\partial x} \\ \frac{\partial}{\partial y} \\ \frac{\partial}{\partial z} \end{bmatrix} \quad (5.23)$$

$$\frac{\partial}{\partial r} = \mathbf{J}^{-1} \frac{\partial}{\partial x} \quad (5.24)$$

or, in matrix notation,

where  $\mathbf{J}$  is the *Jacobian operator* relating the natural coordinate derivatives to the local coordinate derivatives. We should note that the Jacobian operator can easily be found using (5.18). We require  $\partial/\partial x$  and use

$$\frac{\partial}{\partial x} = \mathbf{J}^{-1} \frac{\partial}{\partial r}$$

which requires that the inverse of  $\mathbf{J}$  exists. This inverse exists provided that there is a one-to-one (i.e., unique) correspondence between the natural and the local

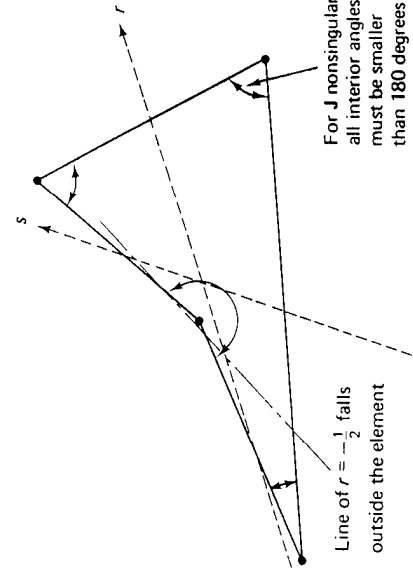
coordinates of the element, as expressed in (5.20) and (5.21). In most formulations the one-to-one correspondence between the coordinate systems (i.e., to each  $r$ ,  $s$ , and  $t$ , there corresponds only one  $x$ ,  $y$ , and  $z$ ) is obviously given, such as for the elements in Figs. 5.3 to 5.6. However, in cases where the element is much distorted or folds back upon itself, as in Fig. 5.7, the unique relation between the coordinate systems does not exist (see also Section 5.3.2 for singularities in the Jacobian transformation, Example 5.17).

Using (5.19) and (5.25), we evaluate  $\partial u/\partial x$ ,  $\partial u/\partial y$ ,  $\partial u/\partial z$ , and can therefore construct the strain-displacement transformation matrix  $\mathbf{B}$ , with

$$\boldsymbol{\epsilon} = \hat{\mathbf{B}} \hat{\mathbf{u}} \quad (5.26)$$

where  $\hat{\mathbf{u}}$  is a vector listing the element nodal point displacements of (5.19), and we note that  $\mathbf{J}$  affects the elements in  $\mathbf{B}$ . The element stiffness matrix corresponding to the local element degrees of freedom is then

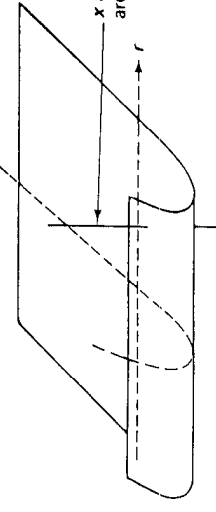
$$\mathbf{K} = \int_V \mathbf{B}^T \mathbf{C} \mathbf{B} dV \quad (5.27)$$



(a) Distorted element

For  $\mathbf{J}$  nonsingular,

all interior angles must be smaller than 180 degrees



(b) Element folding upon itself  
FIGURE 5.7 Elements with possible singular Jacobian.

We should note that the elements of  $\mathbf{B}$  are functions of the natural coordinates  $r$ ,  $s$ , and  $t$ . Therefore, the volume integration extends over the natural coordinate volume, and the volume differential  $dV$  need also be written in terms of the natural coordinates. In general, we have

$$(5.28) \quad dV = \det \mathbf{J} dr ds dt$$

where  $\det \mathbf{J}$  is the determinant of the Jacobian operator in (5.24).

An explicit evaluation of the volume integral in (5.27) is, in general, not effective; in particular, when higher-order interpolations are used or the element is distorted. Therefore, numerical integration is employed. Indeed, numerical integration must be regarded as an integral part of the isoparametric element matrix evaluations. The details of the numerical integration procedure are described in Section 5.7, but the process can briefly be summarized as follows. First, we write (5.27) in the form

$$(5.29) \quad \mathbf{K} := \int_V \mathbf{F} dr ds dt$$

where  $\mathbf{F} = \mathbf{B}^T \mathbf{C} \mathbf{B} \det \mathbf{J}$  and the integration is performed in the natural coordinate system of the element. As stated above, the elements of  $\mathbf{F}$  depend on  $r$ ,  $s$ , and  $t$ , but the detailed functional relationship is usually not calculated. Using numerical integration, the stiffness matrix is now evaluated as

$$(5.30) \quad \mathbf{K} = \sum_{i,j,k} \alpha_{ijk} \mathbf{F}_{ijk}$$

where  $\mathbf{F}_{ijk}$  is the matrix  $\mathbf{F}$  evaluated at points  $r_i$ ,  $s_j$ , and the  $t_k$ , and the  $\alpha_{ijk}$  are given constants which depend on the values of  $r_i$ ,  $s_j$ , and  $t_k$ . The sampling points  $r_i$ ,  $s_j$ , and  $t_k$  of the function and the corresponding weighting factors  $\alpha_{ijk}$  are chosen to obtain maximum accuracy in the integration. Naturally, the integration accuracy can increase as the number of sampling points is increased.

The purpose of the above brief outline of the numerical integration procedure was to complete the description of the general isoparametric formulation. The relative simplicity of the formulation may already be noted. It is the simplicity of the element formulation and the efficiency with which the element matrices can actually be evaluated in the computer that has drawn much attention to the development of the isoparametric and related elements.

The formulation of the element mass matrix and load vectors is now straightforward. Namely, writing the element displacements in the form

$$(5.31) \quad \mathbf{u}(r, s, t) = \mathbf{H} \bar{\mathbf{u}}$$

where  $\mathbf{H}$  is a matrix of the interpolation functions, we have, as in (4.30) to (4.33),

$$(5.32) \quad \mathbf{M} = \int_V \rho \mathbf{H}^T \mathbf{H} dV$$

$$(5.33) \quad \mathbf{R}_S = \int_V \mathbf{H}^T \mathbf{F}^S dV$$

$$(5.34) \quad \mathbf{R}_B = \int_V \mathbf{B}^T \mathbf{F}^B dV$$

$$(5.35) \quad \mathbf{R}_I = \int_V \mathbf{B}^T \mathbf{r}' dV$$

The above matrices are evaluated using numerical integration as indicated for the stiffness matrix  $\mathbf{K}$  in (5.30). In the evaluation we need to use the appropriate function  $\mathbf{F}$ . To calculate the body force vector  $\mathbf{R}_B$  we use  $\mathbf{F} = \mathbf{H}^T \mathbf{f}^B$  det  $\mathbf{J}$ . for the surface force vector we use  $\mathbf{F} = \mathbf{H}^T \mathbf{f}^S$  det  $\mathbf{J}^S$ , for the initial stress load vector we use  $\mathbf{F} = \mathbf{B}^T \mathbf{r}'$  det  $\mathbf{J}$ , and for the mass matrix we have  $\mathbf{F} = \rho \mathbf{H}^T \mathbf{H}$  det  $\mathbf{J}$ . The weight coefficients  $\alpha_{ijk}$  are the same as in the stiffness matrix evaluation if the same order of numerical integration is used. However, in practice, different integration orders may be employed because the required accuracy in the element matrices varies (see Section 5.7).

The above formulation was for one-, two-, or three-dimensional elements.

We shall now consider some specific cases and demonstrate the details of the calculation of element matrices.

**EXAMPLE 5.2:** Derive the displacement interpolation matrix  $\mathbf{H}$ , strain-displacement interpolation matrix  $\mathbf{B}$ , and the Jacobian operator  $\mathbf{J}$  for the three-node truss element shown in Fig. 5.8.

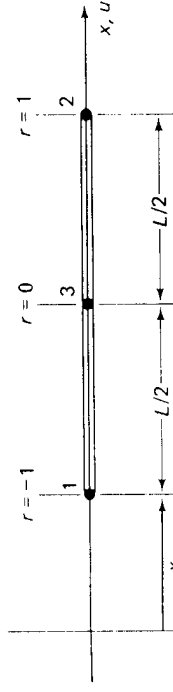


FIGURE 5.8 Truss element with node 3 at center of element.

The interpolation functions of the element were already given in Fig. 5.3. Thus we have

$$(a) \quad \mathbf{H} = \left[ -\frac{r}{2}(1-r) \quad \frac{r}{2}(1+r) \quad (1-r^2) \right]$$

The strain-displacement matrix  $\mathbf{B}$  is obtained by differentiation of  $\mathbf{H}$  with respect to  $r$  and premultiplying the result by the inverse of the Jacobian operator

$$(b) \quad \mathbf{B} = \mathbf{J}^{-1} [(-\frac{1}{2} + r) \quad (\frac{1}{2} + r) \quad -2r]$$

To evaluate  $\mathbf{J}$  formally we use

$$(c) \quad x = -\frac{r}{2}(1-r)x_1 + \frac{r}{2}(1+r)(x_1 + L) + (1-r^2)(x_1 + \frac{L}{2})$$

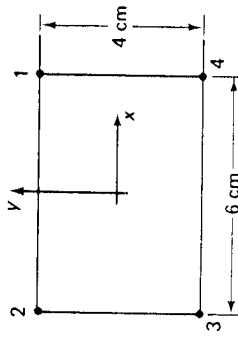
hence

where we may note that because node 3 is at the center of the truss,  $x$  is interpolated linearly between nodes 1 and 2. The same result would be obtained using only nodes 1 and 2 for the geometry interpolation. Using now the relation in (c) we have

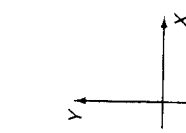
$$(d) \quad \mathbf{J} = \begin{bmatrix} \frac{L}{2} \\ 2 \end{bmatrix}$$

With the relations in (a) to (d), we could now evaluate all finite element matrices and vectors given in (5.27) to (5.35).

**EXAMPLE 5.3:** Establish the Jacobian operator  $\mathbf{J}$  of the two-dimensional elements shown in Fig. 5.9.



Element 1



Element 2

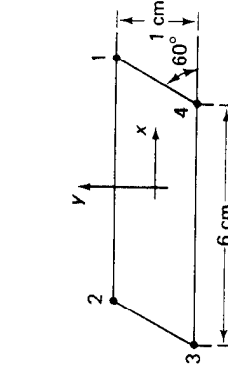


FIGURE 5.9 Some two-dimensional elements.

The Jacobian operator is the same for the global  $X$ - $Y$  and the local  $x$ - $y$  coordinate systems. For convenience we therefore use the local coordinate systems. Substituting into (5.18) and (5.23) using the interpolation functions given in Fig. 5.5, we obtain for element 1:

$$x = 3r; \quad y = 2s$$

$$\mathbf{J} = \begin{bmatrix} 3 & 0 \\ 0 & 2 \end{bmatrix}$$

Similarly, for element 2, we have

$$x = \frac{1}{3}(1+r)(1+s)(3+1/(2\sqrt{3}))+\frac{1}{3}(1-r)(1+s)(-(3-1/(2\sqrt{3}))) + (1-r)(1-s)(-(3+1/(2\sqrt{3}))) + (1+r)(1-s)(3-1/(2\sqrt{3}))$$

$$y = \frac{1}{3}(1+r)(1+s)(1/2)+(1-r)(1+s)(1/2)+(1-r)(1-s)(-1/2) + (1+r)(1-s)(-1/2)$$

and hence

$$\mathbf{J} = \begin{bmatrix} 3 & 0 \\ \frac{1}{2\sqrt{3}} & \frac{1}{2} \end{bmatrix}$$

Also, for element 3,

$$x = \frac{1}{4}(1+r)(1+s)(1)+(1-r)(1+s)(-1)+(1-r)(1-s)(-1) + (1+r)(1-s)(+1)$$

$$y = \frac{1}{4}(1+r)(1-s)(5/4)+(1-r)(1+s)(1/4)+(1-r)(1-s)(-3/4)$$

$$+ (1+r)(1-s)(-3/4)$$

$$\text{therefore, } \mathbf{J} = \frac{1}{4} \begin{bmatrix} 4 & (1+s) \\ 0 & (3+r) \end{bmatrix}$$

We may recognize that the Jacobian operator of a  $2 \times 2$  square element is the identity matrix, and that the entries in the operator  $\mathbf{J}$  of a general element express the amount of distortion from that  $2 \times 2$  square element. Since the distortion is constant at any point  $(r, s)$  of elements 1 and 2 the operator  $\mathbf{J}$  is constant for these elements.

**EXAMPLE 5.4:** Establish the interpolation functions of the two-dimensional element shown in Fig. 5.10.

The individual functions are obtained by combining the basic linear, parabolic, and cubic interpolations corresponding to the  $r$  and  $s$  directions. Thus using the functions in Figure 5.4 we obtain

$$h_3 = \frac{1}{16}(-27r^3 - 9r^2 + 27r + 9) \{ \frac{1}{2}(1+s) \}$$

$$h_6 = \{ (1-r^2) + r^2(27r^3 + 7r^2 - 7) \} \{ \frac{1}{2}(1+s) \}$$

$$h_2 = \{ \frac{1}{2}(1-r) - \frac{1}{2}(1-r^2) + \frac{1}{16}(-9r^3 + r^2 + 9r - 1) \} \{ \frac{1}{2}(1+s) \}$$

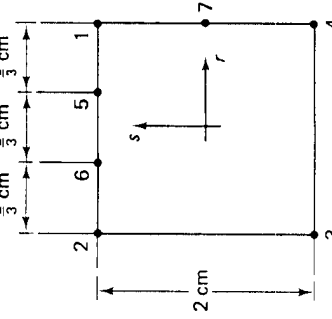
$$h_3 = \frac{1}{4}(1-r)(1-s)$$

$$h_7 = \frac{1}{2}(1-s^2)(1+r)$$

$$h_4 = \frac{1}{4}(1+r)(1-s) - \frac{h_7}{2}$$

$$h_1 = \frac{1}{4}(1+r)(1+s) - \frac{3}{4}h_5 - \frac{3}{4}h_6 - \frac{1}{2}h_7$$

where  $h_1$  is constructed as indicated in Fig. 5.10.



(a) Seven node element  
FIGURE 5.10 A 7-node element.

The displacement interpolation given in (5.19) is

$$\begin{aligned} u &= \frac{1}{4}(1+r)(1+s)u_1 + \frac{1}{4}(1-r)(1+s)u_2 \\ &\quad + \frac{1}{4}(1-r)(1-s)u_3 + \frac{1}{4}(1+r)(1-s)u_4 \\ v &= \frac{1}{4}(1+r)(1+s)v_1 + \frac{1}{4}(1-r)(1+s)v_2 \\ &\quad + \frac{1}{4}(1-r)(1-s)v_3 + \frac{1}{4}(1+r)(1-s)v_4 \end{aligned}$$

The element strains are given by

$$\boldsymbol{\epsilon}^r = [\epsilon_{xx} \quad \epsilon_{yy} \quad \gamma_{xy}]$$

$$\text{where } \epsilon_{xx} = \frac{\partial u}{\partial x}; \quad \epsilon_{yy} = \frac{\partial v}{\partial y}; \quad \gamma_{xy} = \frac{\partial u}{\partial y} + \frac{\partial v}{\partial x}$$

To evaluate the displacement derivatives, we need to evaluate (5.23):

$$\left[ \begin{array}{c} \frac{\partial}{\partial r} \\ \hline \boldsymbol{\partial} \\ \hline \frac{\partial}{\partial s} \end{array} \right] = \left[ \begin{array}{cc} \frac{\partial x}{\partial r} & \frac{\partial y}{\partial r} \\ \frac{\partial x}{\partial s} & \frac{\partial y}{\partial s} \\ \hline \frac{\partial}{\partial y} \end{array} \right] \quad \text{or} \quad \frac{\partial}{\partial r} = \mathbf{J} \frac{\partial}{\partial x}$$

$$\text{where } \frac{\partial x}{\partial r} = \frac{1}{4}(1+s)x_1 - \frac{1}{4}(1-s)x_2 - \frac{1}{4}(1-s)x_3 + \frac{1}{4}(1-s)x_4$$

$$\frac{\partial x}{\partial s} = \frac{1}{4}(1+r)x_1 + \frac{1}{4}(1-r)x_2 - \frac{1}{4}(1-r)x_3 - \frac{1}{4}(1+r)x_4$$

$$\frac{\partial y}{\partial r} = \frac{1}{4}(1+s)y_1 - \frac{1}{4}(1-s)y_2 - \frac{1}{4}(1-s)y_3 + \frac{1}{4}(1-s)y_4$$

$$\frac{\partial y}{\partial s} = \frac{1}{4}(1+r)y_1 + \frac{1}{4}(1-r)y_2 - \frac{1}{4}(1-r)y_3 - \frac{1}{4}(1+r)y_4$$

Therefore, for any value  $r$  and  $s$ ,  $-1 \leq r \leq +1$  and  $-1 \leq s \leq +1$ , we can form the Jacobian operator  $\mathbf{J}$  by using the above expressions for  $\partial x/\partial r$ ,  $\partial x/\partial s$ , and  $\partial y/\partial r$ ,  $\partial y/\partial s$ . Assume that we evaluate  $\mathbf{J}$  at  $r = r_i$  and  $s = s_j$  and denote the operator by  $\mathbf{J}_{ij}$  and its determinant by  $\det \mathbf{J}_{ij}$ . Then we have

$$\left[ \begin{array}{c} \frac{\partial}{\partial x} \\ \hline \frac{\partial}{\partial y} \\ \hline \frac{\partial}{\partial r} \end{array} \right] = \mathbf{J}_{ij}^{-1} \left[ \begin{array}{c} \frac{\partial}{\partial r} \\ \hline \frac{\partial}{\partial s} \\ \hline \frac{\partial}{\partial y} \end{array} \right] \text{at } \begin{array}{l} r=r_i \\ s=s_j \end{array}$$

To evaluate the element strains we use

$$\frac{\partial u}{\partial r} = \frac{1}{4}(1+s)u_1 - \frac{1}{4}(1-s)u_2 - \frac{1}{4}(1-s)u_3 + \frac{1}{4}(1-s)u_4$$

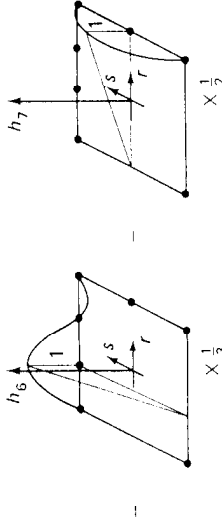
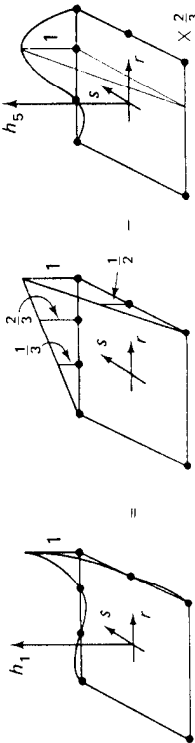
$$\frac{\partial u}{\partial s} = \frac{1}{4}(1+r)u_1 + \frac{1}{4}(1-r)u_2 - \frac{1}{4}(1-r)u_3 - \frac{1}{4}(1+r)u_4$$

$$\frac{\partial v}{\partial r} = \frac{1}{4}(1+s)v_1 - \frac{1}{4}(1-s)v_2 - \frac{1}{4}(1-s)v_3 + \frac{1}{4}(1-s)v_4$$

$$\frac{\partial v}{\partial s} = \frac{1}{4}(1+r)v_1 + \frac{1}{4}(1-r)v_2 - \frac{1}{4}(1-r)v_3 - \frac{1}{4}(1+r)v_4$$

Therefore,

$$\begin{aligned} \left[ \begin{array}{c} \frac{\partial u}{\partial x} \\ \hline \frac{\partial u}{\partial y} \\ \hline \frac{\partial u}{\partial r} \end{array} \right] &= \frac{1}{4}\mathbf{J}_{ij}^{-1} \left[ \begin{array}{c} 1+s_j & 0 & -(1+s_j) & 0 \\ 1+r_i & 0 & 1-r_i & 0 \\ 1-r_i & 0 & -(1-r_i) & 0 \\ 1+r_i & 0 & 1+r_i & 0 \end{array} \right] \mathbf{u} \\ &= \frac{1}{4}\mathbf{J}_{ij}^{-1} \left[ \begin{array}{c} 1+s_j & 0 & -(1+s_j) & 0 \\ 1+r_i & 0 & 1-r_i & 0 \\ 1-r_i & 0 & -(1-r_i) & 0 \\ 1+r_i & 0 & 1+r_i & 0 \end{array} \right] \mathbf{u} \end{aligned} \quad (\text{a})$$



(b) Construction of  $h_1$

**FIGURE 5.10** (cont.)

**EXAMPLE 5.5:** Derive the expressions needed for the evaluation of the stiffness matrix of the isoparametric four-node finite element in Fig. 5.11. Assume plane stress or plane strain conditions.

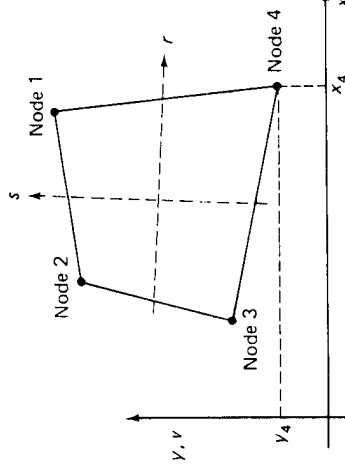


**FIGURE 5.11** Four-node two-dimensional element.

Using the interpolation functions  $h_1$ ,  $h_2$ ,  $h_3$ , and  $h_4$  defined in Fig. 5.5, the coordinate interpolation given in (5.18) is, for this element,

$$\begin{aligned} x &= \frac{1}{4}(1+r)(1+s)h_1 + \frac{1}{4}(1-r)(1+s)h_2 \\ &\quad + \frac{1}{4}(1-r)(1-s)h_3 + \frac{1}{4}(1+r)(1-s)h_4 \\ y &= \frac{1}{4}(1+r)(1+s)v_1 + \frac{1}{4}(1-r)(1+s)v_2 \\ &\quad + \frac{1}{4}(1-r)(1-s)v_3 + \frac{1}{4}(1+r)(1-s)v_4 \end{aligned}$$

and

$$\begin{bmatrix} \frac{\partial v}{\partial x} \\ \frac{\partial v}{\partial y} \end{bmatrix} = \mathbf{J}_I^{-1} \begin{bmatrix} 0 & 1+s_j & 0 & -(1+s_j) & 0 & -1-s_j \\ 0 & 1+r_i & 0 & 1-r_i & 0 & -(1+r_i) \\ 1+r_i & 1+s_j & 1-r_i & -1-r_i & 0 & 0 \end{bmatrix} \mathbf{u} \quad (6)$$

where

$$\hat{\mathbf{u}}^T = [u_1 \ u_2 \ u_3 \ u_4 \ v_1 \ v_2]$$

Evaluating the relations in (a) and (b), we can establish the strain-displacement transformation matrix at the point  $(r_i, s_j)$ ; i.e., we obtain

$$\boldsymbol{\epsilon}_{ij} = \mathbf{B}_{ij} \hat{\mathbf{u}}$$

where the subscripts  $i$  and  $j$  indicate that the strain-displacement transformation is evaluated at the points  $r_i$  and  $s_j$ . For example, if  $x = r$ ,  $y = s$ , i.e., the stiffness matrix of a square element is required that has side lengths equal to 2, the Jacobian operator is the identity matrix, and hence

$$\mathbf{B}_{ij} = \frac{1}{4} \begin{bmatrix} 1+s_j & 0 & -(1+s_j) & 0 & -(1-s_j) & 0 \\ 0 & 1+r_i & 0 & 1-r_i & 0 & -(1+r_i) \\ 1+r_i & 1+s_j & 1-r_i & -1-r_i & -1-s_j & 0 \end{bmatrix}$$

The matrix  $\mathbf{F}_{ij}$  in (5.30) is now simply

$$\mathbf{F}_{ij} = \mathbf{B}_{ij}^T \mathbf{C} \mathbf{B}_{ij} \det \mathbf{J}_{ij}$$

where the material property matrix  $\mathbf{C}$  is given in Table 4.3. In the case of plane stress or plane strain conditions, we integrate in the  $r, s$  plane and assume that the function  $\mathbf{F}$  is constant through the thickness of the element. The stiffness matrix of the element is therefore

$$\mathbf{K} = \sum_{ij} t_{ij} \alpha_{ij} \mathbf{F}_{ij}$$

where  $t_{ij}$  is the thickness of the element at the sampling point  $r_i, s_j$  ( $t_{ij} = 1.0$  in plane strain analysis). With the matrices  $\mathbf{F}_{ij}$  given as above and the weighting factors  $\alpha_{ij}$  being determined, the required stiffness matrix can readily be evaluated.

For the actual implementation it should be noted that in the evaluation of  $\mathbf{J}_{ij}$  and of the matrices defining the displacement derivatives in (a) and (b), only the eight possible derivatives of the interpolation functions  $h_1, \dots, h_4$  are required. Therefore, it is expedient to calculate these derivatives corresponding to the point  $(r_i, s_j)$  once at the start of the evaluation of  $\mathbf{B}_{ij}$  and use them whenever they are required.

It should also be realized that considering the specific point  $(r_i, s_j)$ , the relations in (a) and (b) may be written, respectively, as

$$\begin{aligned} \frac{\partial u}{\partial x} &= \sum_{i=1}^4 \frac{\partial h_i}{\partial x} u_i \\ \frac{\partial u}{\partial y} &= \sum_{i=1}^4 \frac{\partial h_i}{\partial y} u_i \\ \frac{\partial v}{\partial x} &= \sum_{i=1}^4 \frac{\partial h_i}{\partial x} v_i \\ \frac{\partial v}{\partial y} &= \sum_{i=1}^4 \frac{\partial h_i}{\partial y} v_i \end{aligned} \quad (c)$$

and

$$u^S = \frac{1}{2}(1+r)u_1 + \frac{1}{2}(1-r)u_2 \\ v^S = \frac{1}{2}(1+r)v_1 + \frac{1}{2}(1-r)v_2 \quad (d)$$

Hence we have

$$\mathbf{B} = \begin{bmatrix} \frac{\partial h_1}{\partial x} & 0 & \frac{\partial h_2}{\partial x} & 0 & \frac{\partial h_3}{\partial x} & 0 & \frac{\partial h_4}{\partial x} & 0 \\ 0 & \frac{\partial h_1}{\partial y} & 0 & \frac{\partial h_2}{\partial y} & 0 & \frac{\partial h_3}{\partial y} & 0 & \frac{\partial h_4}{\partial y} \\ \frac{\partial h_1}{\partial x} & \frac{\partial h_2}{\partial y} & \frac{\partial h_3}{\partial x} & \frac{\partial h_4}{\partial y} & \frac{\partial h_3}{\partial x} & \frac{\partial h_4}{\partial y} & 0 & 0 \end{bmatrix} \quad (e)$$

where it is implied that in (c) and (d), the derivatives are evaluated at point  $(r_i, s_j)$ , and therefore in (e), we have, in fact, the matrix  $\mathbf{B}_{ij}$ .

**EXAMPLE 5.6:** Derive the expressions needed for the evaluation of the mass matrix of the element considered in Example 5.5.

The mass matrix of the element is given by

$$\mathbf{M} = \sum_{i,j} \alpha_{ij} t_{ij} \mathbf{F}_{ij}$$

$$\mathbf{F}_{ij} = \rho_{ij} \mathbf{H}_{ij}^T \mathbf{H}_{ij} \det \mathbf{J}_{ij}$$

where

$$\mathbf{H}_{ij} = \frac{1}{4} \begin{bmatrix} (1+r_i)(1+s_j) & 0 & 0 & 0 \\ 0 & (1+r_i)(1+s_j) & 0 & 0 \\ (1-r_i)(1-s_j) & 0 & (1+r_i)(1-s_j) & 0 \\ 0 & (1-r_i)(1-s_j) & 0 & (1+r_i)(1-s_j) \end{bmatrix}$$

and  $\mathbf{H}_{ij}$  is the displacement interpolation matrix. The displacement interpolation functions for  $u$  and  $v$  of the four-node element have been given in Example 5.5, and we have

**EXAMPLE 5.7:** Derive the expressions needed for the evaluation of the body force vector  $\mathbf{R}_B$  and the initial stress vector  $\mathbf{R}_I$  of the element considered in Example 5.5.

These vectors are obtained using the matrices  $\mathbf{H}_{ij}$ ,  $\mathbf{B}_{ij}$ , and  $\mathbf{J}_{ij}$  defined in Examples 5.5 and 5.6; i.e., we have

$$\mathbf{R}_B = \sum_{i,j} \alpha_{ij} t_{ij} \mathbf{H}_{ij}^T \mathbf{f}_{ij}^B \det \mathbf{J}_{ij}$$

$$\mathbf{R}_I = \sum_{i,j} \alpha_{ij} t_{ij} \mathbf{B}_{ij}^T \mathbf{t}_{ij}^I \det \mathbf{J}_{ij}$$

where  $\mathbf{f}_{ij}^B$  and  $\mathbf{t}_{ij}^I$  are the body force vector and initial stress vector evaluated at the integration sampling points.

**EXAMPLE 5.8:** Derive the expressions needed in the calculation of the surface force vector  $\mathbf{R}_S$ , when the element edge 1-2 of the four-node isoparametric element considered in Example 5.5 is loaded as shown in Fig. 5.12.

The first step is to establish the displacement interpolations. Since  $s = +1$  at the edge 1-2, we have, using the interpolation functions given in Example 5.5,

$$u^S = \frac{1}{2}(1+r)u_1 + \frac{1}{2}(1-r)u_2 \\ v^S = \frac{1}{2}(1+r)v_1 + \frac{1}{2}(1-r)v_2$$

**EXAMPLE 5.9:** Explain how the expressions given in Examples 5.5 to 5.7 need be modified when the element considered is an axisymmetric element.

In this case two modifications are necessary. Firstly, we consider one radian of the structure. Hence, the thickness to be employed in all integrations is that corresponding to one radian, which means that at an integration point the thickness is equal to the radius at that point:

$$t_{ij} = \sum_{k=1}^4 h_k \Big|_{r_i, s_j} \quad (a)$$

Secondly, it is recognized that also circumferential strains and stresses are developed (see Table 4.2). Hence, the strain-displacement matrix at integration point  $(i, j)$  must be augmented by one row for the hoop strain  $u/R$ , i.e. we have

$$\mathbf{B} = \begin{bmatrix} \cdots & & & & & \\ h_1 & 0 & h_2 & 0 & h_3 & 0 & h_4 & 0 & \frac{1}{r} & 0 & \cdots \\ \cdots & & & & & & & & & & \end{bmatrix} \quad (b)$$

where the first three rows have already been defined in Example 5.5 and  $r$  is equal to the radius. To obtain the strain-displacement matrix at integration point  $(i, j)$  we use (a) to evaluate  $t$  and substitute into (b).

**EXAMPLE 5.10:** Calculate the nodal point forces of the four-node axisymmetric finite element shown in Fig. 5.13 when the element is subjected to centrifugal loading.

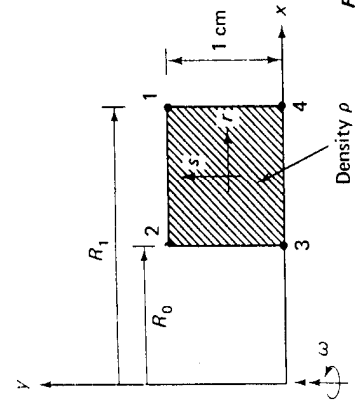


FIGURE 5.12 Pressure distribution along edge 1-2 of a four-node element.

Hence to evaluate  $\mathbf{R}_s$  in (5.34) we can use

$$\mathbf{H}^s = \begin{bmatrix} \frac{1}{2}(1+r) & 0 & \frac{1}{2}(1-r) & 0 & 0 & 0 & 0 \\ 0 & \frac{1}{2}(1+r) & 0 & \frac{1}{2}(1-r) & 0 & 0 & 0 \end{bmatrix}$$

$$\text{and } \mathbf{f}^s = \begin{bmatrix} f_x^s \\ f_y^s \end{bmatrix}$$

where  $f_x^s$  and  $f_y^s$  are the  $x$  and  $y$  components of the applied surface force. These components may have been given as a function of  $r$ .

For the evaluation of the integral in (5.34), we also need the differential surface area  $dS$  expressed in the  $r, s$  natural coordinate system. If  $t_r$  is the thickness,  $dS = t_r dl$ , where  $dl$  is a differential length,

$$dl = \det \mathbf{J}^s dr; \quad \det \mathbf{J}^s = \left\{ \left( \frac{\partial x}{\partial r} \right)^2 + \left( \frac{\partial y}{\partial r} \right)^2 \right\}^{1/2}$$

But the derivatives  $\partial x/\partial r$  and  $\partial y/\partial r$  have been given in Example 5.5. Using  $s = +1$ , we have, in this case,

$$\frac{\partial x}{\partial r} = \frac{x_1 - x_2}{2}, \quad \frac{\partial y}{\partial r} = \frac{y_1 - y_2}{2}$$

Although the vector  $\mathbf{R}_s$  could in this case be evaluated in a closed form solution (provided that the functions used in  $\mathbf{f}^s$  are simple), in order to keep generality in the program that calculates  $\mathbf{R}_s$ , it is expedient to use numerical integration. This way, variable-number-nodes elements can be implemented in an elegant manner in one program. Thus, using the notation defined in this section, we have

$$\mathbf{R}_s = \sum_i \alpha_{it} \mathbf{F}_i$$

$$\mathbf{F}_i = \mathbf{H}_i^{sT} \mathbf{f}_i^s \det \mathbf{J}_i^s$$

It is noted that in this case only one-dimensional numerical integration is required, because  $s$  is not a variable.

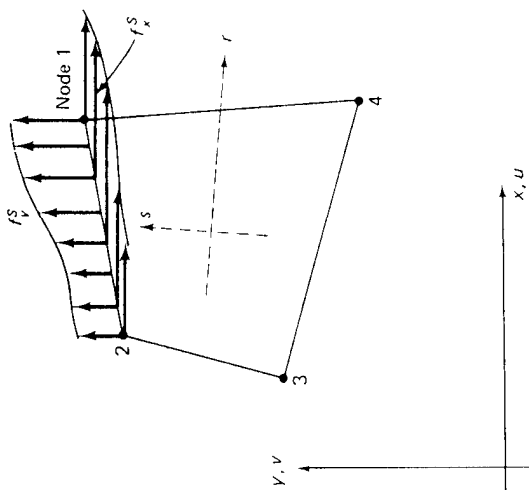


FIGURE 5.13 Four-node axisymmetric element rotating at angular velocity  $\omega$  (rad/sec)

Here we want to evaluate

$$\mathbf{R}_s = \int_V \mathbf{H}^s \mathbf{f}^s dV$$

$$f_x^s = \rho \omega^2 R, \quad f_y^s = 0$$

$$R = \frac{1}{2}(1-r)R_0 + \frac{1}{2}(1+r)R_1$$

$$\mathbf{H} = \begin{bmatrix} h_1 & 0 & h_2 & 0 & h_3 & 0 & h_4 & 0 \\ 0 & h_1 & 0 & h_2 & 0 & h_3 & 0 & h_4 \end{bmatrix}; \quad \mathbf{J} = \begin{bmatrix} \frac{R_1 - R_0}{2} & 0 \\ 0 & \frac{1}{2} \end{bmatrix}$$

and the  $h_i$  are defined in Fig. 5.5. Also, considering one radian

$$dV = \det \mathbf{J} dr ds R = \left( \frac{R_1 - R_0}{4} \right) dr ds \left[ \frac{R_1 + R_0}{2} + \frac{R_1 - R_0}{2} \right]$$

Hence

$$\mathbf{R}_B = \frac{\rho \omega^2 (R_1 - R_0)}{64} \int_{r=s-1}^{r=+1} \int_{s=-1}^{s=+1} \begin{bmatrix} (1+r)(1+s) & 0 \\ 0 & (1+r)(1+s) \\ (1-r)(1+s) & 0 \\ 0 & (1-r)(1+s) \\ (1-r)(1-s) & 0 \\ 0 & (1+r)(1-s) \end{bmatrix} dr ds$$

If we let  $A = R_1 + R_0$  and  $B = R_1 - R_0$ , we have

$$\mathbf{R}_B = \frac{\rho \omega^2 B}{64} \begin{bmatrix} \frac{2}{3}(6A^2 + 4AB + 2B^2) & 0 \\ 0 & \frac{2}{3}(6A^2 - 4AB + 2B^2) \\ \frac{2}{3}(6A^2 - 4AB + 2B^2) & 0 \\ 0 & \frac{2}{3}(6A^2 + 4AB + 2B^2) \\ 0 & 0 \end{bmatrix}$$

**EXAMPLE 5.11:** The four-node plane stress element shown in Fig. 5.14 is subjected to the given temperature distribution. If the nodal point forces corresponding to the stress-free state is  $\theta_0$ , evaluate the nodal point forces to which the element must be subjected in order that there are no nodal point displacements.

In this case we have for the total stresses, due to mechanical strains  $\epsilon$  and thermal strains  $\epsilon^{th}$ ,

$$\tau = C(\epsilon - \epsilon^{th}) \quad (a)$$

where  $\epsilon_{xx}^{th} = \alpha(\theta - \theta_0)$ ,  $\epsilon_{yy}^{th} = \alpha(\theta - \theta_0)$ ,  $\gamma_{xy}^{th} = 0$ . If the nodal point displacements are zero, we have  $\epsilon = 0$ , and the stresses due to the thermal strains can be thought of as initial stresses. Thus, the nodal point forces are

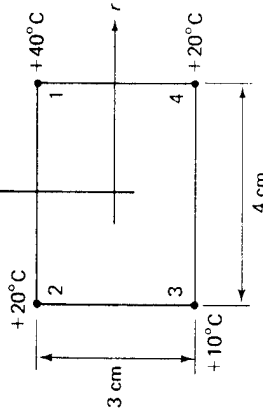
$$\mathbf{R}_I = \int_V \mathbf{B}^T \tau' dV$$

$$\tau' = -\frac{E\alpha}{1-\nu^2} \begin{bmatrix} 1 & \nu & 0 & 0 \\ \nu & 1 & 0 & 0 \\ 0 & 0 & 1-\nu & 0 \\ 0 & 0 & 0 & 2 \end{bmatrix} \left[ \left( \sum_{i=1}^4 h_i \theta_i \right) - \theta_0 \right]$$

and the  $h_i$  are the interpolation functions defined in Fig. 5.5. Also,

$$\mathbf{J} = \begin{bmatrix} 2 & 0 \\ 0 & 1.5 \end{bmatrix}; \quad \mathbf{J}^{-1} = \begin{bmatrix} \frac{1}{2} & 0 \\ 0 & \frac{2}{3} \end{bmatrix}; \quad \det \mathbf{J} = 3$$

Element thickness = 1 cm  
Young's modulus,  $E$   
Roisson's ratio,  $\nu$   
Thermal coefficient of expansion,  $\alpha$



$$[(R_1 + R_0) + (R_1 - R_0)r^2 \begin{bmatrix} 1 \\ 0 \end{bmatrix}] dr ds$$

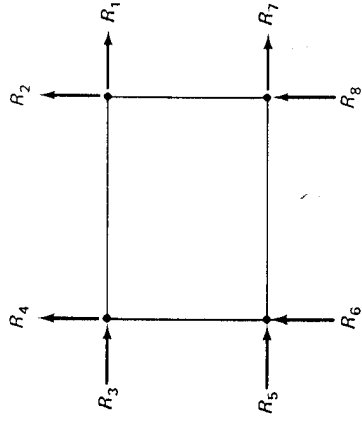


FIGURE 5.14 Nodal point forces due to initial temperature distribution.

$$\mathbf{B} = \begin{bmatrix} \frac{(1+s)}{8} & 0 & 0 & -\frac{(1+s)}{8} & 0 \\ 0 & \frac{(1+r)}{6} & 0 & 0 & \frac{(1-r)}{6} \\ \frac{(1+r)}{6} & \frac{(1+s)}{8} & \frac{(1-r)}{6} & -\frac{(1+s)}{8} & 0 \\ 0 & -\frac{(1-r)}{6} & 0 & 0 & -\frac{(1+r)}{6} \\ -\frac{(1-r)}{6} & -\frac{(1-s)}{8} & -\frac{(1+r)}{6} & \frac{(1-s)}{8} & 0 \end{bmatrix}$$

Hence

$$\mathbf{R}_I = \int_{-1}^{+1} \int_{-1}^{+1} \left[ \begin{array}{ccc} \frac{(1+s)}{8} & 0 & \frac{(1+r)}{6} \\ 0 & \frac{(1+r)}{6} & \frac{(1+s)}{8} \\ -\frac{(1+s)}{8} & 0 & \frac{(1-r)}{6} \end{array} \right] \left[ \begin{array}{c} E\alpha \\ (1+v) \\ 0 \end{array} \right] ds dr$$

$$\mathbf{R}_I = -\frac{E\alpha}{(1-v)} \left[ \begin{array}{ccc} 37.5 - 1.5\theta_0 & 0 & 0 \\ 50 & -2\theta_0 & 0 \\ -37.5 + 1.5\theta_0 & 0 & 0 \end{array} \right]$$

$$+ \left[ \begin{array}{ccc} 40 & -2\theta_0 & 0 \\ -30 & +1.5\theta_0 & 0 \\ -40 & +2\theta_0 & 0 \end{array} \right]$$

$$+ \left[ \begin{array}{ccc} +30 & -1.5\theta_0 & 0 \\ -50 & +2\theta_0 & 0 \end{array} \right]$$

$$[2.5(s+3)(r+3) - \theta_0]3 dr ds$$

It should be noted that the calculation of the initial stress force vector as performed above is one typical step in a thermal stress analysis. In a complete thermal stress analysis the temperatures are calculated as described in Section 7.2, the element load vectors due to the thermal effects are evaluated as illustrated in this example, and the solution of the equilibrium equations of the complete element assembly then yields the nodal point displacements. The element mechanical strains  $\boldsymbol{\epsilon}$  are evaluated from the nodal point displacements and then using (a) the final element stresses are calculated.

**EXAMPLE 5.12:** Consider the elements in Fig. 5.15. Evaluate the consistent nodal point forces corresponding to the surface loading (assuming that the nodal point forces are positive when acting into the direction of the pressure).

Here we want to evaluate

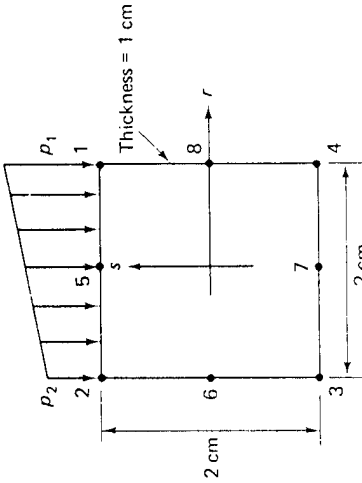
$$\mathbf{R}_S = \int_S \mathbf{H}^S \mathbf{f}^S dS$$

Consider first the two-dimensional interpolations. Since  $s = +1$  at the edge 1-2, we have, using the interpolation functions for the eight-node element (see Fig. 5.5),

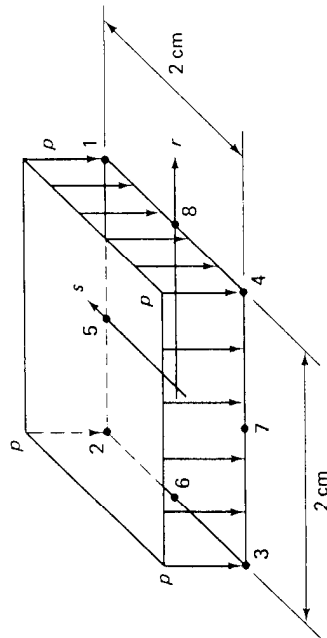
$$h_3 = \frac{1}{4}(1-r^2)(1+s)|_{s=+1} = (1-r^2)$$

$$h_1 = \frac{1}{4}(1+r)(1+s)(r+s-1)|_{s=+1} = \frac{1}{2}r(1+r)$$

$$h_2 = \frac{1}{4}(1-r)(1+s)(s-r-1)|_{s=+1} = -\frac{1}{2}r(1-r)$$



(a) Two-dimensional element subjected to linearly varying pressure along one side



(b) Flat surface of three dimensional element subjected to constant pressure  $p$

FIGURE 5.15 Two- and three-dimensional elements subjected to pressure loading.

which are equal to the interpolation functions of the 3-node bar in Fig. 5.3. Hence

$$\begin{bmatrix} u^S \\ v^S \end{bmatrix} = \begin{bmatrix} \frac{1}{2}r(1+r) & 0 & -\frac{1}{2}r(1-r) & 0 & 0 \\ 0 & \frac{1}{2}r(1+r) & 0 & -\frac{1}{2}r(1-r) & 0 & (1-r^2) \end{bmatrix} \begin{bmatrix} u_1 \\ v_1 \\ u_2 \\ v_2 \\ u_3 \\ v_3 \end{bmatrix}$$

$$\text{Also } \mathbf{f}^S = \begin{bmatrix} f_r^S \\ f_s^S \end{bmatrix} = \begin{bmatrix} 0 & 0 \\ \frac{1}{2}(1+r)p_1 + \frac{1}{2}(1-r)p_2 \end{bmatrix}; \quad \det \mathbf{J}^S = 1$$

Hence

$$\mathbf{R}_S = \int_{-1}^{+1} \frac{t}{2} \begin{bmatrix} 0 & r(1+r) & 0 \\ -r(1-r) & 0 & -r(1-r) \\ 0 & 0 & 2(1-r^2) \end{bmatrix} \begin{bmatrix} 1 \\ (1+r)p_1 + (1-r)p_2 \\ 0 \end{bmatrix} dr$$

$$\mathbf{R}_S = \frac{1}{3} \begin{bmatrix} 0 \\ p_1 \\ p_2 \\ 0 \end{bmatrix} - \frac{1}{2} \begin{bmatrix} 0 \\ 2(p_1 + p_2) \\ 0 \\ 0 \end{bmatrix}$$

For the three-dimensional element we proceed similarly. Since the surface is flat and the loading is normal to it, only the nodal point forces normal to the surface are nonzero (see also (a) above). Also, by symmetry, we know that the forces at nodes 1, 2, 3, 4 and 5, 6, 7, 8 are equal, respectively. Using the interpolation functions of Fig. 5.5, we have for the force at node 1:

$$R_1 = p \int_{-1}^{+1} \int_{-1}^{+1} \frac{1}{4}(1+r)(1+s)(r+s-1) dr ds = -\frac{1}{3}p$$

and for the force at node 5,

$$R_5 = p \int_{-1}^{+1} \int_{-1}^{+1} \frac{1}{4}(1-r^2)(1+s) dr ds = \frac{4}{3}p$$

The total pressure loading on the surface is  $4p$ , which, as a check, is equal to the sum of all the nodal point forces. However, it should be noted that the consistent nodal point forces at the corners of the element act into the opposite direction of the pressure!

**EXAMPLE 5.13:** Calculate the deflection  $u_A$  of the structural model shown in Fig. 5.16.

Because of the symmetry and boundary conditions we only need to evaluate the stiffness coefficient corresponding to  $u_A$ . Here we have for the four-node element

$$\mathbf{J} = \begin{bmatrix} 4 & 0 \\ 0 & 3 \end{bmatrix}, \quad \mathbf{B} = \frac{1}{48} \begin{bmatrix} 3(1-s) & \cdots & 0 \\ \cdots & 0 & -4(1+r) \\ -4(1+r) & \cdots & 3(1-s) \\ 3(1-s) & 3y(1-s) & -2(1-v)(1+r) \\ 3y(1-s) & -2(1-v)(1+r) & ((12)(0.1)) dr ds \end{bmatrix}$$

or

$$k_{77} = 1,336,996.34 \text{ N/cm}$$

Also, the stiffness of the truss is  $AE/L$ , or

$$k = \frac{(1)(30,000)}{8} = 3,750,000 \text{ N/cm}$$

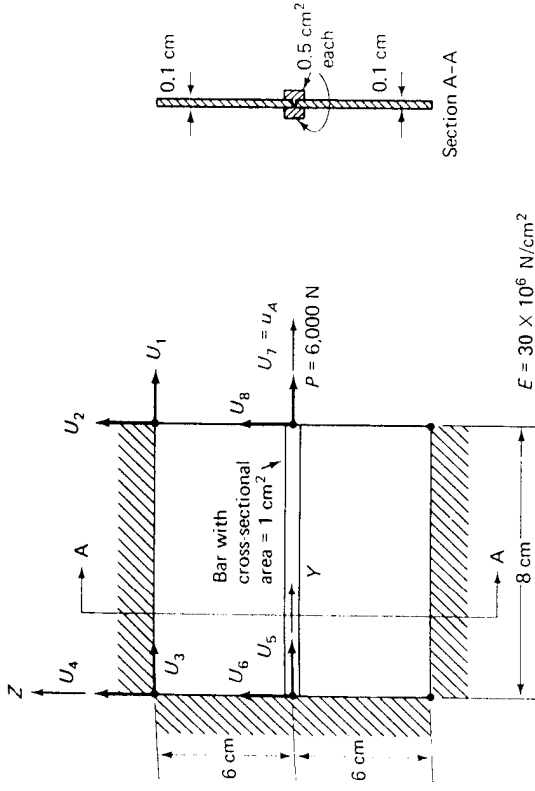


FIGURE 5.16 A simple structural model.

$$k_{\text{total}} = 6.424 \times 10^6 \text{ N/cm}$$

$$u_A = 9.34 \times 10^{-4} \text{ cm}$$

Hence

and

**EXAMPLE 5.14:** Consider the five-node element in Fig. 5.17. Evaluate the consistent nodal point forces corresponding to the stresses given. Using the interpolation functions of Fig. 5.5, we can evaluate the strain-displacement matrix of the element:

$$\mathbf{B} = \frac{1}{8} \begin{bmatrix} (1+s) & 0 & -s(1+s) & 0 \\ 0 & 2(1+r) & 0 & 2(1-r)(1+2s) \\ 2(1+r) & (1+s) & 2(1-r)(1+2s) & -s(1+s) \\ s(1-s) & 0 & 0 & (1-s) \\ 0 & -2(1-r)(1-2s) & -2(1+r) & -2(1+r) \\ -2(1-r)(1-2s) & s(1-s) & s(1-s) & -2(1+r) \\ 0 & -2(1-s^2) & 0 & -2(1-r)s \\ -2(1+r) & 0 & -8(1-r)s & -2(1-s^2) \end{bmatrix}$$

where we used that

$$\mathbf{J} = \begin{bmatrix} 2 & 0 \\ 0 & 1 \end{bmatrix}$$

The required nodal point forces can now be evaluated using (5.35); hence

$$\mathbf{R}_I = \int_{-1}^{+1} \int_{-1}^{+1} \mathbf{B}^T \begin{bmatrix} 0 \\ 10 \\ 20 \end{bmatrix} dr ds$$

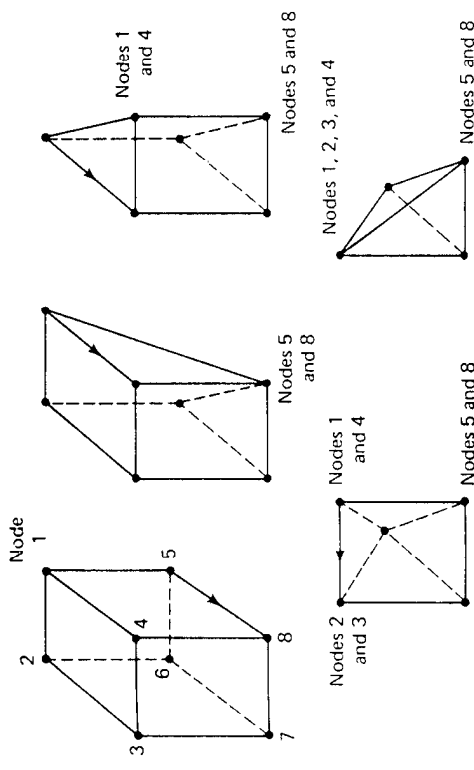


FIGURE 5.17 Five-node element with stresses given.

which gives

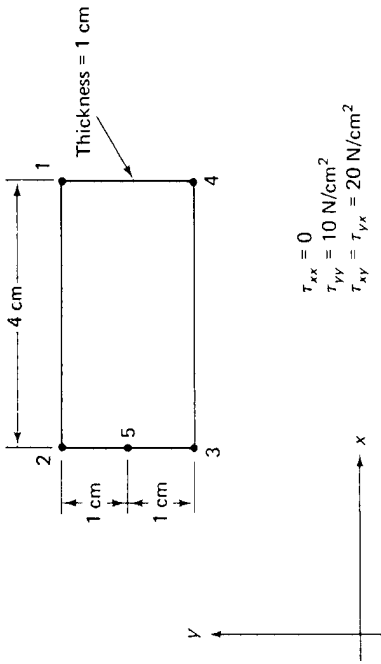
$$\mathbf{R}_I^T = [40 \quad 40 \quad 40 \quad -40 \quad -\frac{80}{3} \quad -40 \quad 0 \quad 0 \quad -\frac{80}{3}]$$

It should be noted that the forces in this vector are also equal to the nodal point consistent forces that correspond to the (constant) surface stresses, which are in equilibrium with the internal stresses given in Fig. 5.17.

### 5.3.2 Triangular Elements

In the previous section we discussed rectangular isoparametric elements which can be used to model very general geometries. However, in some cases the use of triangular or wedge elements may be attractive.

Since the elements discussed in Section 5.3.1 can be distorted, as shown for example in Fig. 5.2, a natural way of generating triangular elements appears to be to simply distort the basic rectangular element into the required triangular form, see Fig. 5.18. This is achieved in practice by assigning the same global node to two corner nodes of the element. We demonstrate this procedure in the following example.



(a) Degeneration of four-node to three-node two-dimensional element

FIGURE 5.18 Degenerate forms of four- and eight-node elements of Figs. 5.5 and 5.6.

(b) Degenerate forms of eight-node three-dimensional element

**EXAMPLE 5.15:** Show that by collapsing the side 1-2 of the four-node quadrilateral element in Fig. 5.19 a constant strain triangle is obtained. Using the interpolation functions of Fig. 5.5, we have

$$\begin{aligned} x &= \frac{1}{4}(1+r)(1+s)x_1 + \frac{1}{4}(1-r)(1+s)x_2 + \frac{1}{4}(1-r)(1-s)x_3 \\ &\quad + \frac{1}{4}(1+r)(1-s)x_4 \\ y &= \frac{1}{4}(1+r)(1+s)y_1 + \frac{1}{4}(1-r)(1+s)y_2 + \frac{1}{4}(1-r)(1-s)y_3 \\ &\quad + \frac{1}{4}(1+r)(1-s)y_4 \end{aligned}$$

Thus, using the conditions  $x_1 = x_2$  and  $y_1 = y_2$  we obtain

$$\begin{aligned} x &= \frac{1}{2}(1+s)x_2 + \frac{1}{4}(1-r)(1-s)x_3 + \frac{1}{4}(1+r)(1-s)x_4 \\ y &= \frac{1}{2}(1+s)y_2 + \frac{1}{4}(1-r)(1-s)y_3 + \frac{1}{4}(1+r)(1-s)y_4 \end{aligned}$$

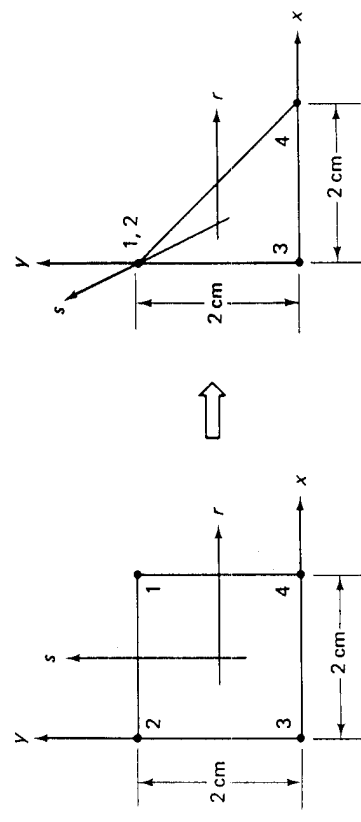


FIGURE 5.19 Collapsing a four-node element to a triangular element.

and hence with the nodal coordinates given in Fig. 5.19

$$\begin{aligned} x &= \frac{1}{2}(1+r)(1-s) \\ y &= (1+s) \end{aligned}$$

It follows that

$$\begin{aligned} \frac{\partial x}{\partial r} &= \frac{1}{2}(1-s) & \frac{\partial y}{\partial r} &= 0 \\ \frac{\partial x}{\partial s} &= -\frac{1}{2}(1+r) & \frac{\partial y}{\partial s} &= 1 \end{aligned}$$

Using the isoparametric assumption, we also have

$$\begin{aligned} u &= \frac{1}{2}(1+s)u_2 + \frac{1}{4}(1-r)(1-s)u_3 + \frac{1}{4}(1+r)(1-s)u_4 \\ v &= \frac{1}{2}(1+s)v_2 + \frac{1}{4}(1-r)(1-s)v_3 + \frac{1}{4}(1+r)(1-s)v_4 \\ \partial u / \partial r &= -\frac{1}{4}(1-s)u_3 + \frac{1}{4}(1-s)u_4; \quad \partial v / \partial r = -\frac{1}{4}(1-s)v_3 + \frac{1}{4}(1-s)v_4 \\ \partial u / \partial s &= \frac{1}{2}u_2 - \frac{1}{4}(1-r)u_3 - \frac{1}{4}(1+r)u_4; \quad \partial v / \partial s = \frac{1}{2}v_2 - \frac{1}{4}(1-r)v_3 - \frac{1}{4}(1+r)v_4 \end{aligned}$$

$$\begin{bmatrix} \frac{\partial}{\partial x} \\ \frac{\partial}{\partial y} \end{bmatrix} = J^{-1} \begin{bmatrix} \frac{\partial}{\partial r} \\ \frac{\partial}{\partial s} \end{bmatrix}$$

Hence

$$\begin{bmatrix} \frac{\partial u}{\partial x} \\ \frac{\partial u}{\partial y} \end{bmatrix} = \begin{bmatrix} \frac{2}{1-s} & 0 \\ \frac{1+r}{1-s} & 1 \end{bmatrix} \begin{bmatrix} 0 & 0 & -\frac{1}{4}(1-s) & 0 & \frac{1}{4}(1-s) & 0 \\ \frac{1}{2} & 0 & -\frac{1}{4}(1-r) & 0 & -\frac{1}{4}(1+r) & 0 \end{bmatrix} \begin{bmatrix} u_2 \\ v_2 \\ u_3 \\ v_3 \\ u_4 \\ v_4 \end{bmatrix}$$

$$\text{and} \quad \begin{bmatrix} \frac{\partial v}{\partial x} \\ \frac{\partial v}{\partial y} \end{bmatrix} = \begin{bmatrix} 0 & 0 & -\frac{1}{2} & 0 & \frac{1}{2} & 0 \\ \frac{1}{2} & 0 & -\frac{1}{2} & 0 & 0 & 0 \end{bmatrix} \begin{bmatrix} u_2 \\ v_2 \\ u_3 \\ v_3 \\ u_4 \\ v_4 \end{bmatrix}$$

Similarly

$$\begin{bmatrix} \frac{\partial v}{\partial x} \\ \frac{\partial v}{\partial y} \end{bmatrix} = \begin{bmatrix} 0 & 0 & 0 & -\frac{1}{2} & 0 & \frac{1}{2} \\ 0 & \frac{1}{2} & 0 & -\frac{1}{2} & 0 & 0 \end{bmatrix} \begin{bmatrix} u_2 \\ v_2 \\ u_3 \\ v_3 \\ u_4 \\ v_4 \end{bmatrix}$$

$$\text{So we obtain} \quad \epsilon = \begin{bmatrix} 0 & 0 & -\frac{1}{2} & 0 & \frac{1}{2} & 0 \\ 0 & \frac{1}{2} & 0 & -\frac{1}{2} & 0 & 0 \\ \frac{1}{2} & 0 & -\frac{1}{2} & -\frac{1}{2} & 0 & \frac{1}{2} \end{bmatrix} \begin{bmatrix} u_2 \\ v_2 \\ u_3 \\ v_3 \\ u_4 \\ v_4 \end{bmatrix}$$

For any values of  $u_2, v_2, u_3, v_3$ , and  $u_4, v_4$  the strain vector is constant and independent of  $r, s$ . Thus, the triangular element is a constant strain triangle.

In the above example we considered only one specific case. However, using the same approach it can be shown that collapsing any one side of a four-node element will always result in a constant strain triangle.

Considering the process of collapsing an element side, it is interesting to note that in the formulation used in Example 5.15 the matrix  $J$  is singular at  $s = +1$ , but this singularity disappears when the strain-displacement matrix is calculated. A practical consequence is that if in a computer program the general formulation of the four-node element is employed to generate a constant strain triangle (as done in Example 5.15), the stresses should not be calculated at the two local nodes that have been assigned the same global node. (Since the stresses are constant throughout the element, they are conveniently evaluated at the center of the element, i.e. at  $r = 0, s = 0$ .)

The same procedure can also be employed in three-dimensional analysis in order to obtain, from the basic eight-node element, wedge or tetrahedral elements. The procedure is illustrated in Fig. 5.18 and in the following example.

**EXAMPLE 5.16:** Show that the three-dimensional tetrahedral element generated in Fig. 5.20 from the eight-node three-dimensional brick element is a constant strain element.

Here we proceed as in Example 5.15. Thus, using the interpolation functions of the brick element (see Fig. 5.6) and substituting the nodal point coordinates of the tetrahedron, we obtain

$$\begin{aligned} x &= \frac{1}{4}(1+r)(1-s)(1-t) \\ y &= \frac{1}{4}(1+s)(1-t) \\ z &= \frac{1}{4}(1+t) \end{aligned}$$

$$J = \begin{bmatrix} \frac{1}{4}(1-s)(1-t) & 0 & 0 \\ -\frac{1}{4}(1+r)(1-t) & \frac{1}{2}(1-t) & 0 \\ -\frac{1}{4}(1+r)(1-s) & -\frac{1}{2}(1+s) & 1 \end{bmatrix}$$

Hence

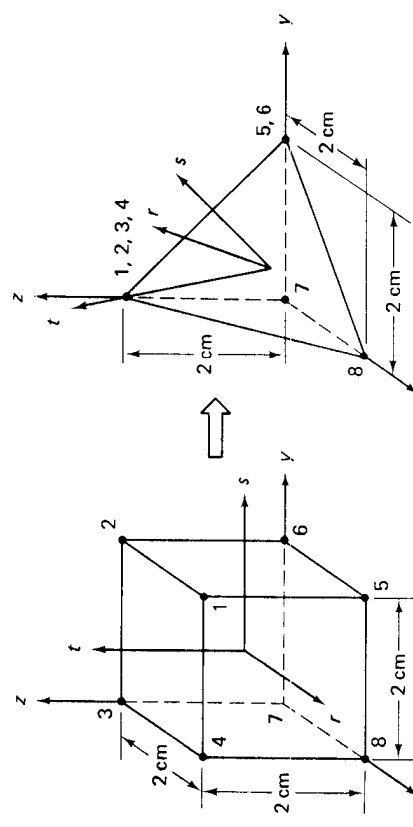


FIGURE 5.20 Collapsing an eight-node brick element into a tetrahedral element.

$$\mathbf{J}^{-1} = \begin{bmatrix} \frac{4}{(1-s)(1-t)} & 0 & 0 \\ \frac{2(1+r)}{(1-s)(1-t)} & \frac{2}{(1-t)} & 0 \\ \frac{2(1+r)}{(1-s)(1-t)} & \frac{(1+s)}{(1-t)} & 1 \end{bmatrix} \quad (a)$$

Using the same interpolation functions for  $u$ , and the conditions that  $u_1 = u_2 = u_3 = u_4$  and  $u_5 = u_6$ , we obtain

$$u = h_4^* u_4 + h_5^* u_5 + h_7^* u_7 + h_8^* u_8$$

with

$$\begin{aligned} h_4^* &= \frac{1}{2}(1+t); & h_5^* &= \frac{1}{4}(1+s)(1-t); \\ h_7^* &= \frac{1}{8}(1-r)(1-t); & h_8^* &= \frac{1}{8}(1+r)(1-s) \end{aligned}$$

Similarly, we also have

$$\begin{aligned} v &= h_4^* v_4 + h_5^* v_5 + h_7^* v_7 + h_8^* v_8 \\ w &= h_4^* w_4 + h_5^* w_5 + h_7^* w_7 + h_8^* w_8 \end{aligned}$$

Evaluating now the derivatives of the displacements  $u$ ,  $v$ , and  $w$  with respect to  $r$ ,  $s$ , and  $t$ , and using  $\mathbf{J}^{-1}$  of (a), we obtain

$$\begin{aligned} \begin{bmatrix} \frac{\partial u}{\partial x} \\ \frac{\partial v}{\partial y} \\ \frac{\partial w}{\partial z} \end{bmatrix} &= \begin{bmatrix} 0 & 0 & 0 & 0 & -\frac{1}{2} & 0 & 0 & \frac{1}{2} & 0 \\ 0 & 0 & 0 & \frac{1}{2} & 0 & 0 & -\frac{1}{2} & 0 & 0 \\ 0 & 0 & \frac{1}{2} & 0 & 0 & 0 & 0 & -\frac{1}{2} & 0 \\ 0 & 0 & 0 & 0 & 0 & 0 & 0 & 0 & 0 \end{bmatrix} \begin{bmatrix} u_4 \\ v_4 \\ w_4 \\ \vdots \\ u_5 \\ v_5 \\ w_5 \\ \vdots \\ u_7 \\ v_7 \\ w_7 \\ \vdots \\ u_8 \\ v_8 \\ w_8 \end{bmatrix} \\ \frac{\partial u}{\partial y} + \frac{\partial v}{\partial x} &= \frac{1}{2}(1+s) - \frac{1}{2}(1-t) \\ \frac{\partial v}{\partial z} + \frac{\partial w}{\partial y} &= \frac{1}{2}(1-r) - \frac{1}{2}(1-s) \\ \frac{\partial u}{\partial z} + \frac{\partial w}{\partial x} &= \frac{1}{2}(1+r) - \frac{1}{2}(1-t) \end{aligned}$$

Hence, the strains are constant for any nodal point displacements, which means that the element can only represent constant strain conditions.

The process of collapsing an element side, or in three-dimensional analysis a number of element sides, may directly yield a desired element, but when higher-order two- or three-dimensional elements are employed some special considerations may be necessary regarding the interpolation functions used. Specifically, when the lower-order elements displayed in Fig. 5.18 are employed, spatially isotropic triangular and wedge elements are automatically generated, but this is not necessarily the case when using higher-order elements, i.e. rectangular and brick elements with more than four and eight nodes in two- and three-dimensional analyses, respectively. In other words, for two-dimensional analysis, although the higher-order element is spatially isotropic (geometrically invariant) in the  $2 \times 2$  square natural coordinate system, the generated triangular element is in general not spatially isotropic.

As an example, we consider the six-node triangular two-dimensional element obtained by collapsing one side of an eight-node element as shown in Fig. 5.21. If the triangular element has sides of equal length, we may want the element to

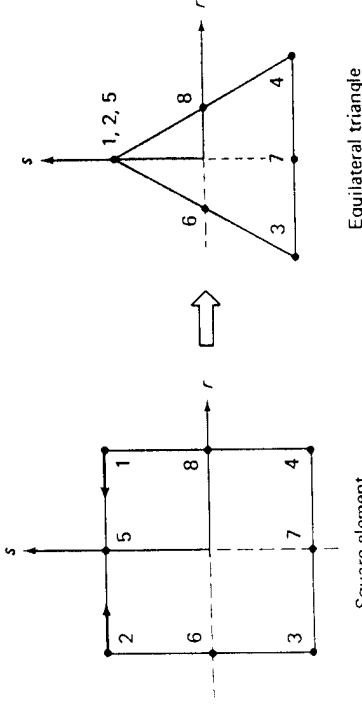


FIGURE 5.21 Collapsing an eight-node element into a triangle.

be spatially isotropic (see Section 4.2.5), i.e., we wish the internal element displacements  $u$  and  $v$  to vary in the same manner for each corner nodal displacement and each midside nodal displacement, respectively. However, the interpolation functions that are generated for the triangle when the side 1-2-5 of the square is simply collapsed do not fulfill the requirement that we should be able to change the numbering of the vertices without a change in the displacement assumptions. In order to fulfill this requirement corrections need be applied to the interpolation functions of the nodes 3, 4, and 7 to obtain the final interpolations,  $h_i^*$ , of the triangular element:

$$\begin{aligned} h_1^* &= \frac{1}{2}(1+s) - \frac{1}{2}(1-t^2) \\ h_3^* &= \frac{1}{4}(1-r)(1-s) - \frac{1}{4}(1-s^2)(1-r) - \frac{1}{4}(1-r^2)(1-s) + \Delta h \\ h_4^* &= \frac{1}{4}(1+r)(1-s) - \frac{1}{4}(1-r^2)(1-s) - \frac{1}{4}(1-s^2)(1+r) + \Delta h \\ h_6^* &= \frac{1}{2}(1-s^2)(1-r) \\ h_7^* &= \frac{1}{2}(1-r^2)(1-s) - 2\Delta h \\ h_8^* &= \frac{1}{2}(1-s^2)(1+r) \end{aligned} \quad (5.36)$$

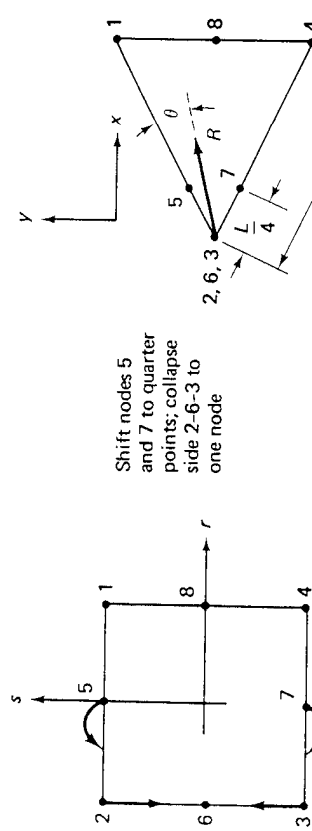
where we added the appropriate interpolations given in Fig. 5.5 and

$$\Delta h = \frac{(1-r^2)(1-s^2)}{8} \quad (5.37)$$

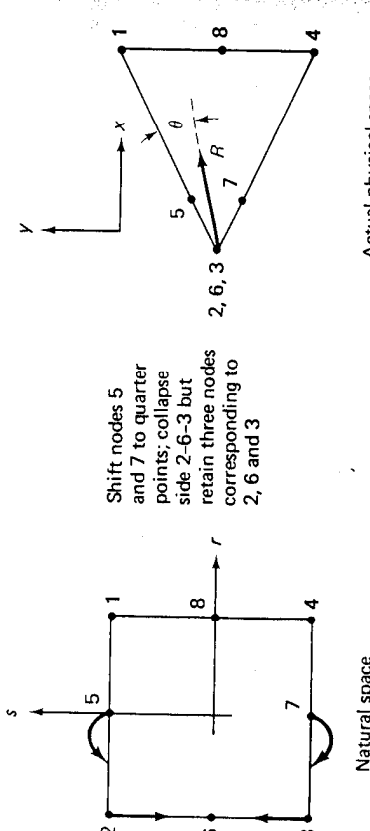
Thus, to generate higher-order triangular elements by collapsing sides of square elements it may be necessary to apply a correction to the interpolation functions used.<sup>15</sup>

In the above considerations, we assumed that a spatially isotropic element is desirable, because the element is to be employed in a finite element assemblage that is used to predict a somewhat homogeneous stress field. However, in some cases, very specific stress variations are to be predicted and in such analyses a spatially non-isotropic element may be more effective. One area of analysis in which specific spatially non-isotropic elements are employed is the field of fracture mechanics. Here it is known that specific stress singularities exist at crack tips, and for the calculation of stress concentration factors or limit loads the use of finite elements that contain the required stress singularities can be effective. Various elements of this sort have been designed, but very simple and attractive elements can be obtained by distorting the higher-order isoparametric ele-

ments.<sup>16-19</sup> Figure 5.22 shows two-dimensional isoparametric elements that have been employed with much success in linear and nonlinear fracture mechanics, because they contain the  $1/\sqrt{R}$  and  $1/R$  stress singularities, respectively. We should note that these elements have the interpolation functions given in (5.36) but with  $\Delta h = 0$ . The same node shifting and side collapsing procedures can also be employed with higher-order three-dimensional elements in order to generate the required three-dimensional stress singularities.<sup>17,19</sup> We demonstrate the procedure of node-shifting to generate a stress singularity in the following example.



(a) Quarter-point triangular element with  $\frac{1}{\sqrt{R}}$  stress singularity at node (2-6-3)



(b) Quarter-point triangular element with  $\frac{1}{R}$  stress singularity at nodes 2, 6, and 3.

**FIGURE 5.22** Two-dimensional distorted (quarter point) isoparametric elements useful in fracture mechanics. Stress singularities are within the element for any angle  $\theta$ . (Note that in (a) the one node (2-6-3) has two degrees of freedom, and that in (b) nodes 2, 3 and 6 each have two degrees of freedom. In case (b) the shifting of nodes 5 and 7 to the quarter points is frequently not performed in practice.)

**EXAMPLE 5.17:** Consider the three-node truss element in Fig. 5.23. Show that when node 3 is specified to be at the quarter point, the stress has a singularity of  $1/\sqrt{x}$  at node 1.

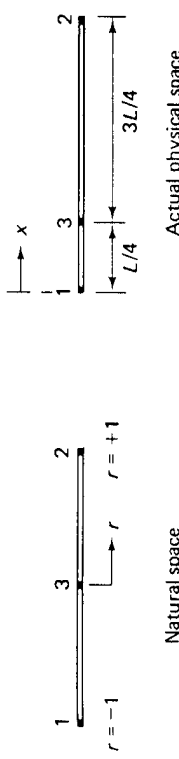


**FIGURE 5.23** Quarter-point one-dimensional element.

We considered a three-node truss already in Example 5.2. Proceeding as before we now have

$$\begin{aligned} x &= \frac{r}{2}(1+r)L + (1-r^2)\frac{L}{4} \\ \text{or} \\ x &= \frac{L}{4}(1+r)^2 \end{aligned} \quad (\text{a})$$

Hence

$$\mathbf{J} = \left[ \frac{L}{2} + \frac{r}{2}L \right]$$

and the strain-displacement matrix is (using (b) of Example 5.2)

$$\mathbf{B} = \left( \frac{1}{L/2 + rL/2} \right) \left[ \left( -\frac{1}{2} + r \right) \left( \frac{1}{2} + r \right) - 2r \right] \quad (\text{b})$$

To show the  $1/\sqrt{x}$  singularity we need to express  $r$  in terms of  $x$ . Using (a) we have

$$r = 2\sqrt{\frac{x}{L}} - 1$$

Substituting this value for  $r$  into (b) we obtain

$$\mathbf{B} = \left[ \left( \frac{2}{L} - \frac{3}{2\sqrt{L}\sqrt{x}} \right) \left( \frac{2}{L} - \frac{1}{2\sqrt{L}\sqrt{x}} \right) \left( \frac{2}{\sqrt{L}\sqrt{x}} - \frac{4}{L} \right) \right]$$

Hence at  $x = 0$  the quarter-point element in Fig. 5.23 has a stress singularity of order  $1/\sqrt{x}$ .

Although the procedure of distorting a rectangular isoparametric element to generate a triangular element can be effective in some cases as discussed above, triangular elements (and in particular spatially isotropic elements) can be constructed directly by using area coordinates. Considering the triangle in Fig. 5.24, the position of a typical interior point  $P$  with coordinates  $x$  and  $y$  is defined by the area coordinates

$$L_1 = \frac{A_1}{A}; \quad L_2 = \frac{A_2}{A}; \quad L_3 = \frac{A_3}{A} \quad (5.38)$$

where the areas  $A_i$ ,  $i = 1, 2, 3$  are defined in the figure and  $A$  is the total area of the triangle. Thus, we also have

$$L_1 + L_2 + L_3 = 1 \quad (5.39)$$

Since element strains are obtained by taking derivatives with respect to the Cartesian coordinates, we need a relation that gives the triangular coordinates in terms of the coordinates  $x$  and  $y$ . Here, we have

$$u = \sum_{i=1}^3 h_i u_i \quad x = \sum_{i=1}^3 h_i x_i \\ v = \sum_{i=1}^3 h_i v_i \quad y = \sum_{i=1}^3 h_i y_i \quad (5.44)$$

where  $h_i = L_i$ ,  $i = 1, 2, 3$ , and the  $h_i$  are functions of the coordinates  $x$  and  $y$ .

Using the relations in (5.44), the various finite element matrices of (5.27) to (5.35) can directly be evaluated. However, just as in the formulation of the rectangular elements (see Section 5.3.1), in practice, it is frequently expedient to use a natural coordinate space in order to describe the element coordinates and displacements. Using the natural coordinate system shown in Fig. 5.24, we have

$$h_1 = 1 - r - s; \quad h_2 = r; \quad h_3 = s \quad (5.45)$$

and the evaluation of the element matrices involves now a Jacobian transformation. Furthermore, all integrations are carried out over the natural coordinates; i.e., the  $r$ -integrations go from 0 to 1 and the  $s$ -integrations go from 0 to  $(1 - r)$ .

**EXAMPLE 5.18:** Using the isoparametric natural coordinate system of Fig. 5.24, establish the displacement and strain-displacement interpolation matrices of a three-node triangular element with

$$x_1 = 0 \quad x_2 = 4 \quad x_3 = 1 \\ y_1 = 0 \quad y_2 = 0 \quad y_3 = 3$$

In this case we have using (5.44)

$$x = 4r + s \\ y = 3s$$

Hence using (5.23)

$$\frac{\partial}{\partial x} = \frac{1}{12} \begin{bmatrix} 3 & 0 \\ -1 & 4 \end{bmatrix} \frac{\partial}{\partial r}$$

$$\mathbf{H} = \begin{bmatrix} 1 - r - s & 0 & r & 0 & s & 0 \\ 0 & (1 - r - s) & 0 & r & 0 & s \end{bmatrix}$$

$$(5.40) \quad (5.41)$$

$$\mathbf{B} = \frac{1}{12} \begin{bmatrix} -3 & 0 & 3 & 0 & 0 & 0 \\ 0 & -3 & 0 & -1 & 0 & 4 \\ -3 & -3 & -1 & 3 & 4 & 0 \end{bmatrix}$$

By analogy to the formulation of higher-order rectangular elements, we can also directly formulate higher-order triangular elements. Namely, using the natural coordinate system of Fig. 5.24 which reduces to

$$L_1 = 1 - r - s \quad L_2 = r \quad L_3 = s \quad (5.46)$$

where the  $L_i$  are the area coordinates of the “unit triangle,” the interpolation functions of a 3 to 6 variable-number-nodes element are given in Fig. 5.25. These functions are constructed in the usual way; namely,  $h_i$  must be unity at node  $i$  and zero at all other nodes (see Example 5.1). The interpolation functions of still higher-order triangular elements are obtained in a similar manner.\*

\* It is interesting to note that the functions of the 6-node triangle in Fig. 5.25 are exactly those given in (5.36), provided the variables  $r$  and  $s$  in Fig. 5.25 are replaced by  $\frac{1}{4}(1 - r)$  and  $\frac{1}{4}(1 - r)(1 + s)$ , respectively, in order to account for the different natural coordinate systems. Hence, the correction  $\Delta h$  in (5.36) can be evaluated from the functions in Fig. 5.25.

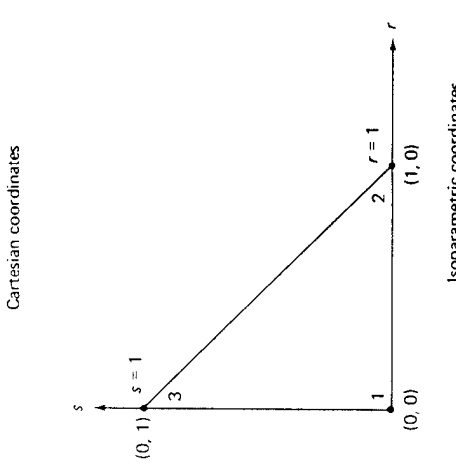
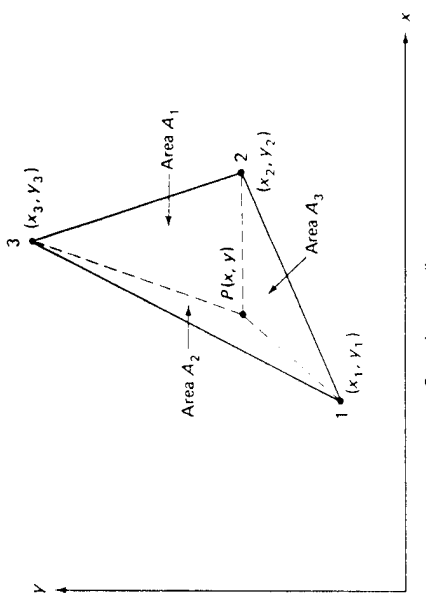


FIGURE 5.24 Description of three-node triangle.

$$x = L_1 x_1 + L_2 x_2 + L_3 x_3 \quad (5.40)$$

$$y = L_1 y_1 + L_2 y_2 + L_3 y_3 \quad (5.41)$$

because these relations hold at points 1, 2 and 3 and  $x$  and  $y$  vary linearly between. Using (5.39) to (5.41) we have

$$\begin{bmatrix} 1 \\ x \\ y \end{bmatrix} = \begin{bmatrix} 1 & 1 & 1 \\ x_1 & x_2 & x_3 \\ y_1 & y_2 & y_3 \end{bmatrix} \begin{bmatrix} L_1 \\ L_2 \\ L_3 \end{bmatrix} \quad (5.42)$$

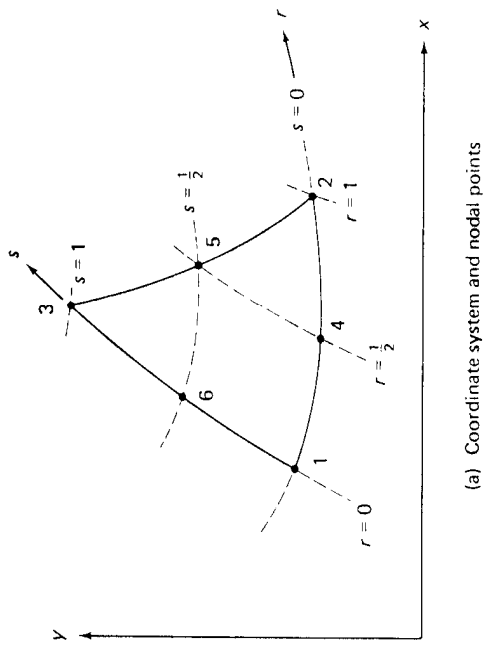
which gives

$$L_i = \frac{1}{2A}(a_i + b_i r + c_i s); \quad i = 1, 2, 3$$

where

$a_1 = x_1 y_2 + x_2 y_3 + x_3 y_1 - x_1 x_2 - y_2 x_3 - y_3 x_1$	$a_2 = x_3 y_1 - x_1 y_3$	$a_3 = x_1 y_2 - x_2 y_1$
$b_1 = y_2 - y_3$	$b_2 = y_3 - y_1$	$b_3 = y_1 - y_2$
$c_1 = x_3 - x_2$	$c_2 = x_1 - x_3$	$c_3 = x_2 - x_1$

As must have been expected, these  $L_i$  are equal to the interpolation functions of a constant strain triangle. Thus, in summary we have for the three-node triangular element in Fig. 5.24,



Include only if node  $i$  is defined

$i = 4$	$i = 5$	$i = 6$
$h_1 = 1-r-s$	$-\frac{1}{2}h_4$	$-\frac{1}{2}h_6$
$h_2 = r$	$-\frac{1}{2}h_4$	$-\frac{1}{2}h_5$
$h_3 = s$	$\dots \dots \dots$	$-\frac{1}{2}h_5$
$h_4 = 4r(1-r-s)$	$\dots \dots \dots$	$-\frac{1}{2}h_6$
$h_5 = 4rs$		
$h_6 = 4s(1-r-s)$		

**FIGURE 5.25** Interpolation functions of three to six variable-number-nodes two-dimensional triangle.

Using the above approach we can now also directly construct the interpolation functions of three-dimensional tetrahedral elements. First, we note that in analogy to (5.46) we now employ *volume coordinates*

$$\begin{aligned} L_1 &= 1 - r - s - t & L_2 &= r \\ L_3 &= s & L_4 &= t \end{aligned} \quad (5.47)$$

where we may check that  $L_1 + L_2 + L_3 + L_4 = 1$ . The  $L_i$  in (5.47) are the interpolation functions of the four-node element in Fig. 5.26 in its natural space. The interpolation functions of a 4 to 10 three-dimensional variable-number-nodes element are given in Fig. 5.27.

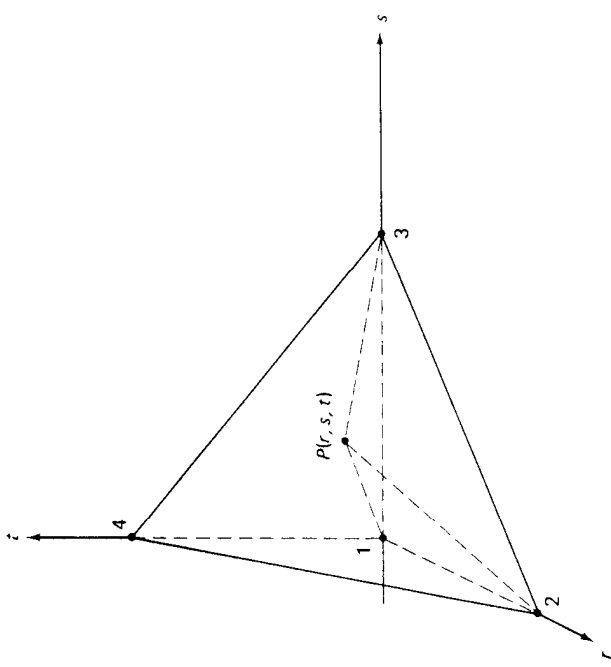


**FIGURE 5.26** Natural coordinate system of tetrahedral element.

To evaluate the element matrices, it is necessary to include the Jacobian transformation as given in (5.24) and to perform the  $r$ -integrations from 0 to 1, the  $s$ -integrations from 0 to  $(1 - r)$ , and the  $t$ -integrations from 0 to  $(1 - r - s)$ . As for the rectangular elements, these integrations are carried out effectively in general analysis using numerical integration, but the integration rules employed are different from those used for rectangular elements (see Section 5.7.4).

### 5.3.3 Element Matrices in Global Coordinate System

So far we considered the calculation of isoparametric element matrices that correspond to local element degrees of freedom. In the evaluation we used local element coordinates  $x$ ,  $y$ , and  $z$ , whichever are applicable, and local element degrees of freedom  $u_i$ ,  $v_i$ , and  $w_i$ . However, we may note that for the two-dimensional element considered in Examples 5.5 to 5.7 the element matrices could have been evaluated using the global coordinate variables  $X$  and  $Y$ , and the global nodal point displacements  $U_i$  and  $V_i$ . Indeed, in the calculations presented, the  $x$  and  $y$  local coordinates and  $u$  and  $v$  local displacement components needed simply to be replaced by the  $X$  and  $Y$  global coordinates and  $U$  and  $V$  global displacement components, respectively. In such case the matrices would have corresponded directly to the global displacement components.

In general, the calculation of the element matrices should be carried out in the global coordinate system, using global displacement components if the number of natural coordinate variables is equal to the number of global variables.

In those cases where the order of the global coordinate system is higher than the order of the natural coordinate system, it is usually most expedient to calculate first the element matrices in the local coordinate system and corresponding to local displacement components. Afterwards, the matrices must be transformed in the usual manner to the global displacement system. Examples are the truss element or the plane stress element when they are oriented arbitrarily in three-dimensional space. However, alternatively, we may include the transformation to the global displacement components directly in the formulation. This is accomplished by introducing a transformation that expresses in the displacement interpolation the local nodal point displacements in terms of the global components.

**EXAMPLE 5.19:** Evaluate the element stiffness matrix of the truss element in Fig. 5.28 using directly global nodal point displacements.

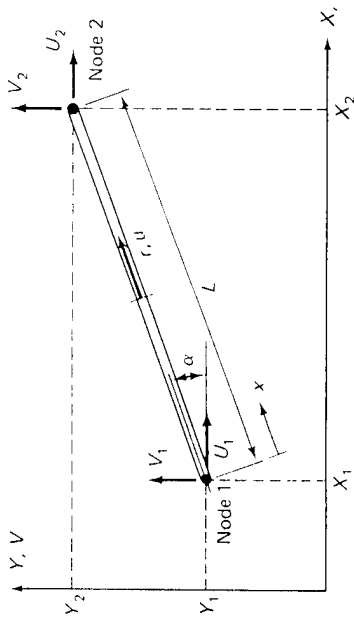


**FIGURE 5.28** Truss element in global coordinate system.

The stiffness matrix of the element is given in (5.27); i.e.,

$$\mathbf{K} = \int_V \mathbf{B}^T \mathbf{C} \mathbf{B} dV$$

where  $\mathbf{B}$  is the strain-displacement matrix and  $\mathbf{C}$  is the stress-strain matrix. For the truss element considered we have

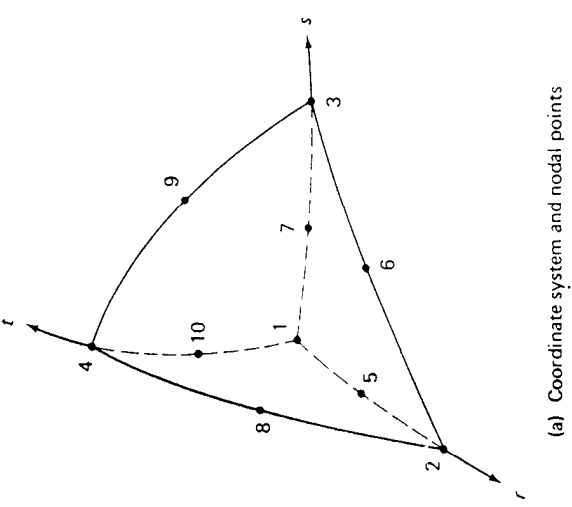
$$\boldsymbol{\epsilon} = [\cos \alpha \sin \alpha] \begin{bmatrix} \frac{1}{2}(1-r)U_1 + \frac{1}{2}(r+1)U_2 \\ \frac{1}{2}(1-r)V_1 + \frac{1}{2}(r+1)V_2 \end{bmatrix}$$

Then using that the strain  $\epsilon = \partial u / \partial x$ , which expressed in the natural coordinate system is  $\epsilon = (2/L) \partial u / \partial r$  (see Section 5.2), we can write the strain-displacement transformation corresponding to the displacement vector  $\mathbf{U}^T = [U_1 \ U_2 \ V_2]$  as

$$\mathbf{B} = \frac{1}{L} [\cos \alpha \quad \sin \alpha \quad \cos \alpha \quad \sin \alpha] \begin{bmatrix} -1 & -1 & \text{zeros} \\ \text{zeros} & \text{zeros} & 1 \end{bmatrix}$$

Also, as given in Section 5.2, we have

$$dV = \frac{AL}{2} dr \quad \text{and} \quad \mathbf{C} = E$$

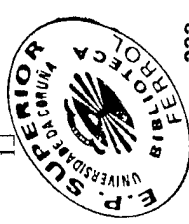


(a) Coordinate system and nodal points

		Include only if node $i$ is defined				
		$i = 6$	$i = 7$	$i = 8$	$i = 9$	$i = 10$
$h_1 = 1-r-s-t$		$-\frac{1}{2}h_5$	$-\frac{1}{2}h_7$	$-\frac{1}{2}h_8$	$-\frac{1}{2}h_9$	$-\frac{1}{2}h_{10}$
$h_2 = r$		$-\frac{1}{2}h_5$	$-\frac{1}{2}h_6$	$-\frac{1}{2}h_7$	$-\frac{1}{2}h_8$	
$h_3 = s$		$-\frac{1}{2}h_6$	$-\frac{1}{2}h_6$	$-\frac{1}{2}h_7$	$-\frac{1}{2}h_8$	
$h_4 = t$		$-\frac{1}{2}h_7$	$-\frac{1}{2}h_8$	$-\frac{1}{2}h_8$	$-\frac{1}{2}h_9$	$-\frac{1}{2}h_{10}$
$h_5 = 4r(1-r-s-t)$						
$h_6 = 4rs$						
$h_7 = 4s(1-r-s-t)$						
$h_8 = 4rt$						
$h_9 = 4st$						
$h_{10} = 4t(1-r-s-t)$						

**FIGURE 5.27** Interpolation functions of four to ten variable-number-nodes three-dimensional tetrahedral element.

Typical examples are two-dimensional elements that are defined in a global plane, and the three-dimensional element in Fig. 5.6. In these cases the Jacobian operator in (5.24) is a square matrix, which can be inverted as required in (5.25), and the element matrices correspond directly to the global displacement components.



Substituting the relations for  $\mathbf{B}$ ,  $\mathbf{C}$ , and  $dV$  and evaluating the integral, we obtain

$$\mathbf{K} = \frac{AE}{L} \begin{bmatrix} \cos^2 \alpha & \cos \alpha \sin \alpha & -\cos^2 \alpha & -\cos \alpha \sin \alpha \\ \sin \alpha \cos \alpha & \sin^2 \alpha & -\sin \alpha \cos \alpha & -\sin^2 \alpha \\ -\cos^2 \alpha & -\cos \alpha \sin \alpha & \cos^2 \alpha & \cos \alpha \sin \alpha \\ -\sin \alpha \cos \alpha & -\sin^2 \alpha & \sin \alpha \cos \alpha & \sin^2 \alpha \end{bmatrix}$$

## 5.4 FORMULATION OF STRUCTURAL ELEMENTS

The concepts of geometry and displacement interpolations that have been employed in the formulation of two- and three-dimensional continuum elements can also be employed in the evaluation of beam, plate, and shell structural element matrices. However, whereas in the formulation of the continuum elements the displacements  $u$ ,  $v$ ,  $w$  (whichever applicable) are interpolated in terms of nodal point displacements of the same kind, in the formulation of structural elements, the displacements  $u$ ,  $v$ , and  $w$  are interpolated in terms of midsurface displacements and rotations. We will show that this procedure corresponds in essence to a “continuum isoparametric element formulation with displacement constraints.” (In addition, there is the major assumption that the stress normal to the mid-surface is zero.) This can be interpreted as using a higher degree of interpolation on the geometry than on the displacements and for this reason the structural elements are also referred to as *superparametric elements* (see Section 5.6), or as *degenerate isoparametric elements*.

Considering the formulation of structural elements, we have already discussed briefly in Section 4.2.3 how beam, plate, and shell elements can be formulated using the Kirchhoff plate theory, in which shear deformations are neglected. In these formulations it is difficult to satisfy interelement continuity on displacements and edge rotations because the plate (or shell) rotations are calculated from the transverse displacements. Furthermore, using an assemblage of flat elements to represent a shell structure, a relatively large number of elements may be required in order to represent the shell geometry to sufficient accuracy.

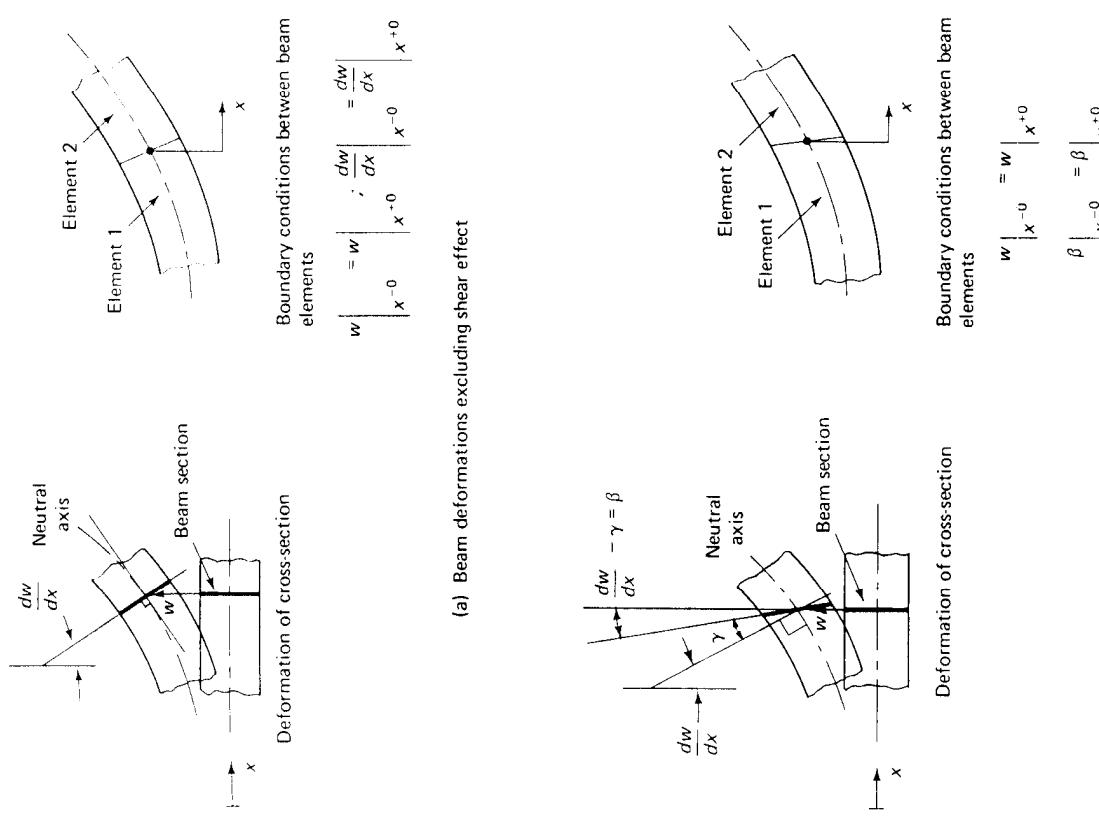
Our objective in this section is to discuss an alternative approach to formulating beam, plate, and shell elements. The basis of this method is a theory that includes the effects of shear deformations. With this theory, the displacements and rotations of the mid-surface normals are independent and the interelement continuity conditions on these quantities can be satisfied directly as in the analysis of continua. In addition, if the concepts of isoparametric interpolation are employed, the geometry of curved shell surfaces is interpolated and can be represented to a high degree of accuracy. In the following sections we discuss first the formulation of beam elements, where we can demonstrate in detail the basic principles used, and we then present the formulation of general plate and shell elements.

### 5.4.1 Beam Elements

The basic assumption in beam-bending analysis excluding shear deformations is that a normal to the mid-surface (neutral axis) of the beam remains straight during deformation and that its angular rotation is equal to the slope

of the beam mid-surface. This kinematic assumption, illustrated in Fig. 5.29(a), leads to the well-known beam-bending governing differential equation in which the transverse displacement  $w$  is the only variable (see Example 3.20). Therefore, using beam elements formulated with this theory, displacement continuity between elements requires that  $w$  and  $dw/dx$  be continuous.

Considering now beam-bending analysis with the effect of shear deformations, we retain the assumption that a plane section originally normal to



(a) Beam deformations excluding shear effect  
(b) Beam deformations including shear effect

FIGURE 5.29 Beam deformation assumptions.

the neutral axis remains plane, but because of shear deformations this section does not remain normal to the neutral axis. As illustrated in Fig. 5.29(b) the total rotation of the plane originally normal to the neutral axis of the beam is due to the rotation of the tangent to the neutral axis and the shear deformation,<sup>20</sup>

$$\beta = \frac{dw}{dx} - \gamma \quad (5.48)$$

where  $\gamma$  is a constant shearing strain across the section. Since the actual shearing stress and strain vary over the section (e.g. a parabolic distribution of shearing stress pertains to a rectangular section), the shearing strain  $\gamma$  in (5.48) is an equivalent constant strain on a corresponding shear area  $A_s$ ,

$$\tau = \frac{V}{A_s}; \quad \gamma = \frac{\tau}{G}; \quad k = \frac{A_s}{A} \quad (5.49)$$

where  $V$  is the shear force at the section considered. The shear correction factor  $k$  can be evaluated using the condition that the constant shear stress in (5.49) when acting on  $A_s$ , must yield the same shear strain energy as the actual shearing stress acting on the actual cross-sectional area  $A$  of the beam.

The finite element formulation of a beam element with the assumption in (5.48) can be obtained using the basic virtual work expressions in (4.1) to (4.20), or the principle of stationarity of the total potential energy (see Example 4.2). In the following we consider first, for illustrative purposes, the formulation of the beam element matrices corresponding to the simple beam element in Fig. 5.30 using the total potential energy approach, and we discuss afterwards the formulation of more general three-dimensional beam elements using the principle of virtual displacements.

Figure 5.30 shows the two-dimensional rectangular cross-section beam considered. The total potential energy of the beam is

$$\Pi = \frac{EI}{2} \int_0^L \left( \frac{d\beta}{dx} \right)^2 dx + \frac{GAk}{2} \int_0^L \left( \frac{dw}{dx} - \beta \right)^2 dx - \int_0^L p w dx - \int_0^L m \beta dx \quad (5.50)$$

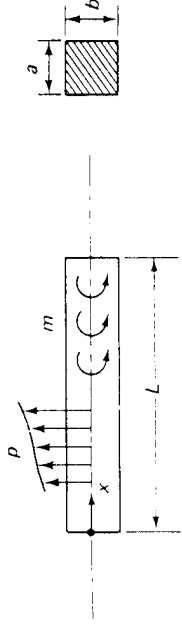
where  $p$  and  $m$  are the transverse and moment loading per unit length. The first two integrals on the r.h.s. of (5.50) represent the strain energy corresponding to bending and shearing deformations, and the last two integrals represent the potential of the external loads. The stationarity condition  $\delta\Pi = 0$  using (5.50) yields

$$EI \int_0^L \left( \frac{d\beta}{dx} \right) \delta \left( \frac{d\beta}{dx} \right) dx + GAk \int_0^L \left( \frac{dw}{dx} - \beta \right) \delta \left( \frac{dw}{dx} - \beta \right) dx \\ - \int_0^L p \delta w dx - \int_0^L m \delta \beta dx = 0 \quad (5.51)$$

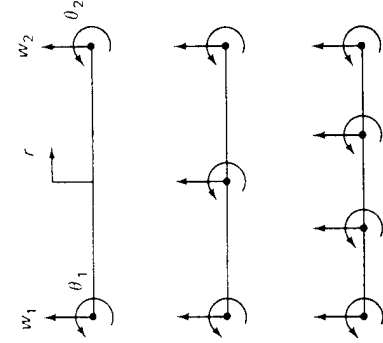
This relation is in fact the principle of virtual displacements corresponding to the beam element deformations. Using now the interpolations

$$w = \sum_{i=1}^q h_i w_i; \quad \beta = \sum_{i=1}^q h_i \theta_i \quad (5.52)$$

where  $q$  is equal to the number of nodes used and the  $h_i$  are the one-dimensional interpolation functions listed in Fig. 5.4, we can directly employ the concepts of



(a) Beam with applied loading  
 $E$  = Young's modulus,  $G$  = shear modulus  
 $k = \frac{5}{6}$ ,  $A = ab$ ,  $I = \frac{ab^3}{12}$



(b) Two, three and four-node models;  $\theta_i = \beta_i$ ,  $i = 1, \dots, q$   
 (Interpolation functions are given in Fig. 5.4)

FIGURE 5.30 Formulation of two-dimensional beam element.

the isoparametric formulations discussed in Section 5.3 to establish all relevant element matrices. Let

$$\begin{aligned} w &= \mathbf{H}_w \hat{w}; & \beta &= \mathbf{H}_\beta \hat{\beta} \\ \frac{\partial w}{\partial x} &= \mathbf{B}_w \hat{w}; & \frac{\partial \beta}{\partial x} &= \mathbf{B}_\beta \hat{\beta} \\ \hat{w}^T &= [w_1 \dots w_q \quad \theta_1 \dots \theta_q] \\ \mathbf{H}_w &= [h_1 \dots h_q \quad 0 \dots 0] \\ \mathbf{H}_\beta &= [0 \dots 0 \quad h_1 \dots h_q] \\ \mathbf{B}_w &= J^{-1} \left[ \frac{\partial h_1}{\partial r} \dots \frac{\partial h_q}{\partial r} \quad 0 \dots 0 \right] \\ \mathbf{B}_\beta &= J^{-1} \left[ 0 \dots 0 \quad \frac{\partial h_1}{\partial r} \dots \frac{\partial h_q}{\partial r} \right] \end{aligned} \quad (5.53) \quad (5.54) \quad (5.55)$$

where

$$\text{and} \quad \begin{aligned} \mathbf{K} &= EI \int_{-1}^1 \mathbf{B}_\beta^T \mathbf{B}_\beta \det J dr + GAk \int_{-1}^1 (\mathbf{B}_w - \mathbf{H}_\beta)^T (\mathbf{B}_w - \mathbf{H}_\beta) \det J dr \\ \mathbf{R} &= \int_{-1}^1 \mathbf{H}_w^T p \det J dr + \int_{-1}^1 \mathbf{H}_\beta^T m \det J dr \end{aligned} \quad (5.56) \quad (5.57)$$

where  $J = \partial x/\partial r$ , then we have for a single element

Also, in dynamic analysis the mass matrix can be calculated using the d'Alembert principle (see (4.21)); hence

$$\mathbf{M} = \int_{-1}^1 \begin{bmatrix} \mathbf{H}_w \\ \mathbf{H}_\beta \end{bmatrix}^T \begin{bmatrix} \rho ab \\ 0 \end{bmatrix} \begin{bmatrix} \mathbf{H}_w \\ \mathbf{H}_\beta \end{bmatrix} \det J \, dx \quad (5.58)$$

In the above evaluations we are using the natural coordinate system of the beam because this is effective in the formulation of more general beam, plate, and shell elements. However, when considering a straight beam of constant cross-section, the integrals can also be evaluated efficiently without using the natural coordinate system as demonstrated in the following example.

**EXAMPLE 5.20:** Evaluate the detailed expressions for the calculation of the stiffness matrix and the load vector of the three-node beam element shown in Fig. 5.31.

The interpolation functions to be used are listed in Fig. 5.4. These functions are given in terms of  $r$  and yield

$$x = \sum_{i=1}^3 h_i x_i$$

Using  $x_1 = 0$ ,  $x_2 = L$ ,  $x_3 = L/2$ , we obtain

$$x = \frac{L}{2}(1+r)$$

Hence, the interpolation functions in terms of  $x$  are

$$h_1 = \frac{2x^2}{L^2} - \frac{3x}{L} + 1$$

$$h_2 = \frac{2x^2}{L^2} - \frac{x}{L}$$

$$h_3 = \frac{4x^2}{L^2} - \frac{4x^2}{L^2}$$

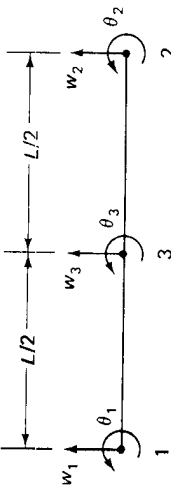
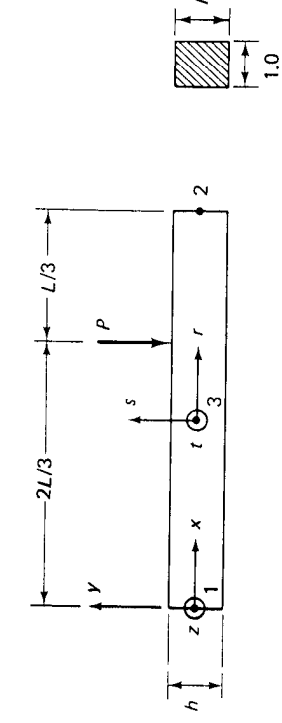


FIGURE 5.31 Three-node beam element considered in Examples 5.20 and 5.22.

Using the notation  $(\cdot)' \equiv \frac{\partial}{\partial x}$  it follows that

$$h'_1 = \frac{4x}{L^2} - \frac{3}{L}$$

$$h'_2 = \frac{4x}{L^2} - \frac{1}{L}$$

$$h'_3 = \frac{4}{L} - \frac{8x}{L^2}$$

Hence with the degrees of freedom ordered as in (5.54) we have

$$\mathbf{K} = \frac{Eh^3}{12} \int_0^L \begin{bmatrix} 0 & 0 & 0 & 0 & 0 & 0 \\ 0 & 0 & 0 & h'_1 & h'_2 & h'_3 \\ 0 & 0 & 0 & h'_1 & h'_2 & h'_3 \\ h'_1 & h'_2 & h'_3 & 0 & 0 & 0 \\ h'_2 & h'_3 & 0 & 0 & 0 & 0 \\ h'_3 & 0 & 0 & 0 & 0 & 0 \end{bmatrix} \left[ \begin{array}{c} h'_1 \\ h'_2 \\ h'_3 \\ -h_1 \\ -h_2 \\ -h_3 \end{array} \right]$$

and

$$\mathbf{R}^T = -\mathbf{P} \begin{bmatrix} -\frac{1}{2} & \frac{2}{3} & \frac{8}{9} & 0 & 0 & 0 \end{bmatrix}$$

The element of Fig. 5.30 can be employed effectively in the analysis of moderately thick and thin beam structures. However, in the analysis of thin beams, the three- or four-node element must be employed, because the two-node element does not represent the bending and shearing deformations to sufficient accuracy.

In order to obtain some insight into the behavior of the beam elements when the beam becomes thin, consider the total potential  $\tilde{\Pi}$ ,

$$\tilde{\Pi} = \int_0^L \left( \frac{d\beta}{dx} \right)^2 dx + \frac{GAk}{EI} \int_0^L \left( \frac{dw}{dx} - \beta \right)^2 dx \quad (5.59)$$

which is obtained by neglecting the load contributions in (5.50) and dividing by  $\frac{1}{2}EI$ . The relation in (5.59) shows the relative importance of the bending and shearing contributions to the stiffness matrix of an element. The bending and shearing contributions are represented by the first and second terms on the r.h.s. of (5.59), respectively, where we note that the factor  $GAk/EI$  in the shearing term can be very large when a thin element is considered. This factor can be interpreted as a penalty number (see Section 3.4) as the element becomes very thin, i.e., we can write

$$\tilde{\Pi} = \int_0^L \left( \frac{d\beta}{dx} \right)^2 dx + \alpha \int_0^L \left( \frac{dw}{dx} - \beta \right)^2 dx; \quad \alpha = \frac{GAk}{EI} \quad (5.60)$$

where  $\alpha \rightarrow \infty$  as  $h \rightarrow 0$ . However, this means that as the beam becomes thin

the constraint of zero shear deformations, i.e.,  $d\psi/dx = \beta$  with  $\gamma = 0$ , will be approached.

The above argument holds for the actual continuous model which is governed by the stationarity condition on  $\Pi$  and the appropriate boundary conditions. Considering now the finite element representation, it is important that the finite element displacement assumptions on  $\beta$  and  $w$  admit that for large values of  $\alpha$  the shearing deformations can be small throughout the domain of the element. If by virtue of the assumptions used on  $w$  and  $\beta$  the shearing deformations cannot be small everywhere, then the element stiffness will grossly overestimate the actual structural stiffness because the penalty number is a multiplier to the erroneous shearing deformations. This is precisely what happens when the two-node beam element of Fig. 5.30 is used, which therefore should not be employed in the analysis of thin beam structures. This conclusion is also applicable to the use of the low-order plate and shell elements discussed in Section 5.4.2. The phenomenon that the thin elements are very stiff has been referred to as “element locking.”<sup>21,22</sup>

Considering the above structural elements, we therefore conclude that, unless the low-order element behavior is “somehow” improved, only high-order elements should be used in the analysis of thin structures. Since the use of low-order elements can be attractive from a cost viewpoint, a considerable amount of research has been spent on finding remedies to improve the behavior of the low-order elements for thin structures. Two procedures have found wide appeal: *the use of selective or reduced integration*<sup>23–25</sup> and *the use of a discrete Kirchhoff theory*.<sup>24,25</sup>

In the above discussion of the beam elements, we assumed that all integrations are performed exactly. The reduced and selective integration procedures are based on the premise that by not integrating the shear strain energy exactly, the effect of “element locking” can be avoided. The difficulty in this procedure is to assure that the element does not contain any spurious zero-energy modes due to the special integration scheme used (which would render the element unreliable) and yet the element must possess good accuracy characteristics. We discuss the approach of reduced and selective integration further in Sections 5.8.1 and 6.5.3.

The procedure used in the discrete Kirchhoff theory to avoid element “locking” is to assume that the shearing strains are so small that the shear strain energy need not be included in the total potential energy functional. However, since the bending strains are given only in terms of the rotations of the cross-sections and we are interpolating these and the transverse displacements, additional equations are needed to relate the nodal point displacements and rotations. These equations are established by invoking the condition that the shearing strains are zero at specific points in the domain of the element. Thus, the basis of the discrete Kirchhoff element formulations is that the Kirchhoff hypothesis is satisfied at discrete points of the element (which, if a large enough number of points is selected, approximates the condition that the hypothesis is satisfied throughout the entire element). The discrete Kirchhoff analysis procedure is most effective in the formulation of low-order elements and we demonstrate the technique in the following simple analysis.

**EXAMPLE 5.21:** Consider the cantilever beam shown in Fig. 5.32. Idealize the cantilever using one two-node element and predict the tip displacement. Also, predict the tip deflection when using a discrete Kirchhoff formulation. The stiffness matrix of a two-node beam element can directly be inferred from the results of Example 5.20 and the interpolation functions listed in Fig. 5.4:

$$\mathbf{K} = \frac{Eh^3}{12} \int_0^L \begin{bmatrix} 0 & 0 \\ 0 & -\frac{1}{L} \\ -\frac{1}{L} & \frac{1}{L} \end{bmatrix} dx$$

$$+ \frac{5Gh}{6} \int_0^L \begin{bmatrix} -\frac{1}{L} & \frac{1}{L} \\ \frac{1}{L} & -\left(1 - \frac{x}{L}\right) \\ -\left(1 - \frac{x}{L}\right) & -\frac{x}{L} \end{bmatrix} dx$$

With  $G = \frac{1}{2}E$  we have

$$\mathbf{K} = \frac{E}{12} \begin{bmatrix} \frac{5h}{L} & \frac{5h}{L} & \frac{5h}{2} & \frac{5h}{2} \\ \frac{5h}{L} & \frac{5h}{L} & -\frac{5h}{2} & -\frac{5h}{2} \\ \frac{5h}{2} & -\frac{5h}{2} & \frac{h^3}{6} + \frac{5hL}{3} & \left(\frac{5hL}{6} - \frac{h^3}{L}\right) \\ -\frac{5h}{2} & -\frac{5h}{2} & \left(\frac{h^3}{L} + \frac{5hL}{3}\right) & \left(\frac{h^3}{L} + \frac{5hL}{3}\right) \end{bmatrix}$$

Since  $w_1 = \theta_1 = 0$ , the governing equilibrium equations for this problem are

$$\begin{bmatrix} \frac{5h}{L} & -\frac{5h}{2} & \frac{5h}{2} & \frac{5h}{2} \\ \frac{5h}{L} & \frac{5h}{L} & -\frac{5h}{2} & -\frac{5h}{2} \\ -\frac{5h}{2} & -\frac{5h}{2} & \frac{h^3}{6} + \frac{5hL}{3} & \left(\frac{5hL}{6} - \frac{h^3}{L}\right) \\ -\frac{5h}{2} & -\frac{5h}{2} & \left(\frac{h^3}{L} + \frac{5hL}{3}\right) & \left(\frac{h^3}{L} + \frac{5hL}{3}\right) \end{bmatrix} \begin{bmatrix} w_2 \\ \theta_2 \\ 0 \\ 0 \end{bmatrix} = \begin{bmatrix} -P \\ 0 \\ 0 \\ 0 \end{bmatrix}$$

which gives

$$\delta = \frac{12PL}{5hE} \left( 1 + \frac{5hL}{4\left(\frac{h^3}{L} + \frac{5hL}{3}\right)} \right)$$

The tip displacement predicted using elementary beam theory is  $\delta = 4PL^3/Eh^3$ ; hence the solution obtained with the two-node element is very inaccurate. (It is interesting to note here that the response using one four-node element with  $h/L = \frac{1}{100}$  is  $\delta = 4.0002PL^3/Eh^3$ .)

However, the solution using the two-node element idealization can be improved significantly with the discrete Kirchhoff theory in the formulation. Firstly, the shear strain energy contribution is neglected in the calculation of the stiffness matrix. Hence, using (5.50) we now have

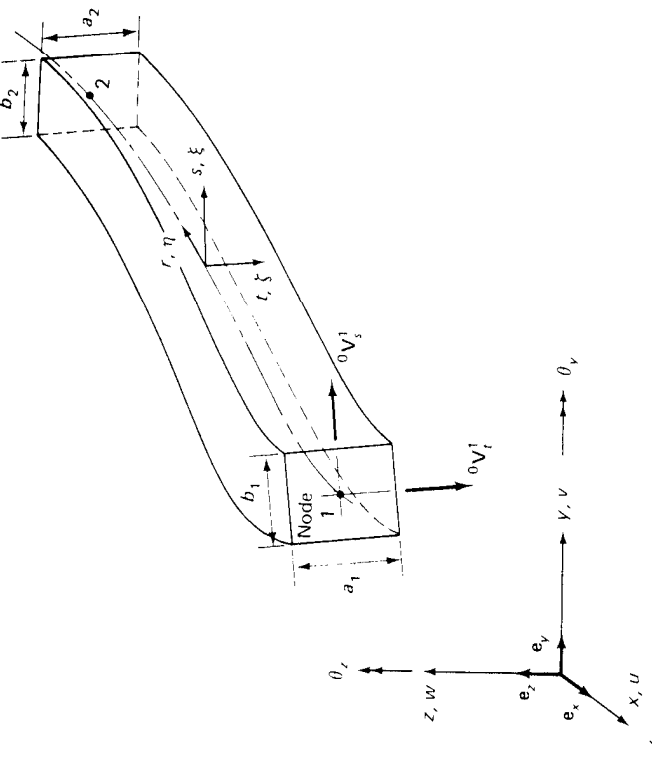


FIGURE 5.32 Analysis of cantilever beam using one two-node element.

$$\mathbf{U} = \frac{1}{2} [\theta_1 \ \theta_2] \frac{Eh^3}{12L} \begin{bmatrix} 1 & -1 & [\theta_1] \\ -1 & 1 & [\theta_2] \end{bmatrix}$$

In the cantilever problem considered  $\theta_1 = 0$ . The second step in using the discrete Kirchhoff formulation is to invoke the constraint that  $\gamma = 0$  in order to relate  $\theta_2$  to  $w_2$ . Using  $\gamma = 0$ , i.e.  $dw/dx = \beta$ , at the midpoint of the element gives

$$\theta_2 = \frac{2w_2}{L}$$

$$\mathbf{U} = \frac{1}{2} [w_2] \frac{Eh^3}{12L} \begin{bmatrix} 4 \\ L^2 \end{bmatrix} [w_2]$$

$$\delta = \frac{3PL^3}{Eh^3}$$

Hence, we now obtain

which is significantly closer to the elementary beam theory solution.

The above discussion and example solution provides only a very brief introduction to the basic concepts employed in discrete Kirchhoff formulations. A particularly difficult step in these formulations is the choice of the appropriate constraints between the nodal point variables. However, the discrete Kirchhoff theory has been used with much success in the formulation of various beam, plate and shell elements, and in particular for the derivation of very effective low-order elements.<sup>25</sup>

The formulation of the two-dimensional beam element of Fig. 5.30 given in (5.50) to (5.58) is a special case of the formulation of more general three-dimensional beam elements. In order to illustrate this point and show how the isoparametric interpolation concepts can be applied to formulate more general beam elements, we consider the three-dimensional beam of rectangular cross-section in Fig. 5.33. In the derivation we assume that an accurate representation of the torsional rigidity is not required. Namely, the torsional interpolation functions that

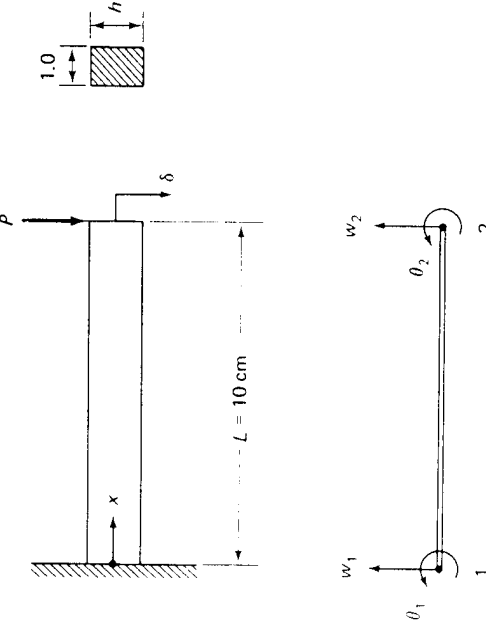


FIGURE 5.33 Three-dimensional beam element.

we will use in the formulation correspond to the exact torsional displacements of a circular section and should be amended for an accurate torsional description of rectangular cross-sections.\* In practice, complex sections such as L and I cross-sections and pipe elbows need be considered. These elements are also more difficult to deal with because again deformation patterns in addition to those used in the formulation given below can be important in the description of the behavior of these beams. For example, in the formulation of a curved pipe element the ovalization of the cross-section must in general be taken into account.<sup>26</sup> However, although we consider in the following only a special three-dimensional beam element the discussion is important because the procedures used in this formulation represent the basic and general steps that are followed also in the formulation of beams of other cross-sectional shapes.

The basic kinematic assumption used in the formulation of the three-dimensional beam element is the same as that employed in the formulation of the two-dimensional element of Fig. 5.30; namely, that plane sections originally normal to the center line axis remain plane and undistorted under deformation, but not necessarily normal to this axis. Based on this assumption, we can formulate the beam element matrices directly using the isoparametric element procedures discussed in Section 5.3.

\* The required amendment is that warping displacements must be interpolated.

Using the natural coordinates  $r$ ,  $s$ , and  $t$ , the Cartesian coordinates of a point in the element with  $q$  nodal points are, before and after deformations:

$$\begin{aligned} \ell_x(r, s, t) &= \sum_{k=1}^q h_k \ell_{xk} + \frac{t}{2} \sum_{k=1}^q a_k h_k \ell_{V_{tx}}^k + \frac{s}{2} \sum_{k=1}^q b_k h_k \ell_{V_{sy}}^k \\ \ell_y(r, s, t) &= \sum_{k=1}^q h_k \ell_{yk} + \frac{t}{2} \sum_{k=1}^q a_k h_k \ell_{V_{ty}}^k + \frac{s}{2} \sum_{k=1}^q b_k h_k \ell_{V_{sz}}^k \\ \ell_z(r, s, t) &= \sum_{k=1}^q h_k \ell_{zk} + \frac{t}{2} \sum_{k=1}^q a_k h_k \ell_{V_{tz}}^k + \frac{s}{2} \sum_{k=1}^q b_k h_k \ell_{V_{zx}}^k \end{aligned} \quad (5.6)$$

where the  $h_k(r)$  are the interpolation functions summarized in Fig. 5.4 and

$\ell_x, \ell_y, \ell_z$  = Cartesian coordinates of any point in the element  
 $\ell_{xk}, \ell_{yk}, \ell_{zk}$  = Cartesian coordinates of nodal point  $k$

$a_k, b_k$  = Cross-sectional dimensions of the beam at nodal point  $k$

$\ell_{V_{tx}}, \ell_{V_{ty}}, \ell_{V_{tz}}$  = Components of unit vector  $\ell_{V_t^k}$  in direction  $t$  at nodal point  $k^*$   
 $\ell_{V_{sx}}, \ell_{V_{sy}}, \ell_{V_{sz}}$  = Components of unit vector  $\ell_{V_s^k}$  in direction  $s$  at nodal point  $k^*$

and the left superscript  $\ell$  denotes the configuration of the element; i.e.,  $\ell = 0$  denotes the original configuration, whereas  $\ell = 1$  corresponds to the configuration in the deformed position. Thus, to obtain the displacement components at any point of the element we have

$$\begin{aligned} u(r, s, t) &= {}^1x - {}^0x \\ v(r, s, t) &= {}^1y - {}^0y \\ w(r, s, t) &= {}^1z - {}^0z \end{aligned} \quad (5.62)$$

and substituting from (5.61) we obtain

$$u(r, s, t) = \sum_{k=1}^q h_k u_k + \frac{t}{2} \sum_{k=1}^q a_k h_k V_{tx}^k + \frac{s}{2} \sum_{k=1}^q b_k h_k V_{sx}^k \quad (5.63)$$

$$v(r, s, t) = \sum_{k=1}^q h_k v_k + \frac{t}{2} \sum_{k=1}^q a_k h_k V_{ty}^k + \frac{s}{2} \sum_{k=1}^q b_k h_k V_{sy}^k \quad (5.64)$$

$$w(r, s, t) = \sum_{k=1}^q h_k w_k + \frac{t}{2} \sum_{k=1}^q a_k h_k V_{tz}^k + \frac{s}{2} \sum_{k=1}^q b_k h_k V_{sz}^k \quad (5.65)$$

where  $V_t^k = {}^1V_t^k - {}^0V_t^k$ ;  $V_s^k = {}^1V_s^k - {}^0V_s^k$

Finally, we express the vectors  $V_t^k$  and  $V_s^k$  in terms of rotations about the Cartesian axes  $x, y, z$ :

$$\begin{aligned} V_t^k &= \boldsymbol{\theta}_k \times {}^0V_t^k \\ V_s^k &= \boldsymbol{\theta}_k \times {}^0V_s^k \end{aligned} \quad (5.66)$$

where  $\boldsymbol{\theta}_k$  is a vector listing the nodal point rotations at nodal point  $k$  (see Fig. 5.33):

$$\boldsymbol{\theta}_k = \begin{bmatrix} \theta_x^k \\ \theta_y^k \\ \theta_z^k \end{bmatrix} \quad (5.67)$$

Using (5.61) to (5.66) we have all the basic equations necessary to establish the displacement and strain interpolation matrices that are employed in the evaluation of the beam element matrices as expressed in (5.27) to (5.35). The

\* Note that these vectors are not necessarily exactly normal to the neutral axis of the beam.

terms in the displacement interpolation matrix  $\mathbf{H}$  are obtained by substituting (5.65) into (5.63). To evaluate the strain-displacement matrix, we recognize that for the beam the only strain components of interest are the longitudinal strain  $\epsilon_{xx}$  and transverse shear strains  $\gamma_{xz}$  and  $\gamma_{yz}$ , where  $\eta, \xi$ , and  $\zeta$  are convected (body-attached) coordinate axes (see Fig. 5.33). Thus, we seek a relation of the form

$$\begin{bmatrix} \epsilon_m \\ \gamma_{xz} \\ \gamma_{yz} \end{bmatrix} = \sum_{k=1}^q \mathbf{B}_k \hat{\mathbf{u}}_k \quad (5.68)$$

$$\hat{\mathbf{u}}_k^T = [u_k \ v_k \ w_k \ \theta_x^k \ \theta_y^k \ \theta_z^k] \quad (5.69)$$

$$\mathbf{B} = [\mathbf{B}_1, \dots, \mathbf{B}_q] \quad (5.70)$$

Following the usual procedure of isoparametric finite element formulation, we have using (5.63)

$$\begin{bmatrix} \frac{\partial u}{\partial r} \\ \frac{\partial u}{\partial s} \\ \frac{\partial u}{\partial t} \end{bmatrix} = \sum_{k=1}^q \begin{bmatrix} \frac{\partial h_k}{\partial r} [1 \ \ (g)_{1i}^k \ \ (g)_{2i}^k \ \ (g)_{3i}^k] \\ h_k [0 \ \ (\hat{g})_{1i}^k \ \ (\hat{g})_{2i}^k \ \ (\hat{g})_{3i}^k] \\ h_k [0 \ \ (\hat{g})_{1i}^k \ \ (\hat{g})_{2i}^k \ \ (\hat{g})_{3i}^k] \end{bmatrix} \quad (5.71)$$

and the derivatives of  $v$  and  $w$  are obtained by simply substituting  $v$  and  $w$  for  $u$ . In (5.70) we have  $i = 1$  for  $u$ ,  $i = 2$  for  $v$  and  $i = 3$  for  $w$ , and we employ the notation:

$$(\hat{g})^k = \frac{b_k}{2} \begin{bmatrix} 0 & -\eta V_{tx}^k & \eta V_{xy}^k \\ \eta V_{rz}^k & 0 & -\eta V_{xz}^k \\ -\eta V_{ry}^k & \eta V_{rx}^k & 0 \end{bmatrix} \quad (5.72)$$

$$(\hat{g})^k = \frac{a_k}{2} \begin{bmatrix} 0 & -\eta V_{tz}^k & \eta V_{tx}^k \\ \eta V_{rz}^k & 0 & -\eta V_{xz}^k \\ -\eta V_{ry}^k & \eta V_{rx}^k & 0 \end{bmatrix} \quad (5.73)$$

To obtain the displacement derivatives corresponding to the coordinate axes  $x, y$ , and  $z$ , we employ the Jacobian transformation

$$\frac{\partial}{\partial \mathbf{x}} = \mathbf{J}^{-1} \frac{\partial}{\partial \mathbf{r}} \quad (5.74)$$

where the Jacobian matrix,  $\mathbf{J}$ , contains the derivatives of the coordinates  $x, y, z$  with respect to the natural coordinates  $r, s$ , and  $t$  (see (5.23)). Substituting from (5.70) into (5.74) we obtain

$$\begin{bmatrix} \frac{\partial u}{\partial x} \\ \frac{\partial u}{\partial y} \\ \frac{\partial u}{\partial z} \end{bmatrix} = \sum_{k=1}^q \begin{bmatrix} J_{11}^{-1} \frac{\partial h_k}{\partial r} (G1)_{1i}^k (G2)_{1i}^k (G3)_{1i}^k \\ J_{21}^{-1} \frac{\partial h_k}{\partial r} (G1)_{2i}^k (G2)_{2i}^k (G3)_{2i}^k \\ J_{31}^{-1} \frac{\partial h_k}{\partial r} (G1)_{3i}^k (G2)_{3i}^k (G3)_{3i}^k \end{bmatrix} \quad (5.75)$$

and, again, the derivatives of  $v$  and  $w$  are obtained by simply substituting  $v$  and  $w$  for  $u$ . In (5.75) we employ the notation

$$(Gm)_m^k = (J_{\bar{n}1}^{-1}(\bar{g})_m^k) \frac{\partial h_k}{\partial r} + (J_{\bar{n}2}^{-1}(\bar{g})_m^k + J_{\bar{n}3}^{-1}(\bar{g})_m^k) h_k \quad (5.76)$$

Using the displacement derivatives in (5.75) we can now calculate the elements of  $\mathbf{B}_k$  by establishing the strain components corresponding to the  $x, y, z$  axes and transforming these components to the local strains  $\epsilon_m, \gamma_{nk}$  and  $\gamma_{nc}$ .

The corresponding stress-strain law to be employed in the formulation is then (using  $k$  as the shear correction factor),

$$\begin{bmatrix} \tau_m \\ \tau_{nk} \\ \tau_{nc} \end{bmatrix} = \begin{bmatrix} E & 0 & 0 \\ 0 & G_k & 0 \\ 0 & 0 & G_k \end{bmatrix} \begin{bmatrix} \epsilon_m \\ \gamma_{nk} \\ \gamma_{nc} \end{bmatrix} \quad (5.77)$$

Considering the formulation in (5.61) to (5.77), it should be recognized that the element can be arbitrarily curved and the cross-sectional dimensions can change along its axis. The width, height, and location of the element neutral axis are interpolated along the element, where it should be noted that if the element is straight and its cross-sectional area is constant, considerable simplifications can result in the calculation of the element matrices (see Example 5.22). Finally, it should also be noted that in addition to representing a general approach to the linear analysis of beam structures, the above formulation is particularly useful as the basis of nonlinear large displacement analysis of beam structures. As discussed in Section 6.3.4, in those analyses initially straight beam elements become curved and distorted, and these deformations can be modeled accurately using the formulation presented above.

**EXAMPLE 5.22:** Show that the application of the general formulation in (5.61) to (5.77) to the beam element in Fig. 5.31 reduces to the use of (5.51).

For the application of the general relations in (5.61) to (5.77) we refer to Figs. 5.31 and 5.33 and thus have

$${}^0\mathbf{V}_t = \begin{bmatrix} 0 \\ 1 \\ 0 \end{bmatrix}; \quad {}^0\mathbf{V}_t = \begin{bmatrix} 0 \\ 0 \\ 1 \end{bmatrix}; \quad a_k = 1, \quad b_k = h, \quad k = 1, 2, 3$$

Hence, the relations in (5.61) reduce to

$$\begin{aligned} {}^0x &= \sum_{k=1}^3 h_k {}^0x_k \\ {}^0y &= \frac{s}{2}h \\ {}^0z &= \frac{t}{2} \end{aligned}$$

We next evaluate (5.65) to obtain (see Section 2.6)

$$\begin{aligned} \mathbf{V}_t^k &= \det \begin{bmatrix} \mathbf{e}_x & \mathbf{e}_y & \mathbf{e}_z \\ \theta_x^k & \theta_y^k & \theta_z^k \\ 0 & 0 & 1 \end{bmatrix} \\ \mathbf{V}_t^k &= \theta_y^k \mathbf{e}_x - \theta_x^k \mathbf{e}_y \end{aligned} \quad (a)$$

or

$$\mathbf{V}_t^k = \begin{bmatrix} \mathbf{e}_x & \mathbf{e}_y & \mathbf{e}_z \\ \theta_x^k & \theta_y^k & \theta_z^k \\ 0 & 1 & 0 \end{bmatrix}$$

$$\mathbf{V}_t^k = -\theta_z^k \mathbf{e}_x + \theta_x^k \mathbf{e}_z \quad (b)$$

or  
The relations in (a) and (b) correspond to the three-dimensional action of the beam. We allow only rotations about the  $z$ -axis, in which case

$$\mathbf{V}_t^k = \mathbf{0}; \quad \mathbf{V}_s^k = -\theta_z^k \mathbf{e}_x$$

Furthermore, we assume that the nodal points can only displace into the  $y$ -direction. Hence, (5.63) yields the displacement assumptions,

$$\begin{aligned} u(r, s) &= -\frac{sh}{2} \sum_{k=1}^3 h_k \theta_z^k \\ v(r, s) &= \sum_{k=1}^3 h_k v_k \end{aligned} \quad (c)$$

where we note that  $u$  is only a function of  $r, s$  and  $v$  is only a function of  $r$ . These relations are identical to the displacement assumptions used before, but with the more conventional beam displacement notation we identified the transverse displacement and section rotation at a nodal point with  $v_k$  and  $\theta_z^k$  instead of  $v_k$  and  $\theta_z^k$ .

Using now (5.70) we obtain

$$\begin{aligned} \begin{bmatrix} \frac{\partial u}{\partial r} \\ \frac{\partial u}{\partial s} \end{bmatrix} &= \sum_{k=1}^3 \begin{bmatrix} -\frac{sh}{2} \frac{\partial \theta_z^k}{\partial r} \\ \frac{h}{2} h_k \end{bmatrix} \theta_z^k \\ \begin{bmatrix} \frac{\partial v}{\partial r} \\ \frac{\partial v}{\partial s} \end{bmatrix} &= \sum_{k=1}^3 \begin{bmatrix} \frac{\partial h_k}{\partial r} \\ 0 \end{bmatrix} v_k \end{aligned} \quad (d)$$

These relations could also directly be obtained by differentiating the displacements in (c) and (d). Since

$$\begin{aligned} \mathbf{J} &= \begin{bmatrix} \frac{L}{2} & 0 \\ 0 & \frac{h}{2} \end{bmatrix}; & \mathbf{J}^{-1} &= \begin{bmatrix} \frac{2}{L} & 0 \\ 0 & \frac{2}{h} \end{bmatrix} \\ \begin{bmatrix} \frac{\partial u}{\partial x} \\ \frac{\partial u}{\partial y} \end{bmatrix} &= \sum_{k=1}^3 \begin{bmatrix} -\frac{h}{2} \frac{2}{L} s \frac{\partial h_k}{\partial r} \\ -h_k \end{bmatrix} \theta_z^k \end{aligned} \quad (e)$$

we obtain

$$\begin{aligned} \begin{bmatrix} \frac{\partial v}{\partial x} \\ \frac{\partial v}{\partial y} \end{bmatrix} &= \sum_{k=1}^3 \begin{bmatrix} \frac{2}{L} \frac{\partial h_k}{\partial r} \\ v_k \end{bmatrix} \\ \text{and} \quad \begin{bmatrix} \frac{\partial v}{\partial x} \\ \frac{\partial v}{\partial y} \end{bmatrix} &= \sum_{k=1}^3 \begin{bmatrix} \frac{2}{L} \frac{\partial h_k}{\partial r} \\ 0 \end{bmatrix} v_k \end{aligned} \quad (f)$$

To analyze the response of the beam in Fig. 5.31 we now use the principle of virtual

work (see (4.12)) with the appropriate strain measures:

$$\int_{-1}^{+1} \int_{-1}^{+1} [\bar{\epsilon}_{xx} \quad \bar{\gamma}_{xy}] \begin{bmatrix} E & 0 \\ 0 & G_k \end{bmatrix} [\epsilon_{xx} \quad \gamma_{xy}] \det J \, ds \, dr = P \bar{v} |_r=0$$

where

$$\begin{aligned} \epsilon_{xx} &= \frac{\partial u}{\partial x}, & \bar{\epsilon}_{xx} &= \frac{\partial \bar{u}}{\partial x} \\ \gamma_{xy} &= \frac{\partial u}{\partial y} + \frac{\partial v}{\partial x}; & \bar{\gamma}_{xy} &= \frac{\partial \bar{u}}{\partial y} + \frac{\partial \bar{v}}{\partial x} \end{aligned}$$

Considering now the relations in (e), (f), (g), and (5.51) we recognize that (g) corresponds to (5.51) if we use  $\beta \equiv \theta_x$ , and  $w \equiv v$ .

In our discussion so far we have considered continuum elements and beam elements separately. However, the very close relationship between these elements should be recognized; the only differences are the kinematic assumption that plane sections initially normal to the neutral axis remain plane, and the stress assumption that stresses normal to the neutral axis are zero. In the beam formulation presented, the kinematic assumption was directly incorporated in the basic geometry and displacement interpolations and the stress assumption was used in the stress-strain law. Since these two assumptions are the only two basic differences between the beam and continuum elements, it appears that the structural element matrices can also be derived from the continuum element matrices by degeneration. We demonstrate this feature in the following example.

**EXAMPLE 5.23:** Assume that the strain-displacement matrix of a four-node plane stress element has been derived. Show how the strain-displacement matrix of a two-node beam element can be established.

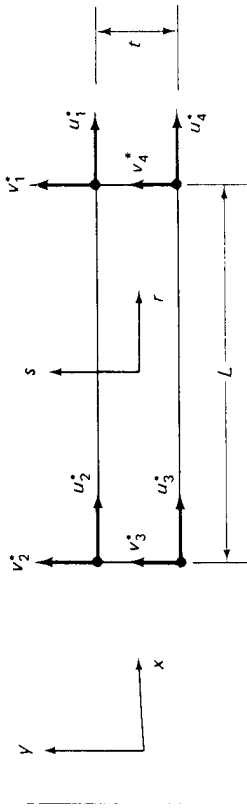
Figure 5.34 shows the plane stress element with its degrees of freedom and the beam element for which we want to establish the strain-displacement matrix. Consider node 2 of the beam element and nodes 2 and 3 of the plane stress element. The entries in the strain-displacement matrix of the plane stress element are

$$\mathbf{B}^* = \begin{bmatrix} u_2^* & v_2^* & u_3^* & v_3^* \\ \cdots & 0 & \frac{1}{2L}(1-r) & -\frac{1}{2L}(1-s) \\ & 0 & -\frac{1}{2L}(1+s) & 0 \\ \frac{1}{2L}(1-r) & -\frac{1}{2L}(1+r) & -\frac{1}{2L}(1-r) & -\frac{1}{2L}(1-s) \end{bmatrix} \quad (\text{a})$$

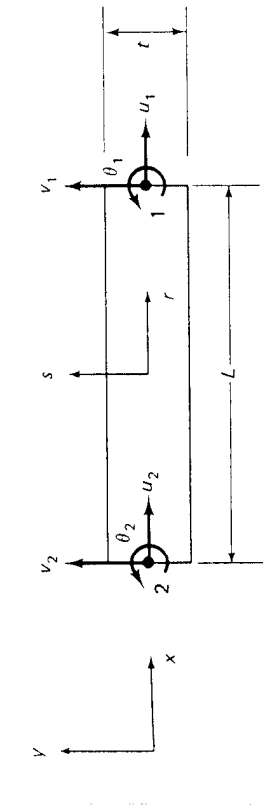
Using now the beam deformation assumptions we have the following kinematic constraints

$$\begin{aligned} u_2^* &= u_2 - \frac{t}{2}\theta_2 \\ u_3^* &= u_2 + \frac{t}{2}\theta_2 \\ v_2^* &= v_2; & v_3^* &= v_2 \end{aligned} \quad (\text{b})$$

These constraints are now substituted to obtain from the elements of  $\mathbf{B}^*$  in (a) the elements of the strain-displacement matrix of the beam. Using the rows of  $\mathbf{B}^*$ , we



(a) Plane stress element



(b) Beam element

FIGURE 5.34 Derivation of beam element from plane stress element.

have with (b),

$$\begin{aligned} -\frac{1}{2L}(1+s)u_2^* - \frac{1}{2L}(1-s)u_3^* &= -\frac{1}{2L}(1+s)\left(u_2 - \frac{t}{2}\theta_2\right) \\ &\quad - \frac{1}{2L}(1-s)\left(u_2 + \frac{t}{2}\theta_2\right) \end{aligned} \quad (\text{c})$$

$$\begin{aligned} \frac{1}{2L}(1-r)v_2^* - \frac{1}{2L}(1+r)v_3^* &= \frac{1}{2L}(1-r)v_2 - \frac{1}{2L}(1+r)v_2 \\ \frac{1}{2L}(1-r)u_2^* - \frac{1}{2L}(1+s)v_2^* - \frac{1}{2L}(1-r)u_3^* - \frac{1}{2L}(1-s)v_3^* &= \frac{1}{2L}(1-r)\left(u_2 - \frac{t}{2}\theta_2\right) - \frac{1}{2L}(1+s)v_2 - \frac{1}{2L}(1-r)\left(u_2 + \frac{t}{2}\theta_2\right) - \frac{1}{2L}(1-s)v_2 \end{aligned} \quad (\text{d})$$

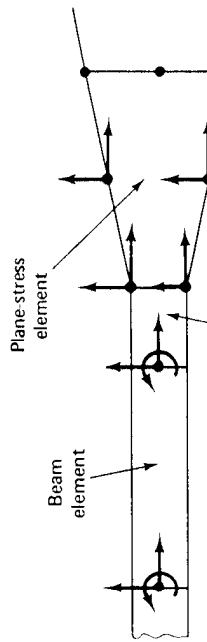
The relations on the r.h.s. of (c), (d), and (e) comprise the entries of the beam strain-displacement matrix

$$\mathbf{B} = \begin{bmatrix} u_2 & v_2 & \theta_2 \\ \cdots & \cdots & \cdots \\ 0 & 0 & 0 \\ 0 & -\frac{1}{L} & 0 \\ 0 & 0 & 0 \\ 0 & -\frac{1}{L} & -\frac{1}{2}(1-r) \end{bmatrix}$$

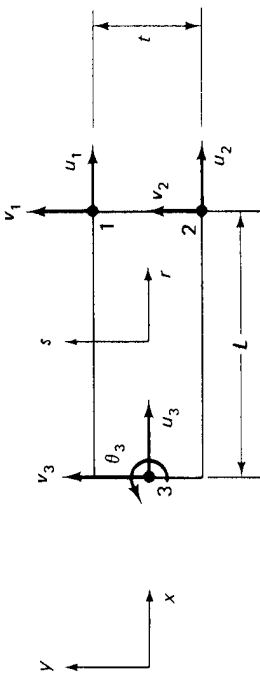
However, the first and third row entries are those that are also obtained using the beam formulation of (5.61) to (5.76). We should note that the zeros in the second row of  $\mathbf{B}$  only express the fact that the strain  $\epsilon_{yy}$  is not included in the formulation. This strain is actually equal to  $-v \epsilon_{xx}$ , because the stress  $\tau_{yy}$  is zero.

The formulation of a structural element using the approach discussed in the above example is computationally inefficient, and is certainly not recommended for general analysis. However, it is instructive to study this approach and recognize that the structural element matrices can in principle be obtained from continuum element matrices by imposing the appropriate static and kinematic assumptions. Moreover, this formulation directly suggests the construction of transition elements that can be used in an effective manner to couple structural and continuum elements without the use of constraint equations (see Fig. 5.35(a)). To demonstrate the formulation of transition elements, we consider in the following example a simple transition beam element.

**EXAMPLE 5.24:** Establish the displacement and strain-displacement interpolation matrices of the transition element shown in Fig. 5.35.



(a) Beam transition element connecting beam and plane stress elements



(b) Transition element

FIGURE 5.35 Two-dimensional beam transition element.

We define the nodal point displacement vector of the element as

$$\mathbf{u}^T = [u_1 \quad v_1 \quad u_2 \quad v_2 \quad u_3 \quad v_3 \quad \theta_3]$$

Since at  $r = +1$  we have plane stress element degrees of freedom, the interpolation functions corresponding to nodes 1 and 2 are (see Fig. 5.5)

$$h_1 = \frac{1}{4}(1+r)(1+s); \quad h_2 = \frac{1}{4}(1+r)(1-s)$$

Node 3 is a beam node and the interpolation function is (see Fig. 5.4)

$$h_3 = \frac{1}{2}(1-r)$$

The displacements of the element are thus

$$\mathbf{u}(r, s) = h_1 u_1 + h_2 u_2 + h_3 u_3 - \frac{t}{2} s h_3 \theta_3$$

$\mathbf{v}(r, s) = h_1 v_1 + h_2 v_2 + h_3 v_3$

Hence, corresponding to the displacement vector in (a) we have

$$\mathbf{H} = \begin{bmatrix} h_1 & 0 & h_2 & 0 & h_3 & 0 & -\frac{t}{2} s h_3 \\ 0 & h_1 & 0 & h_2 & 0 & h_3 & 0 \end{bmatrix}$$

The coordinate interpolation is the same as that of the four-node plane stress element:

$$x(r, s) = \frac{1}{2}(1+r)L$$

$$y(r, s) = \frac{s}{2}t$$

$$\text{Hence } \mathbf{J} = \begin{bmatrix} \frac{L}{2} & 0 \\ 0 & \frac{t}{2} \end{bmatrix}; \quad \mathbf{J}^{-1} = \begin{bmatrix} \frac{2}{L} & 0 \\ 0 & \frac{2}{t} \end{bmatrix}$$

Using (5.25) we thus obtain

$$\mathbf{B} = \begin{bmatrix} \frac{1}{2L}(1+s) & 0 & \frac{1}{2L}(1-s) & 0 & -\frac{1}{L} & 0 & \frac{t}{2L}s \\ 0 & \frac{1}{2t}(1+r) & 0 & -\frac{1}{2t}(1+r) & 0 & 0 & 0 \\ \frac{1}{2t}(1+r) & \frac{1}{2L}(1+s) & -\frac{1}{2t}(1+r) & \frac{1}{2L}(1-s) & 0 & -\frac{1}{L} & -\frac{1}{2}(1-r) \end{bmatrix}$$

We may finally note that the last three columns of the  $\mathbf{B}$ -matrix could also have been derived as described in Example 5.23.

The above presented beam elements represent an alternative to the classical Hermitian beam elements (see Example 4.12), and it must be questioned under what circumstances these beam elements are effective, since for a cubic displacement description twice as many degrees of freedom are required. There is no doubt that in the linear analysis of straight thin beams, the Hermitian elements are much more effective. However, the use of the above elements can be efficient when shear deformations are important, in the analysis of curved structures, in the analysis of stiffened shells (because the beam elements representing the stiffeners are compatible with the shell elements discussed in the next section) and in geometric nonlinear analysis, which is discussed in Section 6.3.4.

#### 5.4.2 Plate and Shell Elements

The same procedures that have been employed in the previous section to formulate beam elements can also directly be used to establish effective plate and shell elements.<sup>21–25,27,28</sup> In the following description we proceed as before; namely, we first discuss the formulation of plate elements, which may be regarded to be simple flat shell elements, and then we proceed to summarize the formulation of general shell elements.

The general shell element formulation presented later contains as a special case the calculation of plate elements that are based on the theory of plates with transverse shear deformations included. This theory uses the assumption that "particles of the plate originally on a line that is normal to the undeformed middle surface remain on a straight line during deformation, but this line is not necessarily normal to the deformed middle surface." With this assumption, the displacement components of a point of coordinates  $x, y, z$  are in the small displacement bending theory:

$$u = z\beta_x(x, y); \quad v = -z\beta_y(x, y); \quad w = w(x, y) \quad (5.78)$$

where  $w$  is the transverse displacement,  $\beta_x$  and  $\beta_y$  are the rotations of the normal to the undeformed middle surface in the  $x$ - $z$  and  $y$ - $z$  planes, respectively, see Fig. 5.36. It is instructive to note that in the Kirchhoff plate theory excluding shear deformations,  $\beta_x = -w_x$  and  $\beta_y = w_y$ .

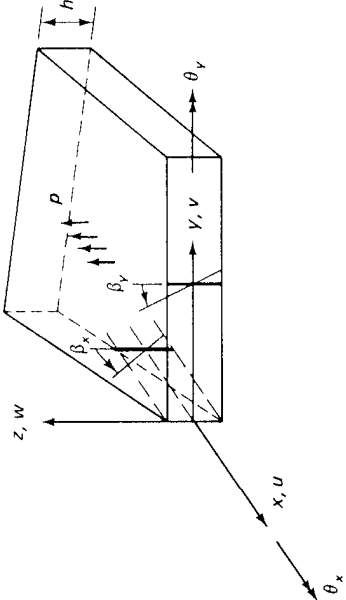


FIGURE 5.36 Deformation assumptions in analysis of plate including shear deformations.

Considering the plate in Fig. 5.36 the bending strains  $\epsilon_{xx}, \epsilon_{yy}, \gamma_{xy}$  vary linearly through the plate thickness and are given by the curvatures of the plate using (5.78),

$$\begin{bmatrix} \epsilon_{xx} \\ \epsilon_{yy} \\ \gamma_{xy} \end{bmatrix} = z \begin{bmatrix} \frac{\partial \beta_x}{\partial x} \\ -\frac{\partial \beta_y}{\partial y} \\ \frac{\partial \beta_x}{\partial y} - \frac{\partial \beta_y}{\partial x} \end{bmatrix} \quad (5.79)$$

whereas the transverse shear strains are assumed to be constant through the thickness

$$\begin{bmatrix} \gamma_{yz} \\ \gamma_{zx} \end{bmatrix} = \begin{bmatrix} \frac{\partial w}{\partial y} - \beta_y \\ \frac{\partial w}{\partial x} + \beta_x \end{bmatrix} \quad (5.80)$$

The state of stress in the plate corresponds to plane stress conditions, i.e.,

$\tau_{zz} = 0$ . Considering an isotropic material we can thus write

$$\begin{bmatrix} \tau_{xx} \\ \tau_{yy} \\ \tau_{xy} \end{bmatrix} = z \frac{E}{1-\nu^2} \begin{bmatrix} 1 & \nu & 0 \\ \nu & 1 & 0 \\ 0 & 0 & \frac{1-\nu}{2} \end{bmatrix} \begin{bmatrix} \frac{\partial \beta_x}{\partial x} \\ -\frac{\partial \beta_y}{\partial y} \\ \frac{\partial \beta_x}{\partial y} - \frac{\partial \beta_y}{\partial x} \end{bmatrix} \quad (5.81)$$

$$\begin{bmatrix} \tau_{yz} \\ \tau_{zx} \end{bmatrix} = \frac{E}{2(1+\nu)} \begin{bmatrix} \frac{\partial w}{\partial y} - \beta_y \\ \frac{\partial w}{\partial x} + \beta_x \end{bmatrix} \quad (5.82)$$

To establish the element equilibrium equations we now proceed as in the formulation of the special two-dimensional beam element of rectangular cross-section (see (5.50) to (5.58)). Considering the plate element the expression for the total potential  $\Pi$  is, with  $p$  equal to the transverse loading per unit area,

$$\Pi = \frac{1}{2} \int_A \int_{-h/2}^{h/2} [\epsilon_{xx} \epsilon_{yy} \gamma_{xy}] \begin{bmatrix} \tau_{xx} \\ \tau_{yy} \\ \tau_{xy} \end{bmatrix} dz dA + \frac{k}{2} \int_A \int_{-h/2}^{h/2} [\gamma_{yz} \gamma_{zx}] \begin{bmatrix} \tau_{yz} \\ \tau_{zx} \end{bmatrix} dz dA - \int_A wp dA \quad (5.83)$$

where  $k$  is again a constant to account for the actual nonuniformity of the shearing stresses. Substituting from (5.79) to (5.83) into (5.83) we thus obtain

$$\Pi = \frac{1}{2} \int_A \mathbf{k}^T \mathbf{C}_b \mathbf{k} dA + \frac{1}{2} \int_A \boldsymbol{\gamma}^T \mathbf{C}_b \boldsymbol{\gamma} dA - \int_A wp dA \quad (5.84)$$

$$\text{where } \mathbf{k} = \begin{bmatrix} \frac{\partial \beta_x}{\partial x} \\ -\frac{\partial \beta_y}{\partial y} \\ \frac{\partial \beta_x}{\partial y} - \frac{\partial \beta_y}{\partial x} \end{bmatrix}; \quad \boldsymbol{\gamma} = \begin{bmatrix} \frac{\partial w}{\partial y} - \beta_y \\ \frac{\partial w}{\partial x} + \beta_x \end{bmatrix} \quad (5.85)$$

$$\mathbf{C}_b = \frac{Eh^3}{12(1-\nu^2)} \begin{bmatrix} 1 & \nu & 0 \\ \nu & 1 & 0 \\ 0 & 0 & \frac{1-\nu}{2} \end{bmatrix}; \quad \mathbf{C}_s = \frac{Ehk}{2(1+\nu)} \begin{bmatrix} 1 & 0 \\ 0 & 1 \end{bmatrix} \quad (5.86)$$

Equilibrium requires that  $\Pi$  is stationary, i.e.,  $\delta\Pi = 0$  where it must be recognized that  $w, \beta_x$ , and  $\beta_y$  are independent variables. Hence, in the finite element analysis of an assemblage of elements, we only need to enforce interelement continuity on  $w, \beta_x$  and  $\beta_y$ , which can readily be achieved in the same way as in the isoparametric finite element analysis of solids.

Using that the total potential must be stationary, we obtain

$$\int_A \delta \mathbf{k}^T \mathbf{C}_b \mathbf{k} dA + \int_A \delta \boldsymbol{\gamma}^T \mathbf{C}_b \boldsymbol{\gamma} dA - \int_A \delta w p dA = 0 \quad (5.88)$$

which may be regarded as the principle of virtual displacements for the plate element.

For the finite element analysis we use

$$\begin{aligned} w &= \sum_{i=1}^q h_i w_i; & \beta_x &= \sum_{i=1}^q h_i \theta_x^i \\ \beta_y &= \sum_{i=1}^q h_i \theta_y^i \end{aligned} \quad (5.89)$$

where the  $h_i$  are the interpolation functions and  $q$  is the number of nodes of the element. With these interpolations we can now proceed in the usual way, and all concepts pertaining to the isoparametric finite elements discussed earlier are directly applicable. For example, some interpolation functions applicable to the formulation of plate elements are listed in Fig. 5.5, and triangular elements can be established as discussed in Section 5.3.2. Since the interpolation functions are given in terms of the isoparametric coordinates  $(r, s)$ , we can also directly calculate the matrices of plate elements that are curved in their plane (to model, for example, a circular plate).

We demonstrate the formulation of a simple 4-node element in the following example.

**EXAMPLE 5.25:** Establish the expressions used in the evaluation of the stiffness matrix of the four-node plate element shown in Fig. 5.37.

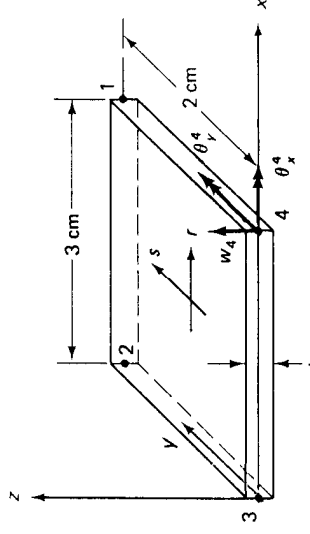


FIGURE 5.37 A four-node plate element.

The calculations are very similar to those performed in the formulation of the two-dimensional plane stress element in Example 5.5.

For the element in Fig. 5.37 we have (see Example 5.3),

$$\mathbf{J} = \begin{bmatrix} 2 & 0 \\ 0 & 1 \end{bmatrix}$$

and then, using the interpolation functions defined in Fig. 5.5:

$$\begin{bmatrix} \frac{\partial w}{\partial x} \\ \frac{\partial w}{\partial y} \end{bmatrix} = \frac{1}{4} \begin{bmatrix} \frac{2}{3} & 0 & (1+s) & -(1+s) & (1-s) & -(1-s) \\ 0 & 1 & (1+r) & -(1-r) & (1-r) & -(1+r) \end{bmatrix} \begin{bmatrix} w_1 \\ w_2 \\ w_3 \\ w_4 \end{bmatrix}$$

with analogous expressions for the derivatives of  $\beta_x$  and  $\beta_y$ . Thus, if we use the

following notation

$$\begin{aligned} \mathbf{K}(r, s) &= \mathbf{B}_x \hat{\mathbf{u}} \\ \mathbf{Y}(r, s) &= \mathbf{B}_y \hat{\mathbf{u}} \\ \mathbf{w}(r, s) &= \mathbf{H}_w \hat{\mathbf{u}} \end{aligned} \quad (5.89)$$

where

$$\begin{aligned} \hat{\mathbf{u}}^T &= [w_1 \quad \theta_x^1 \quad \theta_y^1 \quad w_2 \quad \dots \quad \theta_x^4] \\ \text{We have} \quad \mathbf{B}_x &= \begin{bmatrix} 0 & 0 & \frac{1}{6}(1+s) & \dots & \frac{1}{6}(1-s) \\ 0 & -\frac{1}{4}(1+r) & 0 & \dots & 0 \\ 0 & -\frac{1}{6}(1+s) & \frac{1}{4}(1+r) & \dots & -\frac{1}{4}(1+r) \\ \vdots & \vdots & \vdots & \ddots & \vdots \\ \mathbf{B}_y &= \begin{bmatrix} \frac{1}{4}(1+r) & -\frac{1}{4}(1+r)(1+s) & 0 & \dots & 0 \\ -\frac{1}{6}(1+s) & 0 & \frac{1}{4}(1+r)(1+s) & \dots & \frac{1}{4}(1+r)(1-s) \\ \vdots & \vdots & \vdots & \ddots & \vdots \\ \mathbf{H}_w &= \frac{1}{4}((1+r)(1+s)) \quad \vdots \quad \vdots \quad (1+r)(1-s) \quad \vdots \quad 0 \end{bmatrix} \end{aligned}$$

The element stiffness matrix is then

$$\mathbf{K} = \frac{3}{2} \int_{-1}^{+1} \int_{-1}^{+1} (\mathbf{B}_x^T \mathbf{C}_b \mathbf{B}_x + \mathbf{B}_y^T \mathbf{C}_b \mathbf{B}_y) dr ds \quad (a)$$

and the consistent load vector is

$$\mathbf{R}_S = \frac{3}{2} \int_{-1}^{+1} \int_{-1}^{+1} \mathbf{H}_w^T \rho dr ds \quad (b)$$

where the integrals in (a) and (b) are evaluated using numerical integration (see Section 5.7).

The above isoparametric elements are effective if used as high-order elements and specifically the 9-node and 16-node quadrilateral Lagrangian elements can be employed efficiently. As for the beam element considered above, the low-order elements are much too stiff in modeling thin plates. However, the behavior of these elements can again be improved by neglecting the shear strain energy in the formulation and imposing the Kirchhoff assumption that the shear deformations are zero at discrete points of the element.

As in the discussion of the beam element in Section 5.4.1, where we regarded the formulation of the matrices corresponding to a two-dimensional beam of rectangular cross-section as a special case of a general three-dimensional formulation, we now can regard the formulation of the plate elements above as a special case of a formulation of a general three-dimensional shell element. In this general shell element formulation, we employ the concepts discussed already in Section 5.4.1, and we follow the same formulative steps.

As in the formulation of the continuum and beam elements, we can formulate the shell element for a variable number of nodes. Figure 5.38 shows a nine-node shell element. Using the natural coordinates  $r$ ,  $s$ , and  $t$ , the Cartesian coordinates of a point in the element with  $q$  nodal points are, before and after deformations:

$$\begin{aligned} x(r, s, t) &= \sum_{k=1}^q h_k x_k + \frac{t}{2} \sum_{k=1}^q a_k h_k \epsilon_x V_{nx} \\ y(r, s, t) &= \sum_{k=1}^q h_k y_k + \frac{t}{2} \sum_{k=1}^q a_k h_k \epsilon_y V_{ny} \\ z(r, s, t) &= \sum_{k=1}^q h_k z_k + \frac{t}{2} \sum_{k=1}^q a_k h_k \epsilon_z V_{nz} \end{aligned} \quad (5.90)$$

define two unit vectors  ${}^0\mathbf{V}_1^k$  and  ${}^0\mathbf{V}_2^k$  that are orthogonal to  ${}^0\mathbf{V}_n^k$ :

$${}^0\mathbf{V}_1^k = \frac{\mathbf{e}_y \times {}^0\mathbf{V}_n^k}{\|\mathbf{e}_y \times {}^0\mathbf{V}_n^k\|} \quad (5.93a)$$

where  $\mathbf{e}_y$  is a unit vector into the direction of the  $y$ -axis. (For the special case  ${}^0\mathbf{V}_n^k$  parallel to  $\mathbf{e}_y$ , we may simply use  ${}^0\mathbf{V}_1^k$  equal to  $\mathbf{e}_r$ .) We can now obtain  ${}^0\mathbf{V}_2^k$ ,

$${}^0\mathbf{V}_2^k = {}^0\mathbf{V}_n^k \times {}^0\mathbf{V}_1^k \quad (5.93b)$$

Let  $\alpha_k$  and  $\beta_k$  be the rotations of the normal vector  ${}^0\mathbf{V}_n^k$  about the vectors  ${}^0\mathbf{V}_1^k$  and  ${}^0\mathbf{V}_2^k$ . We then have, because  $\alpha_k$  and  $\beta_k$  are small angles,

$${}^0\mathbf{V}_n^k = -{}^0\mathbf{V}_2^k \alpha_k + {}^0\mathbf{V}_1^k \beta_k \quad (5.94)$$

This relationship can readily be proven when  ${}^0\mathbf{V}_1 = \mathbf{e}_x$ ,  ${}^0\mathbf{V}_2 = \mathbf{e}_y$ , and  ${}^0\mathbf{V}_n = \mathbf{e}_z$ , but since these vectors are tensors, the relationship must also hold in general (see Section 2.6). Substituting from (5.94) into (5.91) we thus obtain

$$\begin{aligned} u(r, s, t) &= \sum_{k=1}^q h_k u_k + \frac{t}{2} \sum_{k=1}^q a_k h_k (-{}^0\mathbf{V}_{2,k}^k \alpha_k + {}^0\mathbf{V}_{1,k}^k \beta_k) \\ v(r, s, t) &= \sum_{k=1}^q h_k v_k + \frac{t}{2} \sum_{k=1}^q a_k h_k (-{}^0\mathbf{V}_{2,k}^k \alpha_k + {}^0\mathbf{V}_{1,k}^k \beta_k) \\ w(r, s, t) &= \sum_{k=1}^q h_k w_k + \frac{t}{2} \sum_{k=1}^q a_k h_k (-{}^0\mathbf{V}_{2,k}^k \alpha_k + {}^0\mathbf{V}_{1,k}^k \beta_k) \end{aligned} \quad (5.95)$$

With the element displacements and coordinates defined in (5.95) and (5.90), we can now proceed as usual with the evaluation of the element matrices. The entries in the displacement interpolation matrix  $\mathbf{H}$  of the shell element are given in (5.95), and the entries in the strain-displacement interpolation matrix can be calculated using the procedures described already in the formulation of the beam element (see Section 5.4.1).

To evaluate the strain-displacement matrix, we obtain from (5.95)

$$\begin{bmatrix} \frac{\partial u}{\partial r} \\ \frac{\partial u}{\partial s} \\ \frac{\partial u}{\partial t} \end{bmatrix} = \sum_{k=1}^q \begin{bmatrix} \frac{\partial h_k}{\partial r} [1 & {}^0\mathbf{V}_{1,k}^k & {}^0\mathbf{V}_{2,k}^k] \\ \frac{\partial h_k}{\partial s} [1 & {}^0\mathbf{V}_{1,k}^k & {}^0\mathbf{V}_{2,k}^k] \\ h_k [0 & {}^0\mathbf{V}_{1,k}^k & {}^0\mathbf{V}_{2,k}^k] \end{bmatrix} \begin{bmatrix} u_k \\ v_k \\ w_k \end{bmatrix} \quad (5.96)$$

and the derivatives of  $v$  and  $w$  are given by simply substituting for  $u$  and  $x$  the variables  $v$  and  $w$ ,  $z$ , respectively. In (5.96) we use the notation

$${}^0\mathbf{V}_1^k = -\frac{1}{2} a_k {}^0\mathbf{V}_2^k; \quad {}^0\mathbf{V}_2^k = \frac{1}{2} a_k {}^0\mathbf{V}_1^k \quad (5.97)$$

To obtain the displacement derivatives corresponding to the Cartesian coordinates  $x$ ,  $y$ ,  $z$ , we use the standard transformation

$$\frac{\partial}{\partial x} = \mathbf{J}^{-1} \frac{\partial}{\partial r} \quad (5.98)$$

where the Jacobian matrix  $\mathbf{J}$  contains the derivatives of the coordinates  $x$ ,  $y$ ,  $z$  with respect to the natural coordinates  $r$ ,  $s$ , and  $t$ . Substituting from (5.96)

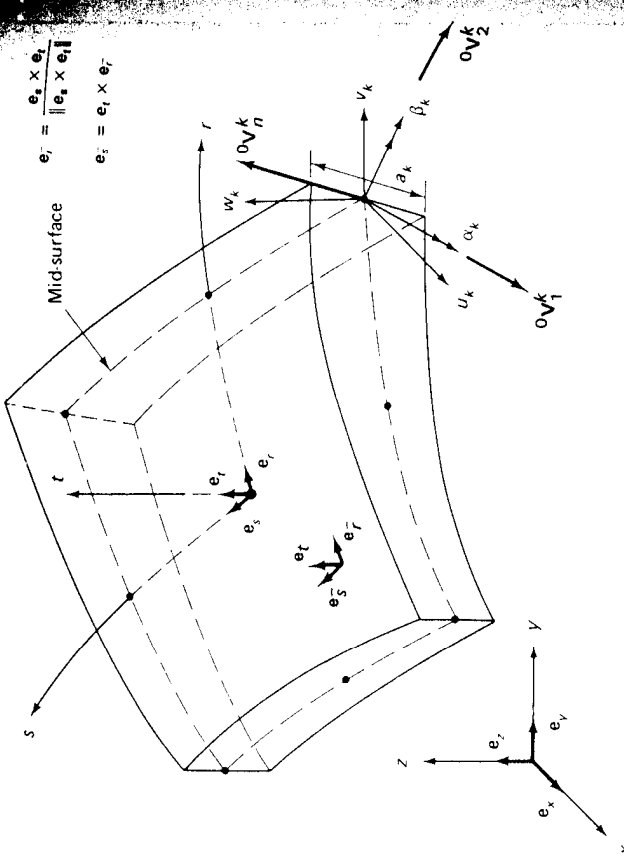


**FIGURE 5.38** Nine-node shell element. Note that the unit vectors  $\mathbf{e}_r$ ,  $\mathbf{e}_s$ ,  $\mathbf{e}_t$  are in general not orthogonal, whereas  $\mathbf{e}_r$ ,  $\mathbf{e}_s$ ,  $\mathbf{e}_t$  are orthogonal.

where the  $h_k(r, s)$  are the interpolation functions summarized in Fig. 5.5 and

- $\ell_x$ ,  $\ell_y$ ,  $\ell_z$  = Cartesian coordinates of any point in the element
- $\ell_{x_k}$ ,  $\ell_{y_k}$ ,  $\ell_{z_k}$  = Cartesian coordinates of nodal point  $k$
- $a_k$  = Thickness of shell in  $t$  direction at nodal point  $k$
- ${}^0\mathbf{V}_{nx}^k$ ,  ${}^0\mathbf{V}_{ny}^k$ ,  ${}^0\mathbf{V}_{nz}^k$  = Components of unit vector  ${}^0\mathbf{V}_n^k$  "normal" to the shell mid-surface in direction  $t$  at nodal point  $k$ \*

and the left superscript  $\ell$  denotes, as in the general beam formulation, the configuration of the element; i.e.  $\ell = 0$  and  $1$  denote the original and final configurations of the shell element. Hence using (5.90), the displacement components are

$$u(r, s, t) = \sum_{k=1}^q h_k u_k + \frac{t}{2} \sum_{k=1}^q a_k h_k {}^0\mathbf{V}_{nx}^k \quad (5.91)$$

$$v(r, s, t) = \sum_{k=1}^q h_k v_k + \frac{t}{2} \sum_{k=1}^q a_k h_k {}^0\mathbf{V}_{ny}^k \quad (5.92)$$

$$w(r, s, t) = \sum_{k=1}^q h_k w_k + \frac{t}{2} \sum_{k=1}^q a_k h_k {}^0\mathbf{V}_{nz}^k \quad (5.93)$$

where  $\mathbf{V}_n^k$  stores the increments in the direction cosines of  ${}^0\mathbf{V}_n^k$ .

$$\mathbf{V}_n^k = {}^1\mathbf{V}_n^k - {}^0\mathbf{V}_n^k \quad (5.94)$$

The components of  $\mathbf{V}_n^k$  can be expressed in terms of rotations at the nodal point  $k$ ; however, there is no unique way of proceeding. An efficient way is to

\* We call  ${}^0\mathbf{V}_n^k$  the *normal* vector although it may not be exactly normal to the mid-surface of the shell in the original configuration, and in the final configuration (for example, because of shear deformations).

into (5.98), we obtain

$$\begin{bmatrix} \frac{\partial u}{\partial x} \\ \frac{\partial u}{\partial y} \\ \frac{\partial u}{\partial z} \end{bmatrix} = \sum_{k=1}^q \begin{bmatrix} \frac{\partial h_k}{\partial x} & g_{1x}^k G_x^k & g_{2x}^k G_x^k \\ \frac{\partial h_k}{\partial y} & g_{1y}^k G_y^k & g_{2y}^k G_y^k \\ \frac{\partial h_k}{\partial z} & g_{1z}^k G_z^k & g_{2z}^k G_z^k \end{bmatrix} \begin{bmatrix} u_k \\ \alpha_k \\ \beta_k \end{bmatrix} \quad (5.99)$$

and the derivatives of  $v$  and  $w$  are obtained in an analogous manner. In (5.99) we have

$$\begin{aligned} \frac{\partial h_k}{\partial x} &= J_{11}^{-1} \frac{\partial h_k}{\partial r} + J_{12}^{-1} \frac{\partial h_k}{\partial s} \\ G_x^k &= t \left( J_{11}^{-1} \frac{\partial h_k}{\partial r} + J_{12}^{-1} \frac{\partial h_k}{\partial s} \right) + J_{13}^{-1} h_k \end{aligned}$$

where  $J_{ij}^{-1}$  is element  $(i,j)$  of  $\mathbf{J}^{-1}$ , and so on.

With the displacement derivatives defined in (5.99) we can now directly assemble the strain-displacement matrix  $\mathbf{B}$  of a shell element. Assuming that the rows in this matrix correspond to all six global Cartesian strain components,  $\epsilon_{xx}, \epsilon_{yy}, \dots, \gamma_{zz}$ , the entries in  $\mathbf{B}$  are constructed in the usual way (see Section 5.3), but then the stress-strain law must contain the shell assumption that the stress normal to the shell surface is zero. Thus, if  $\boldsymbol{\tau}$  and  $\boldsymbol{\epsilon}$  store the Cartesian stress and strain components, we use

$$\boldsymbol{\tau} = \mathbf{C}_{sh} \boldsymbol{\epsilon} \quad (5.100)$$

where

$$\begin{aligned} \boldsymbol{\tau}^T &= [\tau_{xx} \ \tau_{yy} \ \tau_{zz} \ \tau_{xy} \ \tau_{yz} \ \tau_{zx}] \\ \boldsymbol{\epsilon}^T &= [\epsilon_{xx} \ \epsilon_{yy} \ \epsilon_{zz} \ \gamma_{xy} \ \gamma_{yz} \ \gamma_{zx}] \\ &\quad \begin{bmatrix} 1 & v & 0 & 0 & 0 & 0 \\ 0 & 1 & 0 & 0 & 0 & 0 \\ 0 & 0 & 0 & 0 & 0 & 0 \end{bmatrix} \\ \mathbf{C}_{sh} &= \mathbf{Q}_{sh}^T \left( \frac{E}{1-v^2} \right) \begin{bmatrix} 1-v & 0 & 0 \\ \frac{1-v}{2} & 1-v & 0 \\ symmetric & k \frac{1-v}{2} & 0 \\ & & k \frac{1-v}{2} \end{bmatrix} \mathbf{Q}_{sh} \quad (5.101) \end{aligned}$$

and  $\mathbf{Q}_{sh}$  represents a matrix that transforms the stress-strain law from an  $\bar{r}, \bar{s}, \bar{t}$  Cartesian shell-aligned coordinate system to the global Cartesian coordinate system. The elements of the matrix  $\mathbf{Q}_{sh}$  are obtained from the direction cosines of the  $\bar{r}, \bar{s}, \bar{t}$  coordinate axes measured in the  $x, y, z$  coordinate directions,

$$\mathbf{Q}_{sh} = \begin{bmatrix} l_1^2 & m_1^2 & n_1^2 & l_1 m_1 & m_1 n_1 & n_1 l_1 \\ l_2^2 & m_2^2 & n_2^2 & l_2 m_2 & m_2 n_2 & n_2 l_2 \\ l_3^2 & m_3^2 & n_3^2 & l_3 m_3 & m_3 n_3 & n_3 l_3 \\ 2l_1 l_2 & 2m_1 m_2 & 2n_1 n_2 & l_1 m_2 + l_2 m_1 & m_1 n_2 + m_2 n_1 & n_1 l_2 + n_2 l_1 \\ 2l_1 l_3 & 2m_1 m_3 & 2n_1 n_3 & l_1 m_3 + l_3 m_1 & m_1 n_3 + m_3 n_1 & n_1 l_3 + n_3 l_1 \\ 2l_2 l_3 & 2m_2 m_3 & 2n_2 n_3 & l_2 m_3 + l_3 m_2 & m_2 n_3 + m_3 n_2 & n_2 l_3 + n_3 l_2 \\ 2l_1 l_2 l_3 & 2m_1 m_2 m_3 & 2n_1 n_2 n_3 & l_1 m_1 + l_2 m_2 + l_3 m_3 & m_1 n_1 + m_2 n_2 + m_3 n_3 & n_1 l_1 + n_2 l_2 + n_3 l_3 \end{bmatrix} \quad (5.102)$$

$$\begin{aligned} I_1 &= \cos(\mathbf{e}_x, \mathbf{e}_{\bar{r}}) & m_1 &= \cos(\mathbf{e}_y, \mathbf{e}_{\bar{r}}) & n_1 &= \cos(\mathbf{e}_z, \mathbf{e}_{\bar{r}}) \\ I_2 &= \cos(\mathbf{e}_x, \mathbf{e}_{\bar{s}}) & m_2 &= \cos(\mathbf{e}_y, \mathbf{e}_{\bar{s}}) & n_2 &= \cos(\mathbf{e}_z, \mathbf{e}_{\bar{s}}) \\ I_3 &= \cos(\mathbf{e}_x, \mathbf{e}_{\bar{t}}) & m_3 &= \cos(\mathbf{e}_y, \mathbf{e}_{\bar{t}}) & n_3 &= \cos(\mathbf{e}_z, \mathbf{e}_{\bar{t}}) \end{aligned}$$

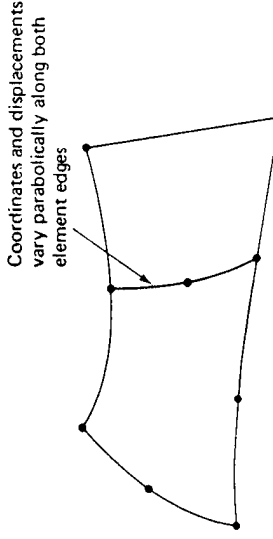
and the relation in (5.101) corresponds to a fourth-order tensor transformation as described in Section 2.6.

It follows that in the analysis of a general shell the matrix  $\mathbf{Q}_{sh}$  may have to be evaluated anew at each integration point that is employed in the numerical integration of the stiffness matrix (see Section 5.7). However, when special shells are considered and, in particular, when a plate is analyzed, the transformation matrix and the stress-strain matrix  $\mathbf{C}_{sh}$  need only be evaluated at specific points and can then be employed repetitively. For example, in the analysis of an assemblage of flat plates, the stress-strain matrix  $\mathbf{C}_{sh}$  need only be calculated once for each flat structural part.

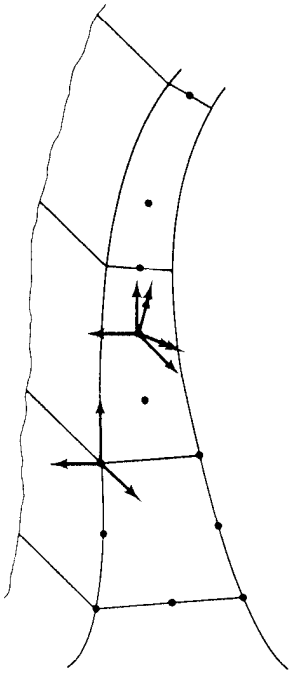
In the above formulation we assumed that the strain-displacement matrix is formulated corresponding to the Cartesian strain components, which can be directly established using the derivatives in (5.99). Alternatively, we could calculate the strain components corresponding to coordinate axes aligned with the shell element midsurface and establish a strain-displacement matrix for these strain components, as we did in the formulation of the general beam element in Section 5.4.1. The relative computational efficiency of these two approaches depends on whether it is more effective to transform the strain components (which always differ at the integration points) or to transform the stress-strain law.

It is instructive to compare the above shell element formulation with a formulation in which flat elements with a superimposed plate bending and membrane stress behavior are employed (see Section 4.2.3). To identify the differences, assume that the general shell element is used as a flat element in the modeling of a shell; then the stiffness matrix of this element could also be obtained by superimposing the plate bending stiffness matrix derived in (5.78) to (5.88) (see Example 5.23) and the plane stress stiffness matrix discussed in Section 5.3. Thus, in this case, the general shell element reduces to a plate bending element plus a plane stress element, but a computational difference lies in the fact that these element matrices are calculated by integrating numerically only in the  $r,s$  element midplanes, whereas in the shell element stiffness calculation numerical integration is also performed in the  $t$ -direction (unless the general formulation is modified for this special case).

The major advantage of the general shell element formulation can now be recognized; namely, using this formulation the geometry of any shell surface can be represented accurately and all displacement compatibility conditions between elements are satisfied directly and in an effective manner. This generality of the analysis capabilities is increased still further if the element is also implemented as a transition element, which can be formulated analogously to the beam transition element discussed in Section 5.4.1. As illustrated in Fig. 5.39, with a shell transition element it is possible to model shell intersections and shell-to-solid transitions using compatible element idealizations without the use of special constraint equations. The above features of generality and accuracy in the representation of a shell geometry can be particularly important in



(a) Shell intersections



(b) Solid to shell intersection

the geometric nonlinear analysis of shell structures, in which any change in the shell geometry must be accounted for accurately. We discuss the formulation of the general shell element for nonlinear analysis in Section 6.3.5.

## 5.5 CONVERGENCE CONSIDERATIONS

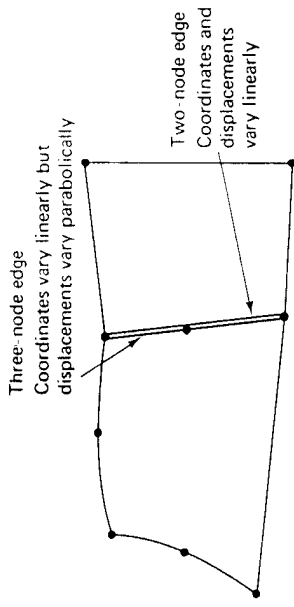
In Section 4.2.5 we discussed the requirements for monotonic convergence of a finite element analysis. The two requirements are that the elements must be compatible and complete. We now want to investigate whether the continuum and structural isoparametric element formulations satisfy these convergence criteria.

### 5.5.1 Continuum Elements

To investigate the compatibility of an element assemblage, we need to consider each edge, or rather face, between adjacent elements. For compatibility it is necessary that the coordinates and the displacements of the elements at the common face be the same. This is the case if the elements have the same nodes on the common face and the coordinates and displacements along the common face are in each element defined by the same interpolation functions. Examples of adjacent elements that preserve compatibility, and that do not, are shown in Fig. 5.40.

Completeness requires that the rigid body displacements and constant strain states be possible. One way to investigate whether these criteria are satisfied for an isoparametric element is to follow the considerations given in Section 4.2.5. However, we now want to get more insight into the specific conditions that per-

(a) Compatible elements



(b) Incompatible elements



**FIGURE 5.40** *Compatible and incompatible two-dimensional elements.*

tain to the isoparametric formulation of a continuum element. For this purpose we consider in the following a three-dimensional continuum element because the one- and two-dimensional elements can be regarded as special cases of these three-dimensional considerations. For the rigid body and constant strain states to be possible, the following displacements defined in the local element coordinate system must be contained in the isoparametric formulation

$$\left. \begin{aligned} u &= a_1 + b_1x + c_1y + d_1z \\ v &= a_2 + b_2x + c_2y + d_2z \\ w &= a_3 + b_3x + c_3y + d_3z \end{aligned} \right\} \quad (5.103)$$

where the  $a_i, b_j, c$  and  $d_j, j = 1, 2, 3$ , are constants. The nodal point displacements corresponding to this displacement field are

$$\left. \begin{aligned} u_i &= a_1 + b_{1i}x_i + c_{1i}y_i + d_{1i}z_i \\ v_i &= a_2 + b_{2i}x_i + c_{2i}y_i + d_{2i}z_i \\ w_i &= a_3 + b_{3i}x_i + c_{3i}y_i + d_{3i}z_i \end{aligned} \right\} \quad (5.104)$$

where  $i = 1, \dots, q$  and  $q = \text{number of nodes}$ . To show that the displacements in (5.103) are possible when the isoparametric formulation is employed, assume that the nodal point displacements of the element are given by (5.104). We should find that, with these nodal point displacements, the displacements in the isoparametric formulation are actually those given in (5.103). In the isopara-

metric formulation we have the displacement interpolation

$$u = \sum_{i=1}^q h_i \mu_i; \quad v = \sum_{i=1}^q h_i \nu_i; \quad w = \sum_{i=1}^q h_i \omega_i$$

which using (5.104) reduces to

$$\left. \begin{aligned} u &= a_1 \sum_{i=1}^q h_i + b_1 \sum_{i=1}^q h_i x_i + c_1 \sum_{i=1}^q h_i y_i + d_1 \sum_{i=1}^q h_i z_i \\ v &= a_2 \sum_{i=1}^q h_i + b_2 \sum_{i=1}^q h_i x_i + c_2 \sum_{i=1}^q h_i y_i + d_2 \sum_{i=1}^q h_i z_i \\ w &= a_3 \sum_{i=1}^q h_i + b_3 \sum_{i=1}^q h_i x_i + c_3 \sum_{i=1}^q h_i y_i + d_3 \sum_{i=1}^q h_i z_i \end{aligned} \right\} \quad (5.105)$$

Since in the isoparametric formulation the coordinates are interpolated in the same way as the displacements, we can use (5.18) to obtain from (5.105)

$$\begin{aligned} u &= a_1 \sum_{i=1}^q h_i + b_1 x + c_1 y + d_1 z \\ v &= a_2 \sum_{i=1}^q h_i + b_2 x + c_2 y + d_2 z \\ w &= a_3 \sum_{i=1}^q h_i + b_3 x + c_3 y + d_3 z \end{aligned} \quad (5.106)$$

The displacements defined in (5.106), however, are the same as those given in (5.104), provided that for any point in the element

$$\sum_{i=1}^q h_i = 1 \quad (5.107)$$

The relation in (5.107) is the condition on the interpolation functions for the completeness requirements to be satisfied. We may note that (5.107) is certainly satisfied at the nodes of an element, because the interpolation function  $h_i$  has been constructed to be unity at node  $i$  with all other interpolation functions  $h_j, j \neq i$ , being zero at that node; but in order that an isoparametric element be properly constructed, the condition must be satisfied for all points in the element.

In the above discussion, we have considered only a three-dimensional continuum element, but the conclusions are also directly applicable to the other isoparametric continuum element formulations. For the one- or two-dimensional continuum elements we simply include only the appropriate displacement and coordinate interpolations in the relations (5.103) to (5.107). We demonstrate the convergence considerations in the following example.

**EXAMPLE 5.26:** Investigate whether the requirements for monotonic convergence are satisfied for the variable-number-nodes elements in Figs. 5.5 and 5.6.

Compatibility is maintained between element edges in two-dimensional analysis and element faces in three-dimensional analysis, provided that the same number of nodes is used on connecting element edges and faces. A typical compatible element layout is shown in Fig. 5.40(a).

The second requirement for monotonic convergence is the completeness condition. Considering first the basic four-node two-dimensional element, we recognize that the arguments leading to the condition in (5.107) are directly applicable, provided only the  $x$  and  $y$  coordinates and  $u$  and  $v$  displacements are considered.

Evaluating  $\sum_{i=1}^4 h_i$  for the element we find

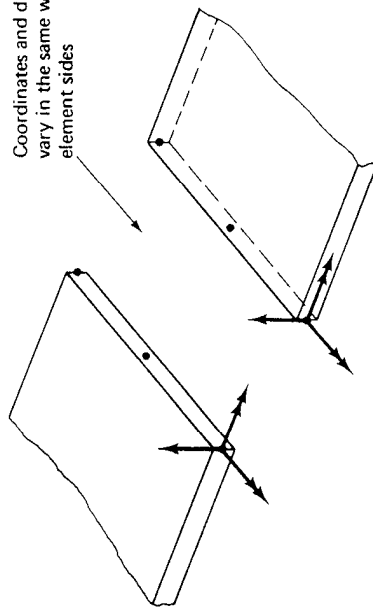
$$\frac{1}{4}(1+r)(1+s) + \frac{1}{4}(1-r)(1+s) + \frac{1}{4}(1+r)(1-s) + \frac{1}{4}(1-r)(1-s) = 1$$

Hence the basic four-node element is complete. We now study the interpolation functions given in Fig. 5.5 for the variable-number-nodes element and find that the total contribution that is added to the basic four-node interpolation functions is always zero for whichever additional node is included. Hence any one of the possible elements defined by the variable number of nodes in Fig. 5.5 is complete. The proof for the three-dimensional elements in Fig. 5.6 is carried out in an analogous manner. It follows, therefore, that the variable-number-nodes continuum elements satisfy the requirements for monotonic convergence.

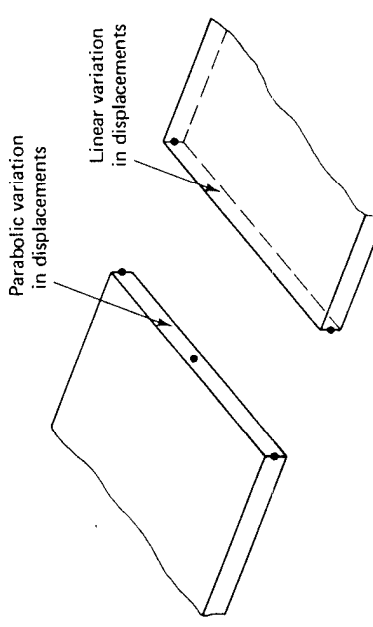
### 5.5.2 Structural Elements

The compatibility requirements between structural elements are satisfied in the same way as when using continuum elements (see Fig. 5.41). Furthermore, the use of transition elements as described in Section 5.4.1 enables also a

Coordinates and displacements vary in the same way along both element sides



(a) Compatible element layout



(b) Incompatible element layout  
FIGURE 5.41 *Compatible and incompatible plate element layouts.*

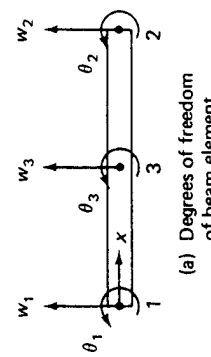
compatible transition between structural and continuum elements. However, some additional considerations are necessary when studying the completeness of a structural or transition element.

We discussed in Section 5.4.1 (see Example 5.23) that the structural elements could be derived from the continuum elements, although such a derivation would in practice be computationally ineffective. The fact that in theory the structural elements can be considered as “continuum elements subject to certain constraints” renders the completeness considerations for the continuum elements somewhat applicable to the structural elements—but only within the limits of the constraints imposed. Therefore, the effect of these constraints must be investigated and each structural element must be subjected to a more detailed convergence analysis. We give an analysis of this type in the following example.

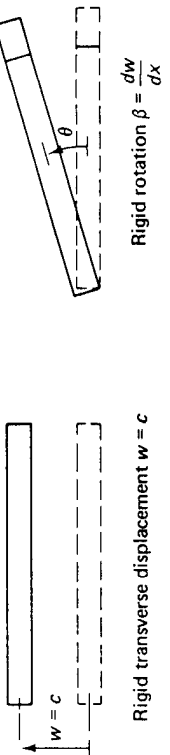
**EXAMPLE 5.27:** Examine whether the convergence requirements are satisfied for the three-node beam element shown in Fig. 5.42(a) and discussed in Example 5.20.

The element is compatible because  $w$  and  $\beta$  continuity is ensured between elements.

The condition given in (5.107) requires that  $\sum_{i=1}^3 h_i = 1$ , which is satisfied here.



(a) Degrees of freedom  
of beam element



(b) Rigid body motions



FIGURE 5.42 Convergence requirements of three-node beam.

However, since this is a structural element, we need to investigate in detail how the conditions of completeness are contained in the formulation.

The element must be able to undergo two rigid body modes (see Fig. 5.42(b)); a rigid transverse displacement and a rigid rotation. The rigid transverse displacement is obtained using  $w_i = c$ ,  $i = 1, 2, 3$ , where  $c$  is a constant. The rigid rotation is obtained using  $w_1 = 0$ ,  $w_2 = \theta L$ ,  $w_3 = \theta L/2$  and  $\beta_i = \theta$ ,  $i = 1, 2, 3$ , where  $\theta$  is a constant. Hence the rigid body mode criterion is satisfied.

The constant strain states of interest are a constant shear strain and a constant bending strain (see Fig. 5.42(c)). For a constant shear strain we want  $\beta = 0$  and  $dw/dx$  equal to a constant. This state is obtained when for the element  $\beta_i = 0$ ,  $i = 1, 2, 3$  and  $w_1 = 0$ ,  $w_2 = \gamma L$ ,  $w_3 = \gamma L/2$ . For a constant bending strain we need  $d\beta_i/dx$  equal to a constant and  $\beta = dw/dx$ . This state is reached when  $\beta = cx$  and  $w = cx^2/2$ , which corresponds to the element nodal point variables  $\beta_1 = 0$ ,  $\beta_2 = cL$ ,  $\beta_3 = cL/2$  and  $w_1 = 0$ ,  $w_2 = cL^2/2$ ,  $w_3 = cL^2/8$ . Hence, the two constant strain states of interest are contained in the element formulation and the element is therefore complete.

Using the information of the above example, it is interesting to note that the two-node beam element (i.e. the element in Fig. 5.42 without the center node) cannot represent the constant bending strain condition without shearing strains, because  $\beta$  and  $w$  vary at most linearly over the element. This observation shows once more why the two-node beam element cannot be used in the analysis of thin structures. (However, the constant bending strain condition would be represented in a discrete Kirchhoff theory element, because the shear deformations are not included in the formulation (see Example 5.21).)

## 5.6 ASSOCIATED ELEMENT FAMILIES

In the isoparametric finite element derivations of continuum elements, we assumed that the element coordinates are interpolated in exactly the same way as the element displacements. We may, however, find it expedient in the solution process to interpolate the coordinates different from the displacements, and certain displacement components different from the others. Thus, there appear to be various possibilities of constructing new elements, and in fact the structural elements presented in Section 5.4 represent already a group of such new elements. In the following sections some considerations pertaining to such elements are discussed.

### 5.6.1 Use of Different Interpolations

In the discussion of the structural elements in Section 5.4, we showed that these elements can be thought of as isoparametric continuum elements with displacement constraints (and the transverse normal stresses were also set to zero). Thus, in this case the element geometry is, in essence, interpolated to a higher degree than the displacements. Elements with a higher degree of interpolation on the coordinates than on the displacements are also called, in general, *superparametric elements*. Considering the convergence properties of such elements, each element formulation must be studied individually in order to identify whether the formulation satisfies the specific compatibility and completeness requirements of the problem considered.

element. In this case the coordinate and displacement interpolations used are, respectively,

$$x = \sum_{i=1}^4 h_i x_i; \quad y = \sum_{i=1}^4 h_i y_i \quad (5.108)$$

$$\left. \begin{aligned} u &= \sum_{i=1}^4 h_i u_i + \alpha_1(1 - r^2) + \alpha_2(1 - s^2) \\ v &= \sum_{i=1}^4 h_i v_i + \beta_1(1 - r^2) + \beta_2(1 - s^2) \end{aligned} \right\} \quad (5.109)$$

where the  $h_1, \dots, h_4$  are as defined in Fig. 5.5 or Example 5.5. The  $\alpha_1, \alpha_2, \beta_1$ , and  $\beta_2$  are additional degrees of freedom, with a higher-order displacement interpolation than is present in the  $h_i$ . If the element considered is rectangular, the additional degrees of freedom allow the element to represent a constant bending moment, and the element will perform much better in many stress analyses.

Considering the actual evaluation of the element stiffness matrix, we note that using the interpolation in (5.109) a matrix of order 12 is obtained, and that the degrees of freedom  $\alpha_1, \alpha_2, \beta_1$ , and  $\beta_2$  are not associated with an element nodal point. To reduce the matrix to order 8, the additional degrees of freedom are eliminated using static condensation (see Section 8.2.4), which is equivalent to minimizing the element total potential energy with respect to the variables  $\alpha_1, \alpha_2, \beta_1$ , and  $\beta_2$ . We shall discuss in Section 5.8.1 that the same objective is pursued by using reduced order or selective numerical integration.

Since the additional degrees of freedom are not associated with nodal point degrees of freedom, in the analysis using the element, displacement incompatibilities arise between elements. Therefore, the element does not satisfy the requirements for monotonic convergence discussed in Section 4.2.5, and an important question is whether the element does converge in a nonmonotonic manner. Referring to Section 4.3.1 where we discussed the patch test, the results are that *the four-node incompatible element converges provided that the element is a rectangle (or parallelogram)* (see Example 4.20).

Although the use of the variable-number-nodes elements given in Figs. 5.5 and 5.6 is considered to be most effective, it should be noted that in three-dimensional analysis, the use of incompatible modes can in some cases decrease the analysis cost considerably. An element that has been used with much success is the eight-node brick element with incompatible modes analogous to those used in (5.109); i.e., the displacement interpolations employed are

$$\left. \begin{aligned} u &= \sum_{i=1}^8 h_i u_i + \alpha_1(1 - r^2) + \alpha_2(1 - s^2) + \alpha_3(1 - t^2) \\ v &= \sum_{i=1}^8 h_i v_i + \beta_1(1 - r^2) + \beta_2(1 - s^2) + \beta_3(1 - t^2) \\ w &= \sum_{i=1}^8 h_i w_i + \gamma_1(1 - r^2) + \gamma_2(1 - s^2) + \gamma_3(1 - t^2) \end{aligned} \right\} \quad (5.110)$$

where the  $\alpha_1, \alpha_2, \dots, \gamma_3$  are displacement components that are not associated with nodal points and are eliminated using static condensation. In analogy to

Another class of elements is obtained when the coordinates are interpolated to a lower degree than the displacements. Typically, for the straight-sided eight-node quadrilateral in Fig. 5.43 the displacements  $u$  and  $v$  are interpolated parabolically, whereas the coordinates  $x$  and  $y$  of the element need only be interpolated linearly because the element edges are straight. Elements with a lower degree of interpolation on the coordinates than on the displacements are called *subparametric elements*. These continuum elements satisfy the monotonic convergence requirements, because, firstly, compatibility is satisfied for the same reasoning that is used in the isoparametric formulation. Secondly, a subparametric element is complete because the associated isoparametric element, which is based only on the coordinate interpolations used, is complete. This follows because the addition of higher-order displacement interpolations does not prevent the element from still undergoing the rigid body modes and constant strain states.

In the above formulations we assumed that each node with displacement degrees of freedom is assigned one degree of freedom corresponding to each unknown displacement. However, in some analyses it is advantageous to interpolate some unknown state variables to a higher degree than the others. In this case, a node may be assigned degrees of freedom corresponding to all state variables or a smaller number. This procedure is employed effectively, for example, in the finite element analysis of fluid flow (see Section 7.4).

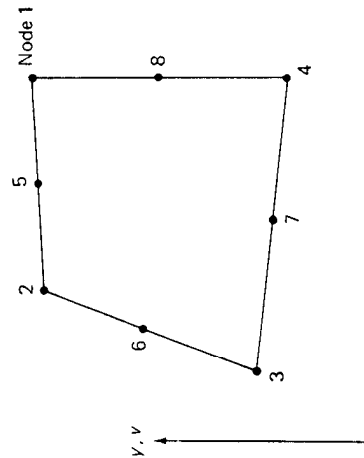


**FIGURE 5.43 Two-dimensional subparametric element.**

### 5.6.2 Addition of Incompatible Modes

An important procedure to improve the behavior of isoparametric elements is the introduction of incompatible modes.<sup>29,30</sup> Consider the simplest case, the addition of incompatible modes to a four-node two-dimensional continuum

the two-dimensional element discussed above, the three-dimensional brick should be rectangular in all three planes. Observing this rule, the element has been employed successfully in a variety of three-dimensional and shell analyses. Finally, it should be noted that the concept of introducing incompatible modes to increase the effectiveness of an element is quite general, and can also be employed in the formulation of higher-order elements.

## 5.7 NUMERICAL INTEGRATION

An important aspect of isoparametric and related finite element analysis is the required numerical integration. The required matrix integrals in the finite element calculations have been written as

$$\left\{ \begin{array}{l} \int F(r) dr, \quad \int F(r, s) dr ds, \\ \int F(r, s) dr ds = \sum_{i,j} \alpha_{ij} F(r_i, s_j) + R_n \end{array} \right\} \quad (5.112)$$

in the one-, two-, and three-dimensional cases, respectively. It was stated that these integrals are in practice evaluated numerically using

$$\left\{ \begin{array}{l} \int F(r) dr = \sum_i \alpha_i F(r_i) + R_n \\ \int F(r, s) dr ds = \sum_{i,j} \alpha_{ij} F(r_i, s_j) + R_n \\ \int F(r, s, t) dr ds dt = \sum_{i,j,k} \alpha_{ijk} F(r_i, s_j, t_k) + R_n \end{array} \right\} \quad (5.113)$$

where the summations extend over all  $i, j$ , and  $k$  specified, the  $\alpha_i$ ,  $\alpha_{ij}$ , and  $\alpha_{ijk}$  are weighting factors, and  $F(r_i)$ ,  $F(r, s_j)$ , and  $F(r, s, t_k)$  are the matrices  $\mathbf{F}(r)$ ,  $\mathbf{F}(r, s)$ , and  $\mathbf{F}(r, s, t)$  evaluated at the points specified in the arguments. The matrices  $\mathbf{R}_n$  are error matrices, which, in practice, are usually not evaluated. Therefore, we use

$$\left\{ \begin{array}{l} \int F(r) dr = \sum_i \alpha_i F(r_i) \\ \int F(r, s) dr ds = \sum_{i,j} \alpha_{ij} F(r_i, s_j) \\ \int F(r, s, t) dr ds dt = \sum_{i,j,k} \alpha_{ijk} F(r_i, s_j, t_k) \end{array} \right\} \quad (5.114)$$

The purpose in this section and Section 5.8.1 is to present the theory and practical implications of numerical integrations. An important point is the integration accuracy that is needed, i.e., the number of integration points required in the element formation.

As presented above, in finite element analysis we integrate matrices, which means that each element of the matrix considered is integrated individually. Hence, for the derivation of the numerical integration formulas we can consider a typical element of a matrix which we denote as  $F$ .

Consider the one-dimensional case first, i.e., the integration of  $\int_a^b F(r) dr$ . In an isoparametric element calculation we would actually have  $a = -1$  and  $b = +1$ .

**brick**

The numerical integration of  $\int_a^b F(r) dr$  is essentially based on passing a polynomial  $\psi(r)$  through given values of  $F(r)$  and then using  $\int_a^b \psi(r) dr$  as an approximation to  $\int_a^b F(r) dr$ . The number of evaluations of  $F(r)$  and the positions of the sampling points in the interval from  $a$  to  $b$  determines how well  $\psi(r)$  approximates  $F(r)$  and hence the error of the numerical integration.

### 5.7.1 Interpolation Using a Polynomial

Assume that  $F(r)$  has been evaluated at the  $n + 1$  distinct points  $r_0, r_1, \dots, r_n$  to obtain  $F_0, F_1, \dots, F_n$  respectively, and that a polynomial  $\psi(r)$  is to be passed through these data. Then there is a unique polynomial  $\psi(r)$  given as

$$\psi(r) = a_0 + a_1 r + a_2 r^2 + \dots + a_n r^n \quad (5.114)$$

Using the condition that  $\psi(r) = F(r)$  at the  $n + 1$  interpolating points, we have

$$\mathbf{F} = \mathbf{V}\mathbf{a} \quad (5.115)$$

$$\left[ \begin{array}{c} F_0 \\ F_1 \\ \vdots \\ F_n \end{array} \right]; \quad \mathbf{F} = \left[ \begin{array}{c} a_0 \\ a_1 \\ \vdots \\ a_n \end{array} \right] \quad \text{where} \quad \mathbf{V} = \left[ \begin{array}{cccc} 1 & r_0 & r_0^2 & \dots & r_0^n \\ 1 & r_1 & r_1^2 & \dots & r_1^n \\ \vdots & \vdots & \vdots & \ddots & \vdots \\ 1 & r_n & r_n^2 & \dots & r_n^n \end{array} \right] \quad (5.116)$$

and  $\mathbf{V}$  is the *Vandermonde matrix*,

$$\mathbf{V} = \left[ \begin{array}{ccccc} 1 & r_0 & r_0^2 & \dots & r_0^n \\ 1 & r_1 & r_1^2 & \dots & r_1^n \\ \vdots & \vdots & \vdots & \ddots & \vdots \\ 1 & r_n & r_n^2 & \dots & r_n^n \end{array} \right] \quad (5.117)$$

Since  $\det \mathbf{V} \neq 0$ , provided that the  $r_i$  are distinct points, we have a unique solution for  $\mathbf{a}$ .

However, a more convenient way to obtain  $\psi(r)$  is to use *Lagrangian interpolation*. First, we recall that the  $(n + 1)$  functions  $1, r, r^2, \dots, r^n$  form an  $(n + 1)$ -dimensional vector space, say  $V_n$ , in which  $\psi(r)$  is an element (see Section 2.2). Since the coordinates  $a_0, a_1, a_2, \dots, a_n$  of  $\psi(r)$  are relatively difficult to evaluate, we seek to use a different basis for the space  $V_n$ , in which the coordinates of  $\psi(r)$  are more easily evaluated. This basis is provided by the fundamental polynomials of Lagrangian interpolation, given as

$$l_j(r) = \frac{(r - r_0)(r - r_1)\dots(r - r_{j-1})(r - r_{j+1})\dots(r - r_n)}{(r_j - r_0)(r_j - r_1)\dots(r_j - r_{j-1})(r_j - r_{j+1})\dots(r_j - r_n)} \quad (5.118)$$

where  $l_j(r_j) = \delta_{jj}$

where  $\delta_{ij}$  is the Kronecker delta; i.e.,  $\delta_{ij} = 1$  for  $i = j$ , and  $\delta_{ij} = 0$  for  $i \neq j$ . Using the property in (5.119), the coordinates of the base vectors are simply the

values of  $F(r)$ , and the polynomial  $\psi(r)$  is

$$\psi(r) = F_0 I_0(r) + F_1 I_1(r) + \dots + F_n I_n(r) \quad (5.120)$$

**EXAMPLE 5.28:** Establish the interpolating polynomial  $\psi(r)$  for the function  $F(r) = 2r - r$  when the data at the points  $r = 0, 1$ , and  $3$  are used. In this case  $r_0 = 0, r_1 = 1, r_2 = 3$ , and  $F_0 = 1, F_1 = 1, F_2 = 5$ .

In the first approach we use the relation in (5.115) to calculate the unknown coefficients  $a_0, a_1$ , and  $a_2$  of the polynomial  $\psi(r) = a_0 + a_1 r + a_2 r^2$ . In this case we have

$$\begin{bmatrix} 1 & 0 & 0 \\ 1 & 1 & 1 \\ 1 & 3 & 9 \end{bmatrix} \begin{pmatrix} a_0 \\ a_1 \\ a_2 \end{pmatrix} = \begin{pmatrix} 1 \\ 1 \\ 5 \end{pmatrix}$$

The solution gives  $a_0 = 1, a_1 = -\frac{2}{3}, a_2 = \frac{2}{3}$ , and therefore  $\psi(r) = 1 - \frac{2}{3}r + \frac{2}{3}r^2$ .

If Lagrangian interpolation is employed, we use the relation in (5.120) which in this case gives

$$\psi(r) = (1) \frac{(r-1)(r-3)}{(-1)(-3)} + (1) \frac{(r)(r-3)}{(1)(-2)} + (5) \frac{(r)(r-1)}{(3)(2)}$$

or, as before,

$$\psi(r) = 1 - \frac{2}{3}r + \frac{2}{3}r^2$$

### 5.7.2 The Newton–Cotes Formulas (one-dimensional integration)

Having established an interpolating polynomial  $\psi(r)$ , we can now obtain an approximation to the integral  $\int_a^b F(r) dr$ . In Newton–Cotes integration, it is assumed that the sampling points of  $F$  are spaced at equal distances, and we define

$$r_0 = a, \quad r_n = b, \quad h = \frac{b-a}{n} \quad (5.121)$$

Using Lagrangian interpolation to obtain  $\psi(r)$  as an approximation to  $F(r)$ , we have

$$\int_a^b F(r) dr = \sum_{i=0}^n \left\{ \int_a^b I_i(r) dr \right\} F_i + R_n \quad (5.122)$$

or, evaluated,

$$\int_a^b F(r) dr = (b-a) \sum_{i=0}^n C_i^n F_i + R_n \quad (5.123)$$

where  $R_n$  is the remainder and the  $C_i^n$  are the Newton–Cotes constants for numerical integration with  $n$  sampling points.

The Newton–Cotes constants and corresponding remainder terms have been published<sup>31</sup> and are summarized in Table 5.1 for  $n = 1$  to  $6$ . The case  $n = 1$  and  $n = 2$  are the well-known trapezoidal rule and Simpson formula. We note that the formulas for  $n = 3$  and  $n = 5$  have the same order of accuracy as the formulas for  $n = 2$  and  $n = 4$ , respectively. For this reason, the even formulas with  $n = 2$  and  $4$  are used in practice.

TABLE 5.1 Newton–Cotes numbers and error estimates.

Number of Intervals $n$	Upper Bound on Error $R_n$ as a Function of the Derivative of $F$					
	$C_0^n$	$C_1^n$	$C_2^n$	$C_3^n$	$C_4^n$	$C_6^n$
1	1	$\frac{1}{2}$	$\frac{1}{2}$	$\frac{1}{6}$	$\frac{1}{4}$	$10^{-1}(b-a)^3 F''(r)$
2	$\frac{1}{6}$	$\frac{1}{6}$	$\frac{4}{3}$	$\frac{3}{8}$	$\frac{3}{8}$	$10^{-3}(b-a)^5 F'''(r)$
3	$\frac{1}{8}$	$\frac{7}{90}$	$\frac{32}{90}$	$\frac{12}{90}$	$\frac{32}{90}$	$10^{-6}(b-a)^7 F''''(r)$
4	$\frac{7}{90}$	$\frac{19}{288}$	$\frac{75}{288}$	$\frac{50}{288}$	$\frac{75}{288}$	$10^{-9}(b-a)^9 F'''''(r)$
5	$\frac{19}{288}$	$\frac{216}{840}$	$\frac{272}{840}$	$\frac{27}{840}$	$\frac{27}{840}$	$10^{-12}(b-a)^{11} F''''''(r)$
6	$\frac{41}{840}$	$\frac{840}{840}$	$\frac{840}{840}$	$\frac{41}{840}$	$\frac{41}{840}$	$10^{-15}(b-a)^{13} F'''''''(r)$

**EXAMPLE 5.29:** Evaluate the Newton–Cotes constants when the interpolating polynomial is of order 2; i.e.,  $\psi(r)$  is a parabola. In this case we have

$$\int_a^b F(r) dr \doteq$$

$$\int_a^b \left[ F_0 \frac{(r-r_1)(r-r_2)}{(r_0-r_1)(r_0-r_2)} + F_1 \frac{(r-r_0)(r-r_2)}{(r_1-r_0)(r_1-r_2)} + F_2 \frac{(r-r_0)(r-r_1)}{(r_2-r_0)(r_2-r_1)} \right] dr$$

Using that  $r_0 = a, r_1 = a+h, r_2 = a+2h$ , where  $h = (b-a)/2$ , the evaluation of the integral gives

$$\int_a^b F(r) dr = \frac{b-a}{6} (F_0 + 4F_1 + F_2)$$

Hence the Newton–Cotes constants are as given in Table 5.1 for the case  $n = 2$ .

**EXAMPLE 5.30:** Use Simpson's rule to integrate  $\int_0^3 (2r-r) dr$ . In this case  $n = 2$  and  $h = \frac{3}{2}$ . Therefore,  $r_0 = 0, r_1 = \frac{3}{2}, r_2 = 3$ , and  $F_0 = 1, F_1 = 1.328427, F_2 = 5$ , and we obtain

$$\int_0^3 (2r-r) dr = \frac{3}{6} [I(1)(1) + (4)(1.328427) + (1)(5)]$$

or

$$\int_0^3 (2r-r) dr \doteq 5.656854$$

The exact result is  $\int_0^3 (2r-r) dr = 5.598868$

Hence the error is  $R = 0.057986$

However, using the upper bound value on the error we would have

$$R < \frac{(3-0)^5}{1000} (\ln 2)^4 (2^4) = 0.448743$$

To obtain greater accuracy in the integration using the Newton-Cotes formulas we need to employ a smaller interval  $h$ ; i.e., include more evaluations of the function to be integrated. Then we have the choice between two different strategies: we may use a higher-order Newton-Cotes formula, or, alternatively, employ the lower-order formula in a repeated manner, in which case the integration procedure is referred to as a *composite formula*. Consider the following example.

**EXAMPLE 5.31:** Increase the accuracy of the integration in Example 5.30 by using half the interval spacing.

In this case we have  $h = \frac{1}{4}$  and the required function values are  $F_0 = 1$ ,  $F_1 = 0.931792$ ,  $F_2 = 1.328427$ ,  $F_3 = 2.506828$ , and  $F_4 = 5$ . The choice lies now between using the higher-order Newton-Cotes formula with  $n = 4$  or applying the Simpson's rule twice, i.e., to the first two intervals and then to the second two intervals. Using the Newton-Cotes formula with  $n = 4$ , we obtain

$$\int_0^3 (2r - r) dr \doteq \frac{3}{90} (7F_0 + 32F_1 + 12F_2 + 32F_3 + 7F_4)$$

Hence

$$\int_0^3 (2r - r) dr \doteq 5.599232$$

On the other hand, using Simpson's rule twice, we consider

$$\int_0^3 (2r - r) dr \doteq \int_0^{3/2} (2r - r) dr + \int_{3/2}^3 (2r - r) dr$$

The integration is performed using

$$\int_0^{3/2} (2r - r) dr \doteq \frac{\frac{3}{2} - 0}{6} (F_0 + 4F_1 + F_2)$$

where  $F_0$ ,  $F_1$ , and  $F_2$  are the function values at  $r = 0$ ,  $r = \frac{3}{4}$ , and  $r = \frac{3}{2}$ , respectively; i.e.,

$$F_0 = 1; \quad F_1 = 0.931792; \quad F_2 = 1.328427 \quad (a)$$

Hence we use

$$\int_0^{3/2} (2r - r) dr \doteq 1.513899$$

Next we need to evaluate

$$\int_{3/2}^3 (2r - r) dr \doteq \frac{3 - \frac{3}{2}}{6} (F_0 + 4F_1 + F_2)$$

where  $F_0$ ,  $F_1$ , and  $F_2$  are the function values at  $r = \frac{3}{2}$ ,  $r = \frac{9}{4}$ , and  $r = 3$ , respectively,

$$F_0 = 1.328427; \quad F_1 = 2.506828; \quad F_2 = 5 \quad (b)$$

Hence we have

$$\int_{3/2}^3 (2r - r) dr \doteq 4.038935$$

Adding the results of (a) and (b), we obtain

$$\int_0^3 (2r - r) dr \doteq 5.602834$$

The use of a composite formula has a number of advantages over the application of high-order Newton-Cotes formulas. A composite formula, such as the repetitive use of the Simpson rule, is easy to employ. Convergence is assured as the interval of sampling decreases, and, in practice, a sampling interval could be used that varies from one application of the basic formula to the next. This is particularly advantageous when there are discontinuities in the function to be integrated. For these reasons, in practice, composite formulas are commonly used.

**EXAMPLE 5.32:** Use a composite formula that employs Simpson's rule to evaluate the integral  $\int_{-1}^{+13} F(r) dr$  of the function  $F(r)$  in Fig. 5.44. This function is best integrated by considering three intervals of integration, as follows:

$$\begin{aligned} \int_{-1}^{13} F(r) dr &= \int_{-1}^2 (r^3 + 3) dr + \int_2^9 [10 + (r - 1)^{1/3}] dr \\ &\quad + \int_9^{13} [\frac{1}{128}(13 - r)^5 + 4] dr \end{aligned}$$

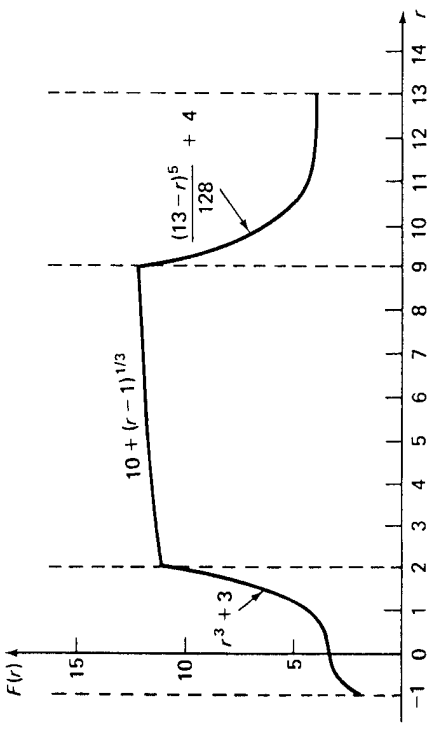


FIGURE 5.44 Function  $F(r)$  integrated in Example 5.32.

We evaluate each of the three integrals using Simpson's rule and have

$$\begin{aligned} \int_{-1}^2 (r^3 + 3) dr &\doteq \frac{2 - (-1)}{6} [(1)(11) + (4)(3.125) + (1)(12)] \\ &\doteq 12.75 \end{aligned}$$

$$\begin{aligned} \int_2^9 [10 + (r - 1)^{1/3}] dr &\doteq \frac{9 - 2}{6} [(1)(11) + (4)(0.650964) + (1)(12)] \\ &\doteq 81.204498 \end{aligned}$$

$$\begin{aligned} \int_9^{13} [\frac{1}{128}(13 - r)^5 + 4] dr &\doteq \frac{13 - 9}{6} [(1)(12) + (4)(4.25) + (1)(4)] \\ &\doteq 5.602834 \end{aligned}$$

or	$\int_0^{13} [r^4(13 - r)^4 + 4] dr \doteq 22$
Hence	$\int_{-1}^{13} F dr \doteq 12.75 + 81.204498 + 22$
or	$\int_{-1}^{13} F dr \doteq 115.954498$

### 5.7.3 The Gauss Formulas (one-dimensional integration)

The basic integration schemes that we considered so far used equally spaced sampling points, although the basic methods could be employed to construct procedures that allow varying the interval of sampling; i.e., the composite formulas have been introduced. The methods considered so far are effective when measurements of an unknown function to be integrated have been taken at equal intervals. However, in the integration of finite element matrices, a subroutine is called to evaluate the unknown function  $F$  at given points, and these points may be anywhere on the element. No additional difficulties arise if the sampling points are not equally spaced. Therefore, it seems natural to try to improve the accuracy that can be obtained for a given number of function evaluations by also optimizing the positions of the sampling points. A very important numerical integration procedure in which both the positions of the sampling points and the weights have been optimized is *Gauss quadrature*. The basic assumption in Gauss numerical integration is that

$$\int_a^b F(r) dr = \alpha_1 F(r_1) + \alpha_2 F(r_2) + \dots + \alpha_n F(r_n) + R_n \quad (5.124)$$

where both the weights  $\alpha_1, \dots, \alpha_n$  and the sampling points  $r_1, \dots, r_n$  are variables. It should be recalled that in the derivation of the Newton–Cotes formulas, only the weights were unknown, and they have been determined from the integration of a polynomial  $\psi(r)$ , which passed through equally spaced sampling points of the function  $F(r)$ . We now calculate also the positions of the sampling points and, therefore, have  $2n$  unknowns to determine a higher-order integration scheme.

In analogy to the derivation of the Newton–Cotes formulas, we use an interpolating polynomial  $\psi(r)$  of the form given in (5.120):

$$\psi(r) = \sum_{j=1}^n F_j J_j(r) \quad (5.125)$$

where  $n$  sampling points are now considered,  $r_1, \dots, r_n$ , which are still unknown. For the determination of the values  $r_1, \dots, r_n$ , we define a function  $P(r)$ ,

$$P(r) = (r - r_1)(r - r_2) \dots (r - r_n) \quad (5.126)$$

which is a polynomial of order  $n$ . We note that  $P(r) = 0$  at the sampling points  $r_1, \dots, r_n$ . Therefore, we can write

$$F(r) = \psi(r) + P(r)\beta_0 + \beta_1 r + \beta_2 r^2 + \dots \quad (5.127)$$

Integrating  $F(r)$  we obtain

$$\int_a^b F(r) dr = \sum_{j=1}^n F_j \left[ \int_a^b I_j(r) dr \right] + \sum_{j=0}^{\infty} \beta_j \left[ \int_a^b r^j P(r) dr \right] \quad (5.128)$$

where it need be noted that in the first integral on the right of (5.128), functions of order  $(n - 1)$  and lower are integrated, and in the second integral the functions that are integrated are of order  $n$  and higher. The unknown values  $r_j, j = 1, 2, \dots, n$ , can now be determined using the conditions

$$\int_a^b P(r) r^k dr = 0 \quad k = 0, 1, 2, \dots, n - 1 \quad (5.129)$$

Then, since the polynomial  $\psi(r)$  passes through  $n$  sampling points of  $F(r)$  and  $P(r)$  vanishes at these points, the conditions in (5.129) mean that the required integral  $\int_a^b F(r) dr$  is approximated by integrating a polynomial of order  $2n - 1$  instead of  $F(r)$ .

In summary, using the Newton–Cotes formulas we use  $(n + 1)$  equally spaced sampling points and integrate exactly a polynomial of order at most  $n$ . On the other hand, in Gauss quadrature we require  $n$  unequally spaced sampling points and integrate exactly a polynomial of order at most  $(2n - 1)$ . Polynomials of orders less than  $n$  and  $(2n - 1)$ , respectively, for the two cases would also be integrated exactly.

To determine the sampling points and the integration weights, we realize that they depend on the interval  $a$  to  $b$ . However, to make the calculations general, we can consider a natural interval from  $-1$  to  $+1$  and deduce the sampling points and weights for any interval. Namely, if  $r_i$  is a sampling point and  $\alpha_i$  is the weight for the interval  $-1$  to  $+1$ , the corresponding sampling point and weight in the integration from  $a$  to  $b$  are

$$\frac{a+b}{2} + \frac{b-a}{2} r_i \quad \text{and} \quad \frac{b-a}{2} \alpha_i$$

respectively.

For the above reasons, consider an interval from  $-1$  to  $+1$ . The sampling points are determined from (5.129) with  $a = -1$  and  $b = +1$ . To calculate the integration weights we substitute for  $F(r)$  in (5.124) the interpolating polynomial  $\psi(r)$  from (5.125) and perform the integration. It should be noted that because the sampling points have been determined, the polynomial  $\psi(r)$  is known, and hence

$$\alpha_j = \int_{-1}^{+1} I_j(r) dr; \quad j = 1, 2, \dots, n \quad (5.130)$$

The sampling points and weights for the interval  $-1$  to  $+1$  have been published and are reproduced in Table 5.2 for values  $n = 1$  to  $6^{32}$ .

The coefficients in Table 5.2 can be calculated directly using (5.129) and (5.130) (see Example 5.33). However, for larger  $n$  the solution becomes cumbersome and it is expedient to use Legendre polynomials to solve for the coefficients, which are thus referred to as Gauss–Legendre coefficients.

**TABLE 5.2** Sampling points and weights in Gauss-Legendre numerical integration (interval  $-1$  to  $+1$ ).

$n$	$r_i$	$\alpha_i$
1	0. (15 zeros)	2. (15 zeros)
2	$\pm 0.57735$	0.2691
3	$\pm 0.77459$	0.6692
4	$\pm 0.86113$	0.94053
5	$\pm 0.90617$	0.98459
6	$\pm 0.93246$	0.95142
	$\pm 0.66120$	0.93864
	$\pm 0.23861$	0.91860
	8.3197	8.3945
	0.46791	0.46791
	39345	39345
	72691	72691

**EXAMPLE 5.33:** Derive the sampling points and weights for two-point Gauss quadrature.

In this case  $P(r) = (r - r_1)(r - r_2)$  and (5.129) gives the two equations

$$\int_{-1}^{+1} (r - r_1)(r - r_2) dr = 0$$

$$\int_{-1}^{+1} (r - r_1)(r - r_2) r dr = 0$$

Solving, we obtain

$$r_1 r_2 = -\frac{1}{3}$$

$$r_1 + r_2 = 0$$

$$\text{Hence } r_1 = -\frac{1}{\sqrt{3}}; \quad r_2 = +\frac{1}{\sqrt{3}}$$

The corresponding weights are obtained using (5.130), which in this case gives

$$\alpha_1 = \int_{-1}^{+1} \frac{r - r_2}{r_1 - r_2} dr$$

$$\alpha_2 = \int_{-1}^{+1} \frac{r - r_1}{r_2 - r_1} dr$$

Since  $r_2 = -r_1$ , we obtain  $\alpha_1 = \alpha_2 = 1.0$ .

**EXAMPLE 5.34:** Use two-point Gauss quadrature to evaluate the integral  $\int_0^3 (2r - r) dr$  considered in Examples 5.30 and 5.31.

Using two-point Gauss quadrature, we obtain, from (5.124),

$$\int_0^3 (2r - r) dr \doteq \alpha_1 F(r_1) + \alpha_2 F(r_2) \quad (\text{a})$$

where  $\alpha_1$ ,  $\alpha_2$  and  $r_1$ ,  $r_2$  are weights and sampling points, respectively. Since the interval is from 0 to 3, we need to determine the values  $\alpha_1$ ,  $\alpha_2$ ,  $r_1$ , and  $r_2$  from the values given in Table 5.2.

$$\begin{aligned} \alpha_1 &= \frac{3}{2}(1); & \alpha_2 &= \frac{3}{2}(1) \\ r_1 &= \frac{3}{2}\left(1 - \frac{1}{\sqrt{3}}\right); & r_2 &= \frac{3}{2}\left(1 + \frac{1}{\sqrt{3}}\right) \end{aligned}$$

where  $1/\sqrt{3} = 0.5773502692$ . Thus

$$F(r_1) = 0.91785978$$

$$\int_0^3 (2r - r) dr \doteq 5.56053551$$

and (a) gives

$$F(r_2) = 2.78916389$$

The Gauss-Legendre integration procedure is commonly used in isoparametric finite element analysis. However, it should be noted that other integration schemes, in which both the weights and sampling positions were varied to obtain maximum accuracy, have been derived also.<sup>31,33</sup> In addition, for the specific objectives in finite element analysis, the basic Gauss quadrature has been applied in modified form as described in Section 5.8.1.

#### 5.7.4 Integrations in Two and Three Dimensions

So far we have considered the integration of a one-dimensional function  $F(r)$ . However, two- and three-dimensional integrals need be evaluated in two- and three-dimensional finite element analyses. Considering the evaluation of rectangular elements, we can apply the above one-dimensional integration formulas successively in each direction.\* As in the analytical evaluation of multidimensional integrals, in this procedure, successively, the innermost integral is evaluated by keeping the variables corresponding to the other integrals constant. Therefore, we have for a two-dimensional integral

$$\int_{-1}^{+1} \int_{-1}^{+1} F(r, s) dr ds = \sum_i \alpha_i \int_{-1}^{+1} F(r_i, s) ds \quad (5.131)$$

$$\int_{-1}^{+1} \int_{-1}^{+1} F(r, s) dr ds = \sum_{i,j} \alpha_i \alpha_j F(r_i, s_j) \quad (5.132)$$

and corresponding to (5.113),  $\alpha_{ij} = \alpha_i \alpha_j$ , where  $\alpha_i$  and  $\alpha_j$  are the integration weights for one-dimensional integration. Similarly, for a three-dimensional integral,

$$\int_{-1}^{+1} \int_{-1}^{+1} \int_{-1}^{+1} F(r, s, t) dr ds dt = \sum_{i,j,k} \alpha_i \alpha_j \alpha_k F(r_i, s_j, t_k) \quad (5.133)$$

and  $\alpha_{ijk} = \alpha_i \alpha_j \alpha_k$ . We should note that it is not necessary in the numerical integration to use the same quadrature rule in the two or three dimensions; i.e., we can employ different numerical integration schemes in the  $r$ ,  $s$ , and  $t$  directions.

**EXAMPLE 5.35:** Given that the  $(i, j)$ th element of a stiffness matrix  $K$  is  $\int_{-1}^{+1} \int_{-1}^{+1} r^2 s^2 dr ds$ . Evaluate the integral  $\int_{-1}^{+1} \int_{-1}^{+1} r^2 s^2 dr ds$  using (1) Simpson's rule in both  $r$  and  $s$ , (2) Gauss quadrature in both  $r$  and  $s$ , and (3) Gauss quadrature in  $r$  and Simpson's rule in  $s$ .

\* This results in much generality of the integration, but for special cases somewhat less costly procedures can be designed.<sup>34</sup>

1. Using Simpson's rule, we have

$$\begin{aligned} \int_{-1}^{+1} \int_{-1}^{+1} r^2 s^2 dr ds &= \int_{-1}^{+1} \frac{1}{3}(1)(1) + (4)(0) + (1)(1)s^2 ds \\ &= \int_{-1}^{+1} \frac{2}{3}s^2 ds = \frac{4}{3}[(1)(\frac{4}{3}) + (4)(0) + (1)(\frac{4}{3})] = \frac{4}{3} \end{aligned}$$

2. Using two-point Gauss quadrature, we have

$$\begin{aligned} \int_{-1}^{+1} \int_{-1}^{+1} r^2 s^2 dr ds &= \int_{-1}^{+1} \left[ (1)\left(\frac{1}{\sqrt{3}}\right)^2 + (1)\left(\frac{1}{\sqrt{3}}\right)^2 \right] s^2 ds \\ &= \int_{-1}^{+1} \frac{2}{3}s^2 ds = \frac{2}{3} \left[ (1)\left(\frac{1}{\sqrt{3}}\right)^2 + (1)\left(\frac{1}{\sqrt{3}}\right)^2 \right] = \frac{4}{3} \end{aligned}$$

3. Finally, using Gauss quadrature in  $r$  and Simpson's rule in  $s$ , we have

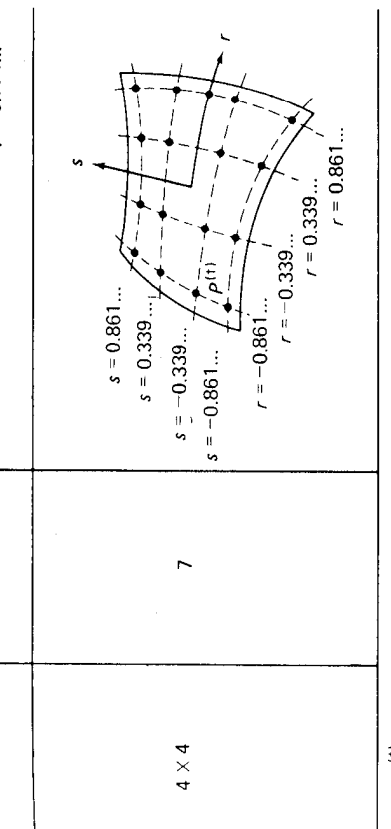
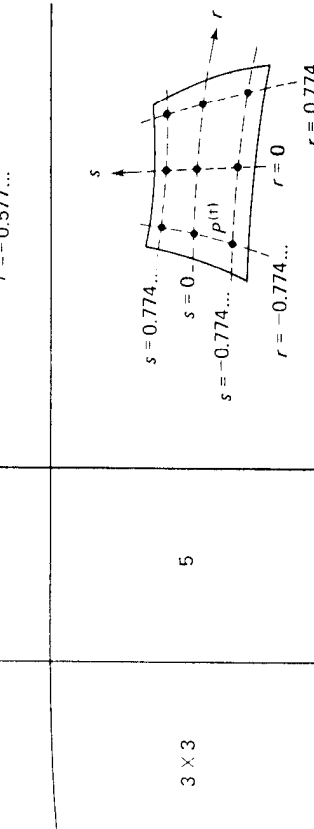
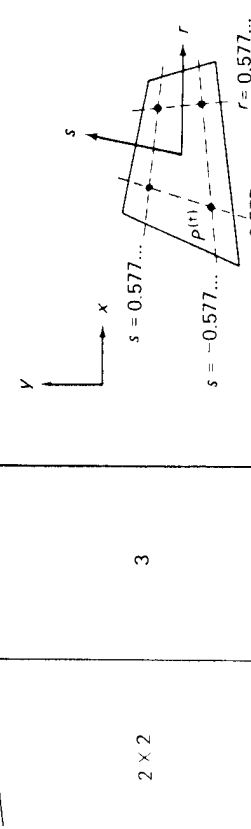
$$\begin{aligned} \int_{-1}^{+1} \int_{-1}^{+1} \left[ (1)\left(\frac{1}{\sqrt{3}}\right)^2 + (1)\left(\frac{1}{\sqrt{3}}\right)^2 \right] s^2 ds \\ = \int_{-1}^{+1} \frac{2}{3}s^2 ds = \frac{4}{3}[(1)(\frac{4}{3}) + (4)(0) + (1)(\frac{4}{3})] = \frac{4}{3} \end{aligned}$$

We should note that the above numerical integrations are exact because both integration schemes, i.e., Simpson's rule and two-point Gauss quadrature, integrate a parabola exactly.

The above procedure is directly applicable to the evaluation of matrices of rectangular elements in which all integration limits are  $-1$  to  $+1$ . Hence, in the evaluation of a two-dimensional finite element, the integrations can be carried out for each entry of the stiffness and mass matrices and load vectors as illustrated in Example 5.35. Based on the information given in Table 5.2 some common Gauss quadrature rules for two-dimensional analysis are summarized in Table 5.3.

Considering next the evaluation of triangular and tetrahedral element matrices, however, the procedure given in Example 5.35 is not applicable directly, because now the integration limits involve the variables themselves. A great deal of research has been spent on the development of suitable integration formulas for triangular domains, and here too formulas of the Newton-Cotes type<sup>36,37</sup> and of the Gauss quadrature type are available.<sup>36,37</sup> As in the solution of rectangular domains, the Gauss quadrature rules are in general more efficient because they yield a higher integration accuracy for the same number of evaluations. Table 5.4 lists the integration stations and integration weights of the Gauss integration formulas published by Cowper.<sup>37</sup>

Integration order	Degree of precision	Location of integration points
2 × 2	3	



(<sup>11</sup>) The location of any integration point in the  $x$ - $y$  coordinate system is given

by :  $x_p = \sum_i h_i (r_p, s_p) x_i$  and  $y_p = \sum_i h_i (r_p, s_p) y_i$

TABLE 5.3 Gauss numerical integrations over rectangular domains. The integration weights are given in Table 5.2 using (5.132).

### 5.8.1 Use of Numerical Integration

In the practical use of the numerical integration procedures presented in the previous section, basically two questions arise; namely, what kind of integration scheme to use, and what order to select. We pointed out that using the Newton-Cotes formulas, ( $n+1$ ) function evaluations are required to integrate without error a polynomial of order  $n$ . On the other hand, if Gauss quadrature is used, a polynomial of order  $(2n-1)$  is integrated exactly with only  $n$  function evaluations. In finite element analysis a large number of function evaluations directly

## 5.8 PRACTICAL CONSIDERATIONS IN ISOPARAMETRIC ELEMENT CALCULATIONS

In previous sections we have presented the basic relations used to derive isoparametric element matrices. However, the proper application of these relations requires that certain choices be made, such as which element to select, what kind and order of numerical integration to use, and so on. Our objective in this section is to discuss some of these practical and important considerations.

increases the cost of analysis, and the use of Gauss quadrature is attractive. However, the Newton-Cotes formulas may be efficient in nonlinear analysis for the reasons discussed in Section 6.5.3.

Having selected a numerical integration scheme, the order of numerical integration to be used in the evaluation of the various finite element integrals needs to be determined. The choice of the order of numerical integration is important in practice, because, firstly, the cost of analysis increases when a higher order integration is employed, and, secondly, using a different integration order, the results can be affected by a very large amount. These considerations are particularly important in three-dimensional analysis.

The matrices to be evaluated by numerical integration are the stiffness matrix  $\mathbf{K}$ , the mass matrix  $\mathbf{M}$ , the body force vector  $\mathbf{R}_b$ , the initial stress vector  $\mathbf{R}_s$ , and the surface load vector  $\mathbf{R}_s$ . In general, the appropriate integration order depends on the matrix that is evaluated and the specific finite element considered. To demonstrate the important aspects, consider the Gauss numerical integration order required to evaluate the matrices of the variable-number-nodes elements discussed in Sections 5.3 and 5.4.

A first observation in the selection of the order of numerical integration is that, in theory, using a high-enough order, all matrices are evaluated exactly. On the other hand, using too low an order of integration, the matrices may be evaluated very inaccurately and, in fact, the problem solution may not be possible. For example, considering an element stiffness matrix, if the order of numerical integration is too low, the matrix can have a larger number of zero eigenvalues than the number of physical rigid body modes. Hence, for a successful solution of the equilibrium equations of the element assemblage, it would be necessary that the deformation modes corresponding to all zero eigenvalues of the element be properly restrained in the assemblage of finite elements, because otherwise the structure stiffness matrix would be singular. A simple example would be the evaluation of the stiffness matrix of a three-node truss element. If one-point Gauss numerical integration is used, the row and column corresponding to the degree of freedom at the midnode of the element would be null vectors, which may result in a structure stiffness matrix that is singular. Therefore, the integration order need in general be higher than a certain limit.

The integration order required to evaluate a specific element matrix without error can be determined by studying the order of the function to be integrated. In the case of the stiffness matrix, we need to evaluate

$$\mathbf{K} = \int_V \mathbf{B}^T \mathbf{C} \mathbf{B} \det \mathbf{J} dV \quad (5.134)$$

where  $\mathbf{C}$  is a constant material property matrix;  $\mathbf{B}$  the strain-displacement matrix in the natural coordinate system  $r, s, t$ ;  $\det \mathbf{J}$  the determinant of the Jacobian transforming local (or global) to natural coordinates (see Section 5.3); and the integration is performed over the element volume in the natural coordinate system. The matrix function  $\mathbf{F}$  to be integrated is, therefore,

$$\mathbf{F} = \mathbf{B}^T \mathbf{C} \mathbf{B} \det \mathbf{J} \quad (5.135)$$

The matrices  $\mathbf{J}$  and  $\mathbf{B}$  have been defined in Sections 5.3 and 5.4.

Integration order	Degree of precision	Integration points	$r$ -coordinates	$s$ -coordinates	Weights
3-point	2		$r_1 = 0.16666\ 66666\ 667$	$s_1 = r_1$	$w_1 = 0.33333\ 33333\ 333$
7-point	5		$r_1 = 0.47014\ 20641\ 051$	$s_1 = r_1$	$w_1 = w_1$
13-point	7		$r_1 = 0.6513\ 01029\ 022$	$s_1 = r_1$	$w_1 = w_1$
			$r_2 = 0.86973\ 97941\ 956$	$s_2 = r_1$	$w_2 = w_1$
			$r_3 = r_1$	$s_3 = r_2$	$w_3 = w_1$
			$r_4 = 0.31286\ 54960\ 049$	$s_4 = r_6$	$w_4 = w_1$
			$r_5 = 0.63844\ 41885\ 698$	$s_5 = r_4$	$w_5 = w_4$
			$r_6 = 0.4869\ 03154\ 253$	$s_6 = r_5$	$w_6 = w_4$
			$r_7 = 0.26034\ 59660\ 790$	$s_7 = r_6$	$w_7 = w_4$
			$r_8 = 0.47930\ 80678\ 419$	$s_8 = r_5$	$w_8 = w_4$
			$r_9 = 0.33333\ 33333\ 333$	$s_9 = r_4$	$w_9 = w_4$
			$r_{10} = 0.14957\ 00444\ 677$	$s_{10} = r_{10}$	$w_{10} = w_{10}$
			$r_{11} = 0.17561\ 52574\ 332$	$s_{11} = r_{10}$	$w_{11} = w_{10}$
			$r_{12} = r_{10}$	$s_{12} = r_{11}$	$w_{12} = w_{10}$
			$r_{13} = r_{13}$	$s_{13} = r_{13}$	$w_{13} = -0.14957\ 00444\ 677$

TABLE 5.4 Gauss numerical integrations over triangular domains; here  $\int_V F dr ds = f_{21} w_1 F(r_1, s_1)$ .

A case for which the order of the variables in  $\mathbf{F}$  can be evaluated with relative ease arises when the four-node two-dimensional element studied in Example 5.5 is used as a rectangular or parallelogram element. It is instructive to consider this case in detail because the procedure of evaluating the required integration order is displayed clearly.

**EXAMPLE 5.36:** Evaluate the required Gauss numerical integration order for the calculation of the stiffness matrix of a four-node rectangular element.

The integration order to be used depends on the order of the variables  $r$  and  $s$  in  $\mathbf{F}$  defined in 5.135. For a rectangular element with sides  $2a$  and  $2b$ , we can write

$$\begin{aligned} x &= ar \\ y &= bs \end{aligned}$$

and consequently the Jacobian matrix  $\mathbf{J}$  is

$$\mathbf{J} = \begin{bmatrix} a & 0 \\ 0 & b \end{bmatrix}$$

Since the elements of  $\mathbf{J}$  are constant, referring to the information given in Example 5.5, the elements of the strain-displacement matrix  $\mathbf{B}$  are therefore functions of  $r$  or  $s$  only. But the determinant of  $\mathbf{J}$  is also constant; hence

$$\mathbf{F} = f(r^2, rs, s^2)$$

where  $f$  denotes “function of.”

Using two-point Gauss numerical integration in the  $r$  and  $s$  directions, all functions in  $r$  and  $s$  involving at most cubic terms are integrated without error; i.e., for integration order  $n$ , the order of  $r$  and  $s$  integrated exactly is  $(2n - 1)$ . Hence two-point Gauss integration is adequate.

In an analogous manner, the required integration order to evaluate exactly the stiffness matrices, mass matrices, and element load vectors of other elements can be assessed. In this context it should be noted that the Jacobian matrix is not constant for nonparallelogram element shapes, which may mean that quite high an integration order would be required to evaluate the element matrices exactly.

We discussed in Sections 3.3.3 and 4.2.5 that provided the convergence criteria are satisfied, the displacement formulation of finite element analysis yields a lower bound on the “exact” strain energy of the system considered; i.e., physically, a displacement formulation results in overestimating the system stiffness. Therefore, by not evaluating the element stiffness matrices exactly in the numerical integration, in fact, better results can be obtained provided that the error in the numerical integration compensates appropriately for the overestimation of structural stiffness due to the finite element discretization.<sup>23,38,39</sup> In other words, a *reduction of the numerical integration order* from the order that is required to evaluate the element stiffness matrix exactly should lead in many cases to improved results. This is indeed the case, and a great deal of research effort has been spent to evaluate the optimum integration order and scheme for isoparametric finite element analysis. In addition to merely using a *reduced integration order*, it may well be beneficial to use *selective integration*, i.e. to

integrate the different strain terms with different orders of integration.<sup>21,40</sup> In certain analyses drastic improvements have been obtained; however, it is instructive to summarize the difficulties encountered in the search for the optimum integration scheme, and make some comments on the practical use of reduced and selective integration.

A first observation is that the bounding property of the displacement analysis is lost. This is in practical analysis usually not a serious shortcoming. However, an important observation is that if the order of integration is too low, the solution obtained may be meaningless. In particular, as pointed out already, if the integration order for the evaluation of an element stiffness matrix is too low to include all displacement modes, the rank of the element matrix will be smaller than if evaluated exactly. This causes solution difficulties if the element is not provided with sufficient stiffness restraint in the assemblage of elements; i.e., the stiffness matrix of the total element assemblage could be singular and is more frequently ill-conditioned. Using certain elements that contain spurious zero energy modes some “rules” have been proposed that should be followed so that no solution instabilities develop.<sup>21</sup> However, in a practical analysis with complex boundary conditions and the use of different kinds of elements to model a structure, these rules may only be of limited value in preventing an ill-conditioned set of equilibrium equations.

It has also been argued that the lowest order of numerical integration required for convergence is that order which would evaluate the volume of the element under consideration without error. However, this rule has to be used with great care. For example, in the formulation of a three-node truss element, using one-point Gauss integration we would evaluate the volume exactly, but, as pointed out earlier, the row and column corresponding to the degree of freedom at the midnode of the element are null vectors!

In summary, considering the use of reduced and selective integrations, it is important that with any special integration scheme the following criteria are satisfied:

1. the element does not contain any spurious zero energy modes (i.e. the rank of the element stiffness matrix is not smaller than evaluated exactly); and
2. the element contains the required constant strain states.

The condition in (1) assures that the governing finite element equations can be solved and that no spurious mechanisms develop in the solution. If condition (2) is also fulfilled we know that the completeness condition is satisfied and therefore convergence as discussed in Sections 4.2.5 and 4.3 can be expected. Hence the above two criteria should, in general, be satisfied for a reliable finite element solution.

If an element based on reduced or selective integration is employed that violates one of the criteria given above, it is necessary to use the element with much care. This is particularly the case in an actual practical analysis where the *reliability of the analysis results is of utmost concern*. The confident use of a reduced or selective integration scheme that does not satisfy the above criteria

must largely depend on experience that has been accumulated when analyzing similar structures with high-order numerical integration, or the knowledge of another reliable numerical solution, or the availability of experimental results. Here it should be noted that in practical analysis reduced integration is in essence always used implicitly whenever the distortion of a finite element is such that with the assigned order of integration the exact stiffness matrix is not evaluated.

In addition to the above considerations, we also need to realize that the order of convergence and the spatial isotropy or directionality of an element stiffness matrix can directly be affected by the integration scheme used. Hence, if by virtue of a specific element selection a certain directionality is purposely introduced in the finite element idealization (see Section 5.8.3), we need to preserve this directionality in the numerically evaluated element stiffness matrices—and vice versa.

In the above discussion we focussed attention on the evaluation of the element stiffness matrices. Considering the element force vectors, it is usually good practice to employ the same integration scheme and the same order of integration as for the stiffness matrices. However, in the evaluation of an element mass matrix, it should be recognized that for a lumped mass matrix only the volume of the element need be evaluated correctly, whereas for the exact evaluation of a consistent mass matrix a higher-order integration may be necessary than in the calculation of the stiffness matrix.

**EXAMPLE 5.37:** Evaluate the stiffness and mass matrices and the body force vector of element 2 of Example 4.3 using Gauss numerical integration.

The expressions to be integrated have been derived in Example 4.3,

$$\mathbf{K} = E \int_0^{80} \left(1 + \frac{x}{40}\right)^2 \begin{bmatrix} -\frac{1}{80} & 0 \\ 0 & \frac{1}{80} \end{bmatrix} \begin{bmatrix} -\frac{1}{80} & 0 \\ 0 & \frac{1}{80} \end{bmatrix} dx \quad (a)$$

$$\mathbf{M} = \rho \int_0^{80} \left(1 + \frac{x}{40}\right)^2 \begin{bmatrix} 1 - \frac{x}{80} & \frac{x}{80} \\ \frac{x}{80} & \frac{1}{80} \end{bmatrix} \begin{bmatrix} (1 - \frac{x}{80}) & \frac{x}{80} \\ \frac{x}{80} & \frac{1}{80} \end{bmatrix} dx \quad (b)$$

$$\mathbf{R}_B = \frac{1}{10} \int_0^{80} \left(1 + \frac{x}{40}\right)^2 \begin{bmatrix} 1 - \frac{x}{80} & \frac{x}{80} \\ \frac{x}{80} & \frac{1}{80} \end{bmatrix} dx \quad (c)$$

The expressions in (a) and (c) are integrated exactly with two-point integration, whereas the evaluation of the integral in (b) requires three-point integration. A higher-order integration is required in the evaluation of the mass matrix, because this matrix is obtained from the displacement interpolation functions, whereas the stiffness matrix is calculated using derivatives of the displacement functions.

Using 1, 2, and 3 point Gauss integration to evaluate (a), (b), and (c) we obtain:

*1-point integration*

$$\mathbf{K} = \frac{12E}{240} \begin{bmatrix} 1 & -1 \\ -1 & 1 \end{bmatrix}, \quad \mathbf{M} = \rho \begin{bmatrix} 480 & 480 \\ 480 & 480 \end{bmatrix}, \quad \mathbf{R}_B = \frac{1}{6} \begin{bmatrix} 96 \\ 96 \end{bmatrix}$$

### 2-point integration

$$\mathbf{K} = \frac{13E}{240} \begin{bmatrix} 1 & -1 \\ -1 & 1 \end{bmatrix}, \quad \mathbf{M} = \rho \begin{bmatrix} 373.3 & 346.7 \\ 346.7 & 1013.3 \end{bmatrix}, \quad \mathbf{R}_B = \frac{1}{6} \begin{bmatrix} 72 \\ 136 \end{bmatrix}$$

### 3-point integration

$$\mathbf{K} = \frac{13E}{240} \begin{bmatrix} 1 & -1 \\ -1 & 1 \end{bmatrix}, \quad \mathbf{M} = \rho \begin{bmatrix} 384 & 336 \\ 336 & 1024 \end{bmatrix}, \quad \mathbf{R}_B = \frac{1}{6} \begin{bmatrix} 72 \\ 136 \end{bmatrix}$$

It is interesting to note that with too low an order of integration the total mass of the element and the total load to which the element is subjected are not taken fully into account.

As discussed above, a suitable integration order for the evaluation of element matrices can be established by studying the order of the polynomials that need be integrated and referring to various considerations concerning a stable and convergent solution. Table 5.5 summarizes the results of such an

Element	Reliable integration order	Reduced integration used in practice (with spurious zero energy mode(s))
4-node	2 × 2	—
4-node distorted	2 × 2	—
8-node	3 × 3	2 × 2
8-node distorted	3 × 3	2 × 2
9-node	3 × 3	2 × 2
9-node distorted	3 × 3	2 × 2

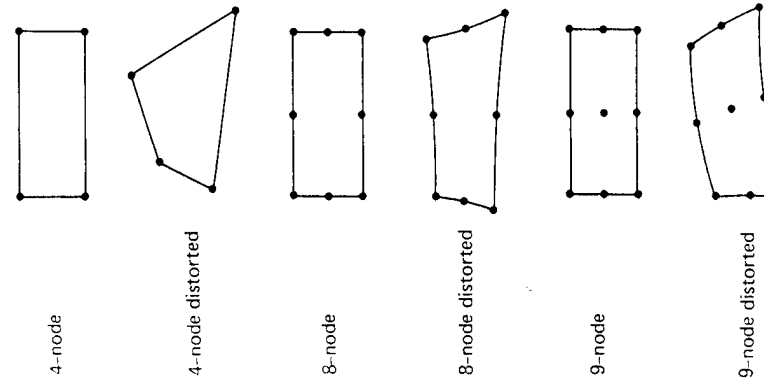


**TABLE 5.5** Gauss numerical integration orders in evaluation of stiffness matrices of two-dimensional rectangular elements (use of Table 5.2).

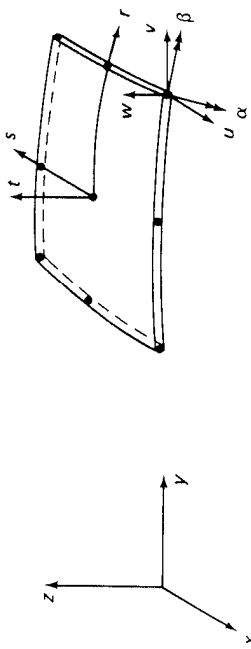
16-node	$4 \times 4$	$3 \times 3$
16-node distorted	$4 \times 4$	$3 \times 3$

TABLE 5.5 (cont.)

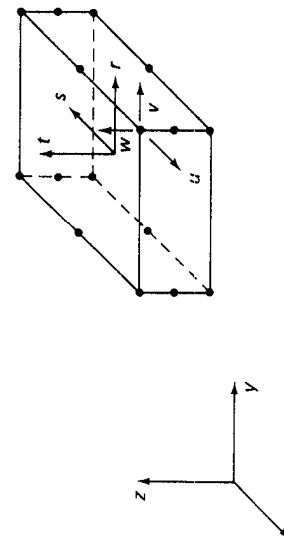
analysis for the appropriate integration orders in the evaluation of the stiffness matrices of two-dimensional elements. This table is presented here in order to give specific guidelines for the choice of the Gauss numerical integration orders in plane stress, plane strain, and axisymmetric analyses. However, the information given in the table is also valuable in deducing appropriate orders of integration for the calculation of the stiffness matrices of other elements.

**EXAMPLE 5.38:** Discuss the required integration order for the evaluation of the shell and three-dimensional elements shown in Fig. 5.45.

Consider first the shell element. The integration in the  $r$ - $s$  plane corresponds to the evaluation of the nine-node element in Table 5.5. Also, the displacements vary



(a) Nine-node shell element



(b) Three-dimensional solid element  
Elements considered in Example 5.38.

linearly with  $t$ . Hence, if the element were flat and rectangular we would evaluate the exact stiffness matrix with  $3 \times 3 \times 2$  Gauss integration corresponding to the  $r$ ,  $s$ ,  $t$  axes. In general, this integration order will also be effective when the element is used in distorted form to model a curved shell.

The required integration order for the evaluation of the stiffness matrix of the three-dimensional solid element can also be deduced from the information given in Table 5.5. The displacements vary linearly in the  $r$ -direction, hence two-point integration is sufficient. In the  $t$ - $s$  planes, i.e. at  $r$  equal to a constant, the element displacements correspond to those of the eight-node element in Table 5.5. Hence,  $2 \times 3 \times 3$  Gauss integration is required to evaluate the element stiffness matrix exactly.

In Table 5.5 we list a reduced integration order that is used in practice and that may for a given finite element mesh result in significantly improved displacement and stress predictions. However, this integration order yields element stiffness matrices that display one or more spurious zero energy modes, which may also be the cause of an unstable (or very inaccurate) solution. As an example, consider the analysis of the simple element assembly in Fig. 5.46.

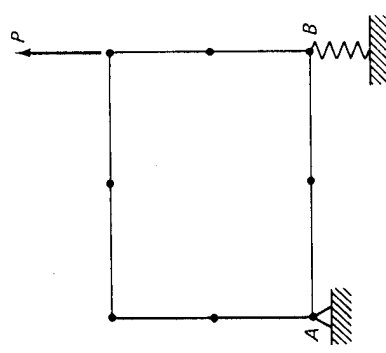


FIGURE 5.46 Eight-node plane stress element supported at  $B$  by a spring.

Using  $2 \times 2$  Gauss integration for the eight-node element, the solution is unstable (the calculated nodal point displacements are very large and have no resemblance with the actual solution), whereas using  $3 \times 3$  Gauss integration (which yields the exact stiffness matrix of the eight-node element), the exact solution—a rigid body rotation about point  $A$ —is calculated.

Finally, considering the information given in Table 5.5, we should note that using the “reliable” integration order we evaluate the stiffness matrices of rectangular elements exactly, whereas the matrices of the distorted elements are, in general, only approximated, but the given integration orders should be sufficient.\* In the above discussion we referred specifically to the evaluation of the element matrices of rectangular elements. But the basic observations summarized above are also applicable to the numerical evaluation of the matrices of trian-

\* Note here that the element distortions may lower significantly the order of strain interpolations (see Section 5.3), and a lower integration order than for the undistorted element may actually be appropriate (also to prevent locking of a plate or shell element, see Section 5.4.1).

gular elements for which, however, a different integration scheme is employed (see Table 5.4).

### 5.8.2 Calculation of Stresses

Assuming that the nodal point displacements of a finite element idealization have been calculated, the stresses within an element are evaluated using the relation

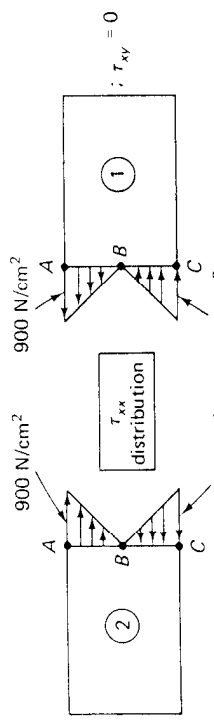
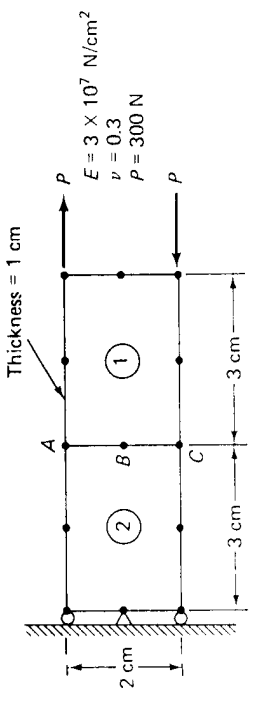
$$\boldsymbol{\tau} = \mathbf{C} \mathbf{B} \mathbf{U} + \boldsymbol{\tau}' \quad (5.136)$$

which was already used in (4.11). The relation in (5.136) gives the stresses at any point of the element, but in practice, the element stresses are only calculated and printed at some specific points. These may be the center of the element, the nodal point locations or the numerical integration points used in the evaluation of the element stiffness matrix. Considering the evaluation of the element stresses, we want to summarize some important observations, some of which we stated already in Section 4.2.6.

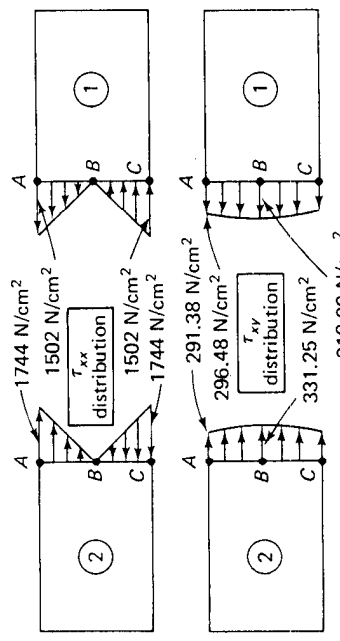
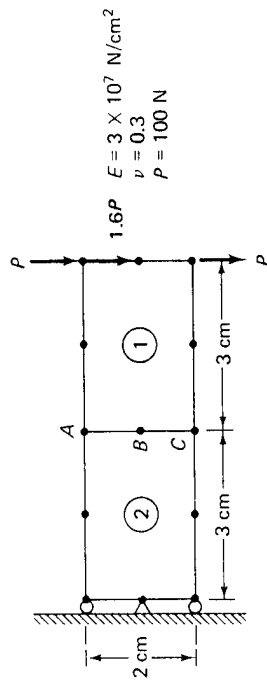
Assume that an element idealization is employed which satisfies all convergence criteria. This does not mean that the predicted stresses are in general continuous across the element boundaries. Hence, considering a compatible element mesh, we would find that the displacements are continuous from element to element, but the stress components are not continuous unless a stress field is analyzed which is contained in the element formulation. A simple analysis that demonstrates this observation is described in Fig. 5.47. When the two eight-node element model of a cantilever is subjected to a bending moment the exact stresses (within beam theory) are predicted, because the eight-node element can represent a constant bending moment exactly (see Example 5.39). Hence, there is no stress discontinuity between the elements. However, the model cannot represent exactly the linearly varying bending moment to be predicted in the analysis of Fig. 5.47(b), which therefore results in stress discontinuities between the elements. The theoretical reason for the stress discontinuities is that only continuity in the displacements, and not their derivatives, is imposed in the analysis (see Sections 4.2.5 and 5.5). For the same reason, imposed stress boundary conditions are only approximately satisfied at a specific boundary point (but they are satisfied in an integral sense).

Based on the convergence considerations discussed earlier (see Section 4.2.5), we note once more that the stress discontinuities between elements and the violation of the local stress boundary conditions will decrease as the element mesh is refined. Therefore, the magnitude of the stress discontinuities between elements can be employed in practice as a measure to indicate whether the finite element idealization has to be refined.

Another observation in the stress calculations is that the stresses at some points in an element can be significantly more accurate when compared with the exact solution than at other points. In particular, it has been observed that the stresses may be considerably more accurate at the Gauss integration points than at the nodal points of an element.<sup>41</sup>



(a) Cantilever subjected to bending moment and finite element solution



(b) Cantilever subjected to tip-shear force and finite element solution

FIGURE 5.47 Predicted longitudinal stress distribution in analysis of cantilever.

The objective in practice is usually to obtain the “best” stress predictions possible once the nodal point displacements have been evaluated. For this purpose, if the difference between the element boundary stresses is not too large, it may be appropriate to simply average them. In an alternative approach, the stresses are only calculated within the elements and then a least squares fit or other interpolation procedure is employed to predict the stresses at the element boundaries or other desired points.<sup>12</sup>

### 5.8.3 Some Modeling Considerations

The establishment of an appropriate finite element model of an actual practical problem depends to a large degree on the following factors: the understanding of the physical problem including a qualitative knowledge of the structural response to be predicted, a thorough knowledge of the basic principles of mechanics, and a good understanding of the finite element procedures available for analysis. Hence, in essence, all the material presented in the previous and the following sections represents important basic knowledge in order that an appropriate finite element model for the analysis of a specific problem can be established. It is our objective in this section to point out a few additional modeling considerations that frequently arise in practice.

A first consideration is the choice of finite elements to be used. Considering the various types of problems that require analysis, it is quite impossible to say that a specific element will always be most effective. However, if we restrict our choice to the isoparametric elements discussed in this chapter, some recommendations can be given.

Table 5.6 summarizes the elements that are usually effective in an actual analysis. We may note that—except for the two-node truss element which is effective because of its simplicity and versatility—the other recommended ele-

ments are higher-order elements, and in particular, the use of parabolic elements is recommended. The reason is that with these elements the cost of using an element and its predictive capability are well-balanced. The predictive capabilities of the parabolic elements can model exactly a constant bending moment, which is important whenever a bending-type stress situation is to be analyzed. We demonstrate this feature in the following example.

**EXAMPLE 5.39:** Consider the eight-node element in Fig. 5.48 when the element is subjected to the nodal point displacements,

$$\begin{aligned} u_1 &= -\delta, & u_2 &= +\delta, & u_3 &= -\delta, & u_4 &= +\delta \\ v_5 &= -\frac{\delta}{2}, & v_6 &= \frac{\delta}{2}, & v_7 &= -\frac{\delta}{2} \end{aligned} \quad (a)$$

and all other nodal point displacements are equal to zero. Evaluate the element strains.

To establish the element strains we evaluate first the element displacements corresponding to the nodal point displacements given in (a). Using

$$u = \sum_{i=1}^8 h_i u_i; \quad v = \sum_{i=1}^8 h_i v_i$$

where the interpolation functions  $h_i$  are given in Fig. 5.5, we obtain

$$\begin{aligned} u &= -rs\delta & v &= -\frac{1}{2}(1-r^2)\delta \\ \epsilon_{xx} &= -s\delta; & \epsilon_{yy} &= 0; & \gamma_{xy} &= 0 \end{aligned} \quad (b)$$

We note that these strains are those of a beam in pure bending (with  $v = 0$ ).

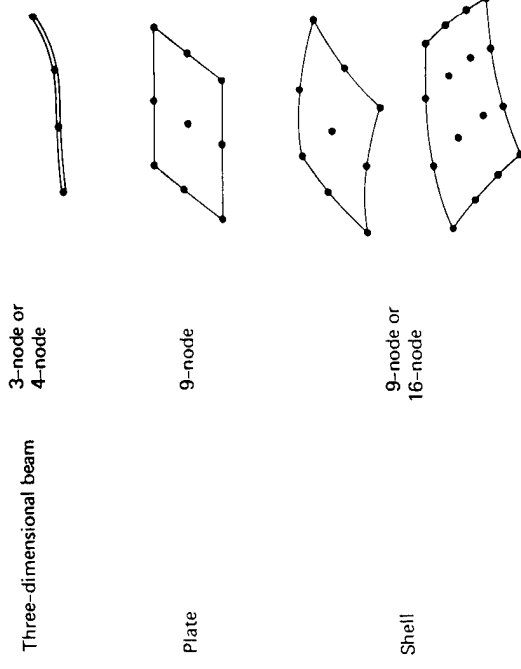


TABLE 5.6 (cont.)

Type of Problem	Element
Truss or cable	2-node
Two-dimensional	8-node or 9-node Plane stress Plane strain Axisymmetric
Three-dimensional	20-node

TABLE 5.6 Isoparametric elements usually effective in analysis.

layouts. Figure 5.49(a) illustrates with a simple example how the use of the variable-number-nodes elements can be effective in constructing transition regions. As another means, constraint equations are frequently useful to preserve compatibility between elements in a transition region. A simple application of constraint equations is shown in Fig. 5.49(b).

Another consideration in the design of a finite element layout is that, except when explicit advantage of element distortions can be taken (see Section 5.3.2), the performance of the isoparametric elements is generally best when they are used without distortions; for example, the rectangular elements should be



**FIGURE 5.48** 2 by 2 eight-node element subjected to bending deformations.

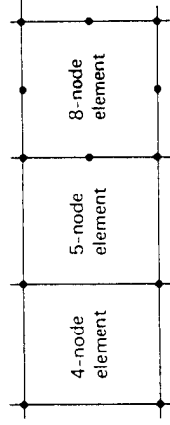
Table 5.6 also shows that for the plate and shell analyses the nine-node and sixteen-node Lagrangian elements are recommended. It is important to use these elements instead of the eight- and twelve-node elements which do not have the internal nodes and "lock" when the element thickness to length ratio becomes small (see Section 5.4).

We show in Table 5.6 only rectangular elements, but in essence the above recommendations are also applicable to the use of triangular elements; i.e., the parabolic and cubic elements are usually most effective.

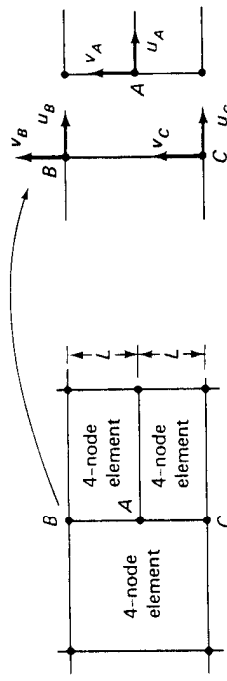
Once a certain element has been chosen, we must decide on the total element layout to be used in the analysis. In this process the element sizes and the number of elements must be selected, and we must decide on the use of mesh grading. The decisions to be made are very problem-dependent but again some general guidelines can be given.

We discussed in Section 5.8.2 the calculation of element stresses and pointed out that, considering an area of a structure in which the exact solution would predict stress continuity, the stresses of a finite element analysis would not (necessarily) be continuous between elements unless a very fine finite element idealization is used. Namely, the stress discontinuities between elements decrease as the finite element idealization is refined and convergence to the "exact" solution is reached. These observations led to the conclusion that the amount of stress discontinuities between elements are a measure of the "appropriateness" of the finite element mesh used. Hence, the overall objective in the design of a finite element mesh is that in an area where high solution accuracy is required, the stress discontinuities between elements should be small, whereas larger stress discontinuities can be tolerated away from the areas of interest. The actual amount of stress discontinuities that can be tolerated depends on the accuracy required in the analysis.

The above objective may require some mesh grading; i.e., a finer finite element mesh in certain areas than in others, and this may require the use of transition zones. Figure 5.49 shows some typical transitions with compatible element

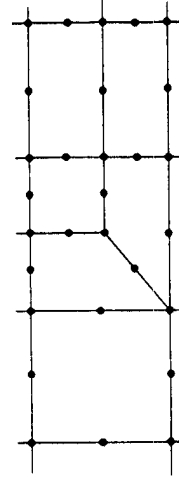


(a) 4-node to 8-node element transition region



Constraint equations:  
 $u_A = (u_C + u_B)/2$   
 $v_A = (v_C + v_B)/2$

(b) 4-node to 4-node element transition;  
from 1 to 2 layers



(c) 8-node to 8-node element transition region;  
from 1 to 2 layers

**FIGURE 5.49** Some transitions with compatible element layouts.

"truly rectangular" with element interior angles of 90 degrees, straight element sides and the noncorner nodes located at the physical positions that correspond to their  $r$ ,  $s$ , and  $t$  values.<sup>43</sup> In this case the Jacobian operator between the natural and physical coordinate systems is a diagonal matrix with constant entries and hence does not affect the order of strain interpolations.

The effect of distorting elements on the accuracy of the analysis results depends to a large degree on the problem considered and the elements used. Although not desirable, in practice distortions of elements cannot be avoided, such as in the modeling of boundaries and transition regions. If the analysis results must be very accurate in these areas, a comparatively larger number of elements must be employed to model these regions in order to compensate for the loss in predictive capabilities of the distorted elements.

Since element distortions often cannot be avoided in practice—and similarly for incompatibilities between elements—a frequent question is: What is the effect of the element distortions and incompatibilities in one area of the mesh on the response that is predicted in another area of this mesh? The precise effect is again dependent on the specific problem considered, and the elements and mesh layout used. However, a major guideline in answering this question is provided by the use of the *St. Venant principle*.<sup>44</sup> Considering a finite element mesh, based on this principle we can expect that the effect of element incompatibilities and distortions will in general be small at a "reasonable" distance from these elements. The actual influence can, however, only be measured using the guidelines given above or by comparison with a more accurate solution.

Finally, we note that in order to assess the actual accuracy of a finite element analysis, without the knowledge of the exact solution to the problem it may be necessary to rerun the analysis with a finer finite element mesh until the changes in the analysis results are sufficiently small. At this point it is assumed that the finite element solution has converged to the "exact" solution of the mechanical model which, it is assumed, represents accurately enough the actual physical problem (see Section 4.2.5). The selection of optimal meshes in these successive finite element solutions is currently subject to much research effort.<sup>45</sup>

## 5.9 COMPUTER PROGRAM IMPLEMENTATION OF ISOPARAMETRIC FINITE ELEMENTS

In Section 5.3 we discussed the isoparametric finite element formulation and showed the specific expressions needed in the calculation of four-node plane stress (or plane strain) elements (see Example 5.5). An important advantage of isoparametric element calculations is the similarity between the calculations of different elements. For example, the calculation of three-dimensional elements is a relatively simple extension from the calculation of two-dimensional elements. Also, in one subroutine, elements with a variety of nodal point configurations can be calculated if an algorithm for selecting the appropriate interpolation functions is used (see Section 5.3).

The purpose of this section is to give an actual computer program for the calculation of the stiffness matrix of four-node isoparametric elements. In

essence, SUBROUTINE QUADS given below is the computer program implementation of the procedures presented in Example 5.5. In addition to the plane stress and plane strain analysis capability, axisymmetric conditions can also be analyzed. It is believed that by showing the actual computer implementation of the element, the relative ease of implementing isoparametric elements is demonstrated best. The input and output variables and the flow of the program are described by means of comment cards.

```

SUBROUTINE QUADS(NEL,ITYPE,NINT,THIC,YM,PR,XI,S,ROUT)
C
C   P R O G R A M
C   TO CALCULATE ISOPARAMETRIC QUADRILATERAL ELEMENT STIFFNESS
C   MATRIX FOR AXISYMMETRIC, PLANE STRESS AND PLANE STRAIN
C   CONDITIONS
C
C   -- INPUT VARIABLES --
C   NEL      = NUMBER OF ELEMENT
C   ITYPE    = ELEMENT TYPE
C   PR.0 = AXISYMMETRIC
C   PR.1 = PLANE STRAIN
C   PR.2 = PLANE STRESS
C   GAUSS  = GAUSS NUMERICAL INTEGRATION ORDER
C   KINT    = THICKNESS OF ELEMENT
C   TMC    = YOUNG'S MODULUS
C   PR     = POISSON'S RATIO
C   IX(2,4) = ELEMENT NODE COORDINATES
C   S(8,8)  = STIFFNESS MATRIX ON SOLUTION EXIT
C   ROUT    = OUTPUT PRINTING FILE
C
C   -- OUTPUT --
C   S(8,8)  = STIFFNESS MATRIX
C
C   IMPLICIT REAL*8(K=-4,0,2)
C   SQR(X)=DSQRT(X)
C   AS(X)=DBS(X)
C
C   * * * THIS PROGRAM IS USED IN SINGLE PRECISION ARITHMETIC ON CDC *
C   * * * EQUIPMENT AND DOUBLE PRECISION ARITHMETIC ON IBM OR UNIVAC *
C   * * * MACHINES. FOR SINGLE OR DOUBLE PRECISION ARITHMETIC ACTIVATE *
C   * * * DPACTIVATE OR AJUST ABOVE AND DATA K/G/M7 CARDS.
C
C   DIMENSION D(4,4),B(4,8),X(2,4),S(8,8),IG(8,4),WGT(8,4),DB(4)
C
C   MATRIX IG STORES GAUSS - LEGENDRE SAMPLING POINTS
C
C   DATA IG/
C   1   0.00,   0.00,   0.00,   0.00,
C   2   1.570265189600, 0.7056669241500, 0.00,
C   3   -3.39981043584900, .34785485137500 /
C
C   MATRIX WGT STORES GAUSS - LEGENDRE WEIGHTING FACTORS
C
C   DATA WGT /
C   1   0.00,   0.00,   1.00,   1.00,
C   2   0.00,   0.5555555555600, .88686888888900,
C   3   0.5555555555600, 0.7056669241500, .652115154662500,
C   4   1.5524515865500, .34785485137500 /
C
C   OBtain STRESS - STRAIN LAW
C
C   PATH/(1,+ PR)
C   G*PR/(1,- 2.*PR)
C   B*P + G
C
C   PLANE STRAIN ANALYSIS
C
C   D(1,*1)=R
C   D(1,*2)=G
C   D(1,*3)=0.
C   D(2,*1)=G
C   D(2,*2)=R
C   D(2,*3)=0.
C   D(3,*1)=0.
C   D(3,*2)=0.
C   D(3,*3)=1/2.
C   IP(ITYPE,EQ,1) THIC=1.
C   IP(ITYPE,EQ,1) GO TO 20
C
C   AXISYMMETRIC ANALYSIS
C
C   011*1=G
C   012*1=G
C   D(3,*1)=0.
C   D(4,*1)=G
C
QUADS0001
QUADS0002
QUADS0003
QUADS0004
QUADS0005
QUADS0006
QUADS0007
QUADS0008
QUADS0009
QUADS0010
QUADS0011
QUADS0012
QUADS0013
QUADS0014
QUADS0015
QUADS0016
QUADS0017
QUADS0018
QUADS0019
QUADS0020
QUADS0021
QUADS0022
QUADS0023
QUADS0024
QUADS0025
QUADS0026
QUADS0027
QUADS0028
QUADS0029
QUADS0030
QUADS0031
QUADS0032
QUADS0033
QUADS0034
QUADS0035
QUADS0036
QUADS0037
QUADS0038
QUADS0039
QUADS0040
QUADS0041
QUADS0042
QUADS0043
QUADS0044
QUADS0045
QUADS0046
QUADS0047
QUADS0048
QUADS0049
QUADS0050
QUADS0051
QUADS0052
QUADS0053
QUADS0054
QUADS0055
QUADS0056
QUADS0057
QUADS0058
QUADS0059
QUADS0060
QUADS0061
QUADS0062
QUADS0063
QUADS0064
QUADS0065
QUADS0066
QUADS0067
QUADS0068
QUADS0069
QUADS0070
QUADS0071
QUADS0072
QUADS0073
QUADS0074
QUADS0075
QUADS0076
QUADS0077
QUADS0078
QUADS0079

```

```

C EVALUATE THE JACOBIAN MATRIX AT POINT (R,S)
C QUAD0041
C QUAD0042
C QUAD0043
C QUAD0044
C QUAD0045
C QUAD0046
C QUAD0047
C QUAD0048
C QUAD0049
C QUAD0050
C QUAD0051
C QUAD0052
C QUAD0053
C QUAD0054
C QUAD0055
C QUAD0056
C QUAD0057
C QUAD0058
C QUAD0059
C COMPUTE THE DETERMINANT OF THE JACOBIAN MATRIX AT POINT (R,S)
C
C DET = XJ(1,1)* XJ(2,2) - XJ(2,1)* XJ(1,2)
C IF (DET<=0.0) STOP(100)
C WRITE (IOUT,20001) NEL
C STOP
C COMPUTE INVERSE OF THE JACOBIAN MATRIX
C
C COMPUTE GLOBAL DERIVATIVE OPERATOR B
C
C QUAD0101
C QUAD0102
C QUAD0103
C QUAD0104
C QUAD0105
C QUAD0106
C QUAD0107
C QUAD0108
C QUAD0109
C QUAD0110
C QUAD0111
C QUAD0112
C QUAD0113
C QUAD0114
C QUAD0115
C QUAD0116
C QUAD0117
C QUAD0118
C QUAD0119
C QUAD0120
C QUAD0121
C QUAD0122
C QUAD0123
C QUAD0124
C QUAD0125
C QUAD0126
C QUAD0127
C QUAD0128
C QUAD0129
C QUAD0130
C QUAD0131
C QUAD0132
C
C FOR PLANE STRESS ANALYSIS CONDENSE STRESS-STRAIN MATRIX
C
C DO 10 I=1,3
C     DO 10 J=1,3
C        D(I,J)=D(I,J) - D(4,J)*A
C 10    DO 30 J=1,8
C      C CALCULATE ELEMENT STIFFNESS
C
C 20 DO 30 I=1,8
C      DO 30 J=1,8
C         S(I,J)=0.
C 30    IF(I,JEQ.0) GO TO 20
C
C CALL STMXXX,B,DET,R1,S1,XBAR,NEL,TYPE,IOUT
C
C ADD CONTRIBUTION TO ELEMENT STIFFNESS
C
C IF ((TYPE.GT.1) XBAR.NINT.MOT(1).NINT*XBAR*DET
C VT=(NINT*XNINT)*MOT(1).NINT*XNINT*XBAR*DET
C DO 40 J=1,8
C 40 IF(J.EQ.1) S1(1,J)=B(I,K,L)*B(L,J)
C CONTINUE
C
C 50 S1(1,J)=S1(1,J)+STIFF*DET(L,J)
C 60 S1(J,1)=S1(J,1)+STIFF*DET
C 70 CONTINUE
C 80 CONTINUE
C
C 90 DO 90 J=1,8
C 90 S1(J,1)=S1(J,1)
C 90 S1(J,1)=S1(J,1)
C
C RETURN
C
C END
C
C SUBROUTINE STMXX(XX,B,DET,R1,S1,XBAR,NEL,TYPE,IOUT)
C
C P R O G R A M
C TO EVALUATE THE STRAIN-DISPLACEMENT TRANSFORMATION MATRIX B
C AT POINT (R,S) FOR A QUADRILATERAL ELEMENT
C
C IMPLICIT REAL(GN-H,C-2)
C DIMENSION XX(2,4),B(4,1),P(2,4),XJ(2,2)
C
C R=1.0+R
C SP=1.0+S
C RM=1.0-R
C SM=1.0-S
C
C INTERPOLATION FUNCTIONS
C
C H(1) = 0.25* RP* SP
C H(2) = 0.25* RP* SP
C H(3) = 0.25* RP* SP
C H(4) = 0.25* RP* SP
C
C NATURAL COORDINATE DERIVATIVES OF THE INTERPOLATION FUNCTIONS
C
C 1. WITH RESPECT TO R
C
C P(1,1) = 0.25* SP
C P(1,2) = - P(1,1)
C P(1,3) = - 0.25* SM
C P(1,4) = - P(1,3)
C
C 2. WITH RESPECT TO S
C
C P(2,1) = 0.25* RP
C P(2,2) = 0.25* RP
C P(2,3) = - P(2,2)
C P(2,4) = - P(2,1)
C
C
```

## REFERENCES

- I. C. Taig, "Structural Analysis by the Matrix Displacement Method," English Electric Aviation Report S017, 1961.
- B. M. Irons, "Engineering Application of Numerical Integration in Stiffness Method," *A.I.A.A. Journal*, Vol. 4, 1966, pp. 2035-2037.
- B. M. Irons, "Numerical Integration Applied to Finite Element Methods," Conference on the Use of Digital Computers in Structural Engineering, University of Newcastle, England, 1966.
- B. M. Irons and O. C. Zienkiewicz, "The Isoparametric Finite Element System—

a New Concept in Finite Element Analysis," *Proceedings, Conference on Recent Advances in Stress Analysis*, Royal Aeronautical Society, London, 1968.

5. J. G. Ergatoudis, "Iso-parametric Finite Elements in Two- and Three-Dimensional Analysis," Ph.D. dissertation, University of Wales, Swansea, 1968.
6. J. G. Ergatoudis, B. M. Irons, and O. C. Zienkiewicz, "Curved, Isoparametric, Quadrilateral Elements for Finite Element Analysis," *International Journal of Solids and Structures*, Vol. 4, 1968, pp. 31-42.
7. J. G. Ergatoudis, B. M. Irons, and O. C. Zienkiewicz, "Three-Dimensional Analysis of Arch Dams and Their Foundations," *Symposium on Arch Dams*, Institute of Civil Engineering, London, Mar. 1968.
8. R. W. Clough, "Comparison of Three Dimensional Elements," *Symposium on Applied Finite Element Methods in Civil Engineering*, Vanderbilt University, Nashville, 1969, pp. 1-26.
9. O. C. Zienkiewicz, B. M. Irons, J. G. Ergatoudis, S. Ahmad, and F. C. Scott, "Isoparametric and Associated Element Families for Two- and Three-Dimensional Analysis," *Finite Element Methods in Stress Analysis* (I. Holand and K. Bell, eds.), Tapir, Trondheim, 1969, Chap. 13.
10. S. Ahmad, "Curved Finite Elements in the Analysis of Solid, Shell and Plate Structures," Ph.D. dissertation, University of Wales, Swansea, 1969.
11. S. Ahmad, B. M. Irons, and O. C. Zienkiewicz, "Analysis of Thick and Thin Shell Structures by Curved Elements," *International Journal for Numerical Methods in Engineering*, Vol. 2, 1970, pp. 419-451.
12. S. Ahmad, B. M. Irons, and O. C. Zienkiewicz, "Curved Thick Shell and Membrane Elements with Particular Reference to Axi-Symmetric Problems," *Proceedings, 2nd Conference on Matrix Methods in Structural Mechanics*, Wright-Patterson A.F.B., Ohio, 1968.
13. W. Pilkey, K. Saczalski, and H. Schaeffer (eds.), *Structural Mechanics Computer Programs*, University Press of Virginia, Charlottesville, Va., 1974.
14. K. J. Bathe, "ADINA—A Finite Element Program for Automatic Dynamic Incremental Nonlinear Analysis," Report AVL 82448-1, M.I.T., Sept. 1975 (rev. Dec. 1978).
15. R. E. Newton, "Degeneration of Brick-Type Isoparametric Elements," *Int. J. Num. Meth. Eng.*, Vol. 7, 1973, pp. 579-581.
16. R. D. Henshell and K. G. Shaw, "Crack Tip Finite Elements are Unnecessary," *Int. J. Num. Meth. Eng.*, Vol. 9, 1975, pp. 495-507.
17. R. S. Barsoum, "On the Use of Isoparametric Finite Elements in Linear Fracture Mechanics," *Int. J. Num. Meth. in Eng.*, Vol. 10, 1976, pp. 25-37.
18. R. S. Barsoum, "Triangular Quarter-Point Elements on Elastic and Perfectly-Plastic Crack Tip Elements," *Int. J. Num. Meth. Eng.*, Vol. 11, 1977, pp. 85-98.
19. R. S. Barsoum, "A Degenerate Solid Element for Linear Fracture Analysis of Plate Bending and General Shells," *Int. J. Num. Meth. in Eng.*, Vol. 10, pp. 551-564, 1976.
20. R. D. Mindlin, "Influence of Rotary Inertia and Shear on Flexural Motion of Isotropic Elastic Plates," *J. Appl. Mech.*, Vol. 18, pp. 31-38, 1951.
21. T. J. R. Hughes, R. L. Taylor, and W. Kanoknukulchai, "A Simple and Efficient Finite Element for Plate Bending," *Int. J. Num. Meth. in Eng.*, Vol. 11, 1977, pp. 1529-1543.
22. O. C. Zienkiewicz, J. Bauer, K. Morgan, and E. Onate, "A Simple and Efficient Element for Axisymmetric Shells," *Int. J. Num. Meth. in Eng.*, Vol. 11, 1977, pp. 1545-1558.
23. E. D. Pugh, E. Hinton, and O. C. Zienkiewicz, "A Study of Quadrilateral Plate Bending Elements with Reduced Integration," *Int. J. Num. Meth. in Eng.*, Vol. 12, 1978, pp. 1059-1078.
24. J. A. Stricklin, W. Haisler, P. Tisdale, and R. Gunderson, "A Rapidly Converging Triangular Plate Element," *A.I.A.A.J.*, Vol. 7, 1969, pp. 80-81.
25. J. L. Batoz, K. J. Bathe, and L. W. Ho, "A Study of Three-node Triangular Plate Bending Elements," *Int. J. Num. Methods in Eng.*, Vol. 15, pp. 1771-1812, 1980.
26. K. J. Bathe and C. Almeida, "A Simple and Effective Pipe Elbow Element—Linear Analysis," *J. Applied Mech.*, Vol. 47, 1980, pp. 93-100.
27. E. Ramm, "A Plate/Shell Element for Large Deflection and Rotations," in *Formulations and Computational Algorithms in Finite Element Analysis*, (K. J. Bathe, J. T. Oden, and W. Wunderlich, eds.), M.I.T. Press, 1977.
28. K. J. Bathe and S. Bolourchi, "A Geometric and Material Nonlinear Plate and Shell Element," *J. Computers and Structures*, Vol. 11, pp. 23-48, 1980.
29. E. L. Wilson, R. L. Taylor, W. Doherty, and J. Ghaboussi, "Incompatible Displacement Models," in *Numerical and Computer Methods in Structural Mechanics* (S. J. Fenves, N. Perrone, J. Robinson, and W. C. Schnobrich, eds.), Academic Press, Inc., New York, 1973.
30. H. H. Dovey, "Extension of Three-Dimensional Analysis to Shell Structures Using the Finite Element Idealization," Report UC SESM 74-2, Department of Civil Engineering, University of California, Berkeley, January 1974.
31. C. E. Fröberg, *Introduction to Numerical Analysis*, Addison-Wesley Publishing Company, Reading, Mass., 1969.
32. A. N. Lozan, N. Davids, and A. Levenson, "Table of the Zeros of the Legendre Polynomials of Order 1-16 and the Weight Coefficients for Gauss' Mechanical Quadrature Formula," *Bulletin of the American Mathematical Society*, Vol. 48, 1942, pp. 739-743.
33. A. H. Stroud and D. Secrest, *Gaussian Quadrature Formulas*, Prentice-Hall, Inc., Englewood Cliffs, N.J., 1966.
34. B. M. Irons, "Quadrature Rules for Brick-Based Finite Elements," *International Journal for Numerical Methods in Engineering*, Vol. 3, 1971, pp. 293-294.
35. P. Silvester, "Newton-Cotes Quadrature Formulae for N-dimensional Simplices," *Proc. 2nd Can. Congr. Appl. Mech.*, Waterloo, Canada, 1969.
36. P. C. Hammer, O. P. Marloue, and A. H. Stroud, "Numerical Integration over Simplices and Cones," *Math. Tabl. Natn. Res. Coun. Wash.*, Vol. 10, 1956, pp. 130-137.
37. G. R. Cowper, "Gaussian Quadrature Formulas for Triangles," *Int. J. Num. Meth. in Eng.*, Vol. 7, 1973, pp. 405-408.
38. W. P. Doherty, E. L. Wilson, and R. L. Taylor, "Stress Analysis of Axisymmetric Solids Utilizing Higher Order Quadrilateral Finite Elements," Report UC SESM 69-3, Structural Eng. Lab., Univ. of California, Berkeley, 1969.
39. O. C. Zienkiewicz, R. L. Taylor, and J. M. Too, "Reduced Integration Techniques in General Analysis of Plates and Shells," *International Journal for Numerical Methods in Engineering*, Vol. 3, 1971, pp. 275-290.
40. S. F. Pawsey and R. W. Clough, "Improved Numerical Integration of Thick Shell Finite Elements," *International Journal for Numerical Methods in Engineering*, Vol. 3, 1971, pp. 575-586.
41. J. Barlow, "Optimal Stress Locations in Finite Element Models," *Int. J. Num. Meth. Eng.*, Vol. 10, 1976, pp. 243-251.
42. E. Hinton and J. S. Campbell, "Local and Global Smoothing of Discontinuous